Spring 2017

SEASONAL CHANGES IN GEOMORPHOLOGY AND SEDIMENT VOLUME OF NEW HAMPSHIRE BEACHES: Insights into a Highly-Engineered, Paraglacial, Bedrock-Influenced Mixed Sand and Gravel Coastal System

Kaitlyn McPherran
University of New Hampshire, Durham

SEASONAL CHANGES IN GEOMORPHOLOGY AND SEDIMENT VOLUME OF NEW HAMPSHIRE BEACHES:

Insights into a Highly-Engineered, Paraglacial, Bedrock-Influenced Mixed Sand and Gravel Coastal System

BY

KAITLYN A. MCPHERRAN

Bachelor of Science, Geology

California State University, Chico, 2014

THESIS

Submitted to the University of New Hampshire

in Partial Fulfillment of

the Requirements for the Degree of

Master of Science

in

Oceanography

May, 2017

This thesis has been examined and approved in partial fulfillment of the requirements for the degree of Master of Science in Oceanography by:

Thesis Advisor Larry G. Ward, Research Associate Professor

Center for Coastal & Ocean Mapping

Department of Earth Sciences

Thomas C. Lippmann, Associate Professor

Center for Coastal & Ocean Mapping

Department of Earth Sciences

Joel E. Johnson, Associate Professor

Department of Earth Sciences

On February 24, 2017

Original approval signatures are on file with the University of New Hampshire Graduate School.

ACKNOWLEGEMENTS

Funding was provided by the University of New Hampshire Department of Earth Sciences in the form of a Teaching Assistantship and an EOS/ESRC – Earth Sciences Student Research Fund, by the Bureau of Ocean Energy Management (Contract M14ACOOO10), and by the University of New Hampshire/National Ocean and Atmospheric Administration Joint Hydrographic Center (Award Number NA10NOS4000073). Without this support, this research would not have been possible.

I sincerely thank my committee members, Dr. Larry Ward, Dr. Thomas Lippmann, and Dr. Joel Johnson for their invaluable guidance and support.

I gratefully acknowledge Dr. Thomas Lippmann for use of his GNSS equipment. I would also like to thank Diamond Tachera, Stephanie Ward, and Alexandra Padilla for their assistance with field work. Finally, I would like to thank Jon Hunt, María José Marín Jarrín, Kelly Nifong, Zachary McAvoy, and Maxlimer Vallee de Ichaso for aiding with data analysis.

Table of Contents

LIST OF FIGURES

LIST OF TABLES

ABSTRACT

SEASONAL CHANGES IN GEOMORPHOLOGY AND SEDIMENT VOLUME OF NEW HAMPSHIRE BEACHES:
Insights into a Highly-Engineered, Paraglacial, Bedrock-Influenced Mixed Sand and Gravel Coastal System

by

Kaitlyn A. McPherran

University of New Hampshire, May 2017

Coastal systems worldwide are undergoing increasing pressure as a result of growing anthropogenic influences, accelerated eustatic sea-level rise, and more intense storms due to climate change. Beaches in New Hampshire have not been systematically studied to assess seasonal changes in beach morphology, erosional and accretional trends, controls on beach processes, or the impact of climate change. In order to further the understanding of a highly-engineered, paraglacial, bedrock-influenced coastal system, six major New Hampshire beaches were monitored from July 2015 to August 2016 for changes in beach morphology and sediment volume. A GNSS rover beach profiling system was utilized to measure beach profiles. Post-processing of the GNSS data revealed that the paths of the profiles often deviated from a shore-perpendicular line. Therefore, a novel processing method was developed to correct and interpolate the profiles to shore-perpendicular lines for comparison. In addition, sediment samples were collected on the upper, middle, and lower beach during summer 2015 to characterize the beaches. Seasonal changes in beach morphology, in addition to sediment grain size distribution, were utilized to classify the beaches and provide insights into beach behavior and possible controls.

Overall, the three northern beaches (Wallis Sands, Foss Beach, and Jenness Beach) are bimodal, granular to pebbly fine to medium sand, dissipative beaches. These beaches tend to be narrow, flat, and featureless welded barriers bounded by bedrock headlands or glacial deposits. The northern beaches tended to undergo vertical erosion and accretion on the scale of weeks to months across the entire width of the beach. Two of the three northern beaches had stations that underwent major net sediment volume changes over the study period. For example, a station on Foss Beach accreted up to an average of 0.87m^3 per meter of beach width, while a station on Jenness Beach eroded an average 0.59m^3 per meter of beach width. The southern three beaches (North Hampton Beach, Hampton Beach, and Seabrook Beach) are unimodal, granular to pebbly medium to coarse sand, intermediate to reflective beaches. The southern beaches are wide barriers with well-developed berms and large sediment volumes. These beaches tended to undergo major erosion and accretion of the berm, including berm crest retreat/advance on the scale of weeks to months. The southern beaches generally ended the study period with negative net sediment volume change (0.2-0.6m^3 eroded per meter of beach width, with a maximum of 0.67m^3 eroded per meter of beach width at southern Seabrook Beach). The results of this study suggest that New Hampshire beaches are vulnerable to erosion under current and future threats of sea-level rise and more intense storms related to climate change.

CHAPTER 1. INTRODUCTION

Beaches have long been recognized for their aesthetic, recreational, and economic value. More recently, beaches have also come to be better appreciated as fragile ecological and geological systems, capable of providing habitat, resources, and even protection from storms. Growing population, expanding demand for coastal and oceanic resources, changing coastal management strategies, and accelerated eustatic (global) sea-level rise due to climate change (IPCC, 2014) have applied increasing pressure on coastal systems worldwide. Furthermore, in many regions, including much of the Atlantic coast of the United States, the recent rate of relative sea-level rise has been much higher than that of eustatic sea-level rise, creating sea-level rise “hotspots” of increased coastal erosion (Sallenger et al., 2012).

Many areas along the New England coastline have experienced significant coastal erosion, as determined by large-scale regional shoreline change analysis studies and smaller-scale studies of beach morphology and sediment budgets (Hill et al., 2002; Kelley et al., 2005; Hapke et al., 2010). For example, sections of Plum Island, Massachusetts have eroded at an estimated rate of 4m/yr in recent decades, while in Maine, average shoreline change north of the Morse River has been an estimated at 2.5m/yr of erosion in recent decades (U.S. Army Corps of Engineers, 2009; Hapke et al., 2010).

New England is also periodically affected by powerful, destructive storms, both tropical storms (e.g. depressions and hurricanes) and extratropical storms (e.g. nor’easters). In 1991, Hurricane Bob (though downgraded to a tropical storm upon landfall) heavily damaged parts of New England, causing over $525 million dollars of damage in Massachusetts (Mayfield, 1992). Wind gusts during the storm exceeded 26m/s in Portsmouth, New Hampshire, and storm surge peaked at 4.6m in Buzzard’s Bay, Massachusetts, causing major coastal erosion (Mayfield, 1992). Recently, Winter Storm Jonas (2016), a

Category 4 (“Crippling”) winter storm, had historic snowfall records in the eastern United States (O’Leary, 2016). Jonas was responsible for wind speeds along the New Hampshire coast up to 20m/s and wave heights of 5m at Jeffreys Ledge (~40km offshore) (NDBC, 2009a, 2016).

Accordingly, many coastlines throughout the world have been heavily engineered and manipulated to protect lives and infrastructure, often with unforeseen negative effects (Pilkey and Wright, 1988). Therefore, new strategies for increasing coastal resiliency are currently being developed, including “soft” solutions (such as beach nourishment), and “green” solutions (such as artificial kelp, oyster reefs, and biodegradable structures) (Pilkey and Cooper, 2012). These new types of coastal management strategies differ greatly from the traditional approach of “hard” solutions, which include seawalls and groins (Pilkey and Cooper, 2012). All coastal management strategies, however, require an in-depth understanding of the morphology, sedimentology, and controlling processes of the coast under a variety of conditions. Consequently, a thorough understanding of the physical and geological processes involved in coastal systems and their interactions with engineering structures is necessary to create and maintain a sustainable balance between human influences and coastal environments.

Like many coastal areas in the western Gulf of Maine (WGOM) (Figure 1-1), the New Hampshire (NH) coastal region is heavily developed and features near-contiguous engineering structures along the entire coast (Blondin, 2016). Therefore, NH beaches provide an opportunity to study the beach morphology and sedimentology of a highly engineered, bedrock-influenced, paraglacial coastal system under a variety of seasonal conditions. Though only 21km in length, the NH coastline includes most of the beach types found in this region, varying from small pocket beaches bounded by headlands and glacial features to barrier islands (FitzGerald et al., 1993; Fitzgerald and Van Heteren, 1999).

The NH coastline has undergone limited shoreline change in recent decades, but the beaches appear to experience large seasonal elevation changes (with respect to sea-level). This apparent stability of the position of the coast is likely a result of extensive bedrock outcrops, glacial features, and engineering structures which tend to anchor and protect the shoreline, as well as a negligible to low rate of relative sea-level rise until recently (see Present Sea-Level, below). However, this shoreline stability is expected to be significantly challenged by the acceleration in eustatic sea-level rise and the increase in storm frequency and intensity related to climate change (IPCC, 2014).

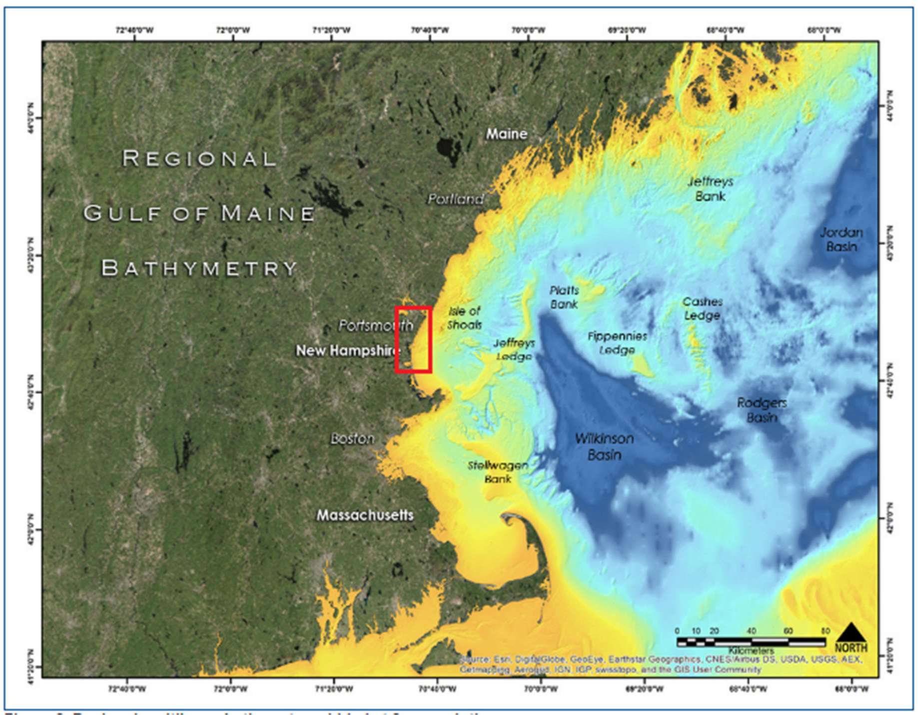

Figure 1-1: Map of the New England region and the Gulf of Maine. The bathymetry, gridded at 8m resolution, is indicated by color, where warmer colors indicate shallower water areas and cooler colors indicate deeper areas. The NH coast is boxed in red. Map from University of New Hampshire Joint Hydrographic Center/Center for Coastal and Ocean Mapping (modified from Johnson and Nagel, 2016).

Despite the extensive development of the coast and clear need for long-term coastal data acquisition, only a few, limited studies have been conducted in NH to evaluate changes in beach morphology and sedimentology, either on seasonal bases or in response to storms. Additionally, the sediment sources, sinks, transport mechanisms, and overall coastal sediment budgets of the NH coastal system are largely unknown. To begin addressing these issues, and to further the current understanding of highly-engineered, paraglacial, bedrock-influenced coastlines, six major NH beaches (Wallis Sands, Foss Beach, Jenness Beach, North Hampton Beach, Hampton Beach, and Seabrook Beach) were studied from July 2015 through August 2016. Beach monitoring stations were established at each beach to determine morphologic and elevation changes over the study period (Figure 1-2). Seasonal and storm-related changes were determined and volumetric changes in beach sediment were quantified. Finally, the beaches were classified based on geomorphology and sediment grain size.

The results of the study provide insights into the stability of the coastline and a baseline for long-term monitoring of the beaches to further the understanding of the potential impacts of sea-level rise and climate change. Additionally, the use of Global Navigation Satellite System (GNSS) technologies to monitor beach changes was investigated, with the aim of maximizing efficiency and accuracy while understanding potential sources of uncertainty. Furthermore, a novel processing method was developed to correct and interpolate the profiles to overlying, shore-perpendicular lines for comparison. Finally, the initial research conducted during this study formed the basis of a long-term volunteer beach monitoring effort that is currently under development in NH.

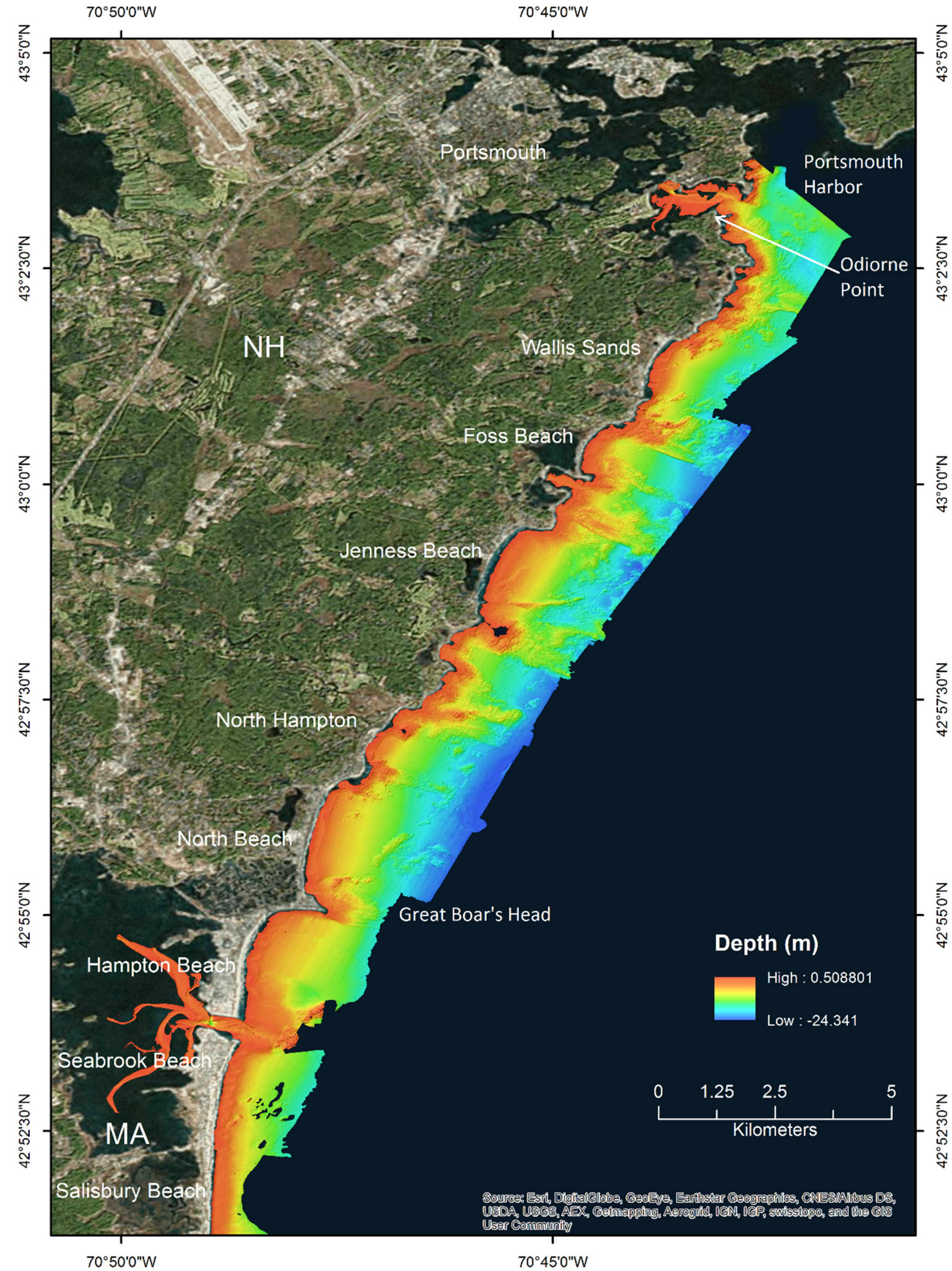

Figure 1-2: Map of the study area, including the New Hampshire coastline and offshore bathymetry, extending from the Piscataqua River in the north to Seabrook in the south. Major beaches and features are labelled in white. Beaches included in this study are: Wallis Sands, Foss Beach, Jenness Beach, North Hampton Beach, Hampton Beach, and Seabrook Beach. Modified from Ward et al., 2016.

CHAPTER 2. BACKGROUND

GEOLOGIC SETTING

Bedrock Geology

The coast of NH is heavily influenced by exposed bedrock, which occurs as headlands between beaches, and as outcrops onshore that extend offshore (Ward et al., 2016b). The bedrock that outcrops along the coast is composed of the Late Proterozoic or Ordovician Rye Complex, the Ordovician or Silurian Kittery formation (Merrimack Group), and the Silurian Newburyport Complex (Bennett et al., 1997; Lyons et al., 2006). The Rye Complex is exposed in all the outcrops north of Great Boar's Head (Figure 1-2), and is composed of "migmatite of gray, foliated, sheared or mylonitized two-mica granite and pegmatite, minor hornblende-biotite diorite, intruding metapelites and metavolcanic rocks" (Lyons et al., 2006). The Rye Complex is in faulted contact with the Kittery Formation, which underlies the northern half of Hampton Beach (Figure 1-2), outcropping both on the beach and offshore (Bennett et al., 1997). The Kittery Formation is composed of "tan, graded-bedded, calcareous metasandstone and purple and green phyllite" (Lyons et al., 2006). The southern half of Hampton Beach and all of Seabrook Beach (Figure 1-2) are underlain by the Silurian Newburyport granite, which is composed of "gray medium-grained porphyritic granite with microcline phenocrysts" (Goldsmith et al., 1983; Wones and Goldsmith, 1991).

Glacial History

During the most recent glaciation (Wisconsin), the Laurentide Ice Sheet covered all or parts of northern New England and the Gulf of Maine from approximately 180,000 to 14,800 cal. B.P. (Figure 2-1) (Dyke et al., 2002a; Shaw et al., 2006). The ice sheet extended south to Cape Cod and east into the Gulf of Maine to Georges Bank (Figure 2-1) (Dyke et al., 2002b; Shaw et al., 2006). Maximum ice thickness is estimated to have been 1500m in NH (Moore, 1987), occurring between 26,000 and 23,000 cal. B.P. (Dyke et al., 2002b). The coast of NH was ice free by ~14.8ka cal. B.P. (Figure 2-1) (Shaw et al., 2006)

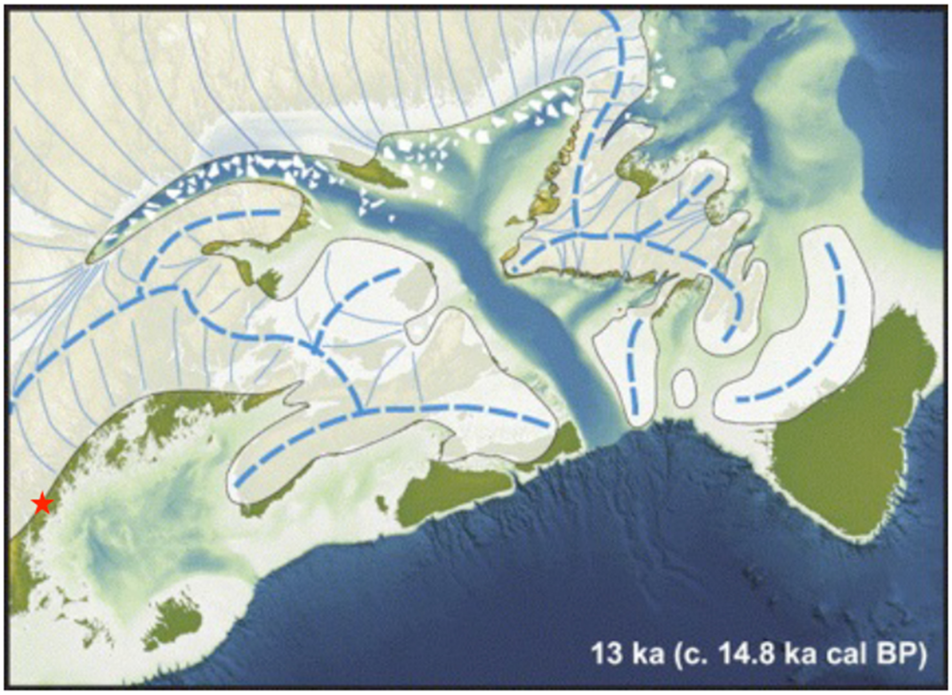

Figure 2-1: Extent of the Laurentide Ice Sheet in Atlantic Canada at 14.8 cal. B.P. The red star represents the current location of the New Hampshire seacoast region, which is thought to have been ice-free by 14.8 cal. B.P. Modified from Shaw et al. (2006).

<u>*Surficial Geology*</u>

As a result of the Wisconsin glaciation, the surficial geology of NH, including the coastal region, consists mainly of reworked glacial deposits and exposed bedrock. The glacial and glaciofluvial erosion during and immediately following the glaciation removed much of the sediment cover, exposing basement bedrock in NH and in the WGOM (Uchupi and Bolmer, 2008). A variety of glacial features were deposited, including drumlins (such as Great Boar's Head (Figure 1-2) at the northern end of Hampton Beach), moraines, outwash plains, glacial till, and glaciomarine muds (Bradley, 1964; Novotny, 1969; Uchupi and Bolmer, 2008). The sediment that composes New England beaches is sourced from inland, updrift, and offshore, including large amounts of sediment stored in submerged paleodeltas and drowned glacial features (Belknap et al., 1989; Duffy et al., 1989; Kelley et al., 1992; Barnhardt et al., 1997).

SEA-LEVEL

Sea-Level History

Due to the Wisconsin glaciation and associated isostatic depression and rebound of the crust in the northeastern United States, the WGOM experienced a complex sea-level history, including a transgression, a regression, and finally, a transgression that is still occurring today (Figure 2-2). The relative sea-level history for the coasts of Massachusetts (Oldale et al., 1993; Barnhardt et al., 1995; Hein et al., 2007) and Maine (Belknap et al., 1987; Barnhardt et al., 1995; Kelley et al., 2010) have been studied extensively and are relatively well-constrained. A preliminary sea-level curve was developed for the NH shelf, however, it is not as well constrained as the Massachusetts and Maine curves (Birch, 1990). The extent of the Presumpscot Formation in NH and the drowned forest at Odiorne Point in NH (discussed below) suggest that the NH sea-level curve more closely follows the Maine sea-level curve, therefore, the Maine sea-level curve is discussed here.

The Presumpscot Formation is a nearshore glaciomarine blue-gray silt and silty clay located in Maine, NH, and the WGOM (Bloom, 1959; Oldale, 1989). The deposition has been radiometrically dated to 18-12ka, corresponding to glacial retreat in the region (Oldale, 1989). NH surficial geology maps suggest that the Presumpscot extends at least 60m above present sea-level in New Hampshire, consistent with the +75m sea-level highstand in southern Maine between 14,000-12,500 cal. B.P., and inconsistent with the +30m highstand level in Massachusetts during the same time period (Bloom, 1959; Oldale et al., 1993; Koteff and Moore, 1994; Kelley et al., 2010; Earth Systems Research Center, 2017).

The remains of a drowned forest are present in the intertidal zone at Odiorne Point, Rye, NH (Figure 1-2). Dendrochronology and radiocarbon age dating suggest that the tree stumps were killed by rising sea-level and salt water incursion approximately 3,660-3,490 cal. B.P., consistent with the slow transgression of the past 4,000 years (cal. B.P.) demonstrated by the Maine sea-level curve (Lyon and Harrison, 1960; Harrison and Lyon, 1963; Kelley et al., 2010).

At the end of the Wisconsin glaciation (~14,000 cal. B.P.), the ocean was in contact with the retreating ice front due to the depression of the crust, leading to a sea-level transgression. The magnitude of the highstand varies along the coast due to the different ice thicknesses and levels of isostatic depression; the highstand extended to approximately 30m above present in northern Massachusetts and approximately 75m above present in southern Maine (Figure 2-2) (Oldale et al., 1993; Kelley et al., 2010).

Due to the removal of the ice sheet, the crust in the WGOM began to isostatically rebound at a rate that exceeded eustatic sea-level rise. This rebound led to a Gulf of Maine relative sea-level lowstand at ~12,500 cal. B.P. (Figure 2-2) This lowstand was ~55m below current sea-level in Maine and ~45m below current sea-level in Massachusetts (Belknap et al., 1987; Oldale et al., 1993; Kelley et al., 2010). As isostatic crustal rebound began to slow in the WGOM, eustatic sea-level rise overtook isostatic rebound, leading to a sea-level transgression of ~40m in Maine, which progressed quickly until ~11,500 cal. B.P. (Barnhardt et al., 1995; Kelley et al., 2010). Between 11,500 and 7,500 cal. B.P., a “slowstand” occurred in Maine, with a sea-level rise of less than 5m (Barnhardt et al., 1995; Kelley et al., 2010). Evidence of this “slowstand” is not present in Massachusetts, where sea-level rose more steadily to present sea-level (Oldale et al., 1993). Post-glacial eustatic sea-level rise slowed, as did crustal rebound, causing relative sea-level rise to also slow from ~4,000 cal. B.P. to present (Barnhardt et al., 1995; Belknap et al., 2002). The very slow sea-level rise of the past 4,000 years has allowed for the formation of beaches, marshes, and barrier systems in New England (Ward et al., 2008; Hapke et al., 2010; Kelley et al., 2010).

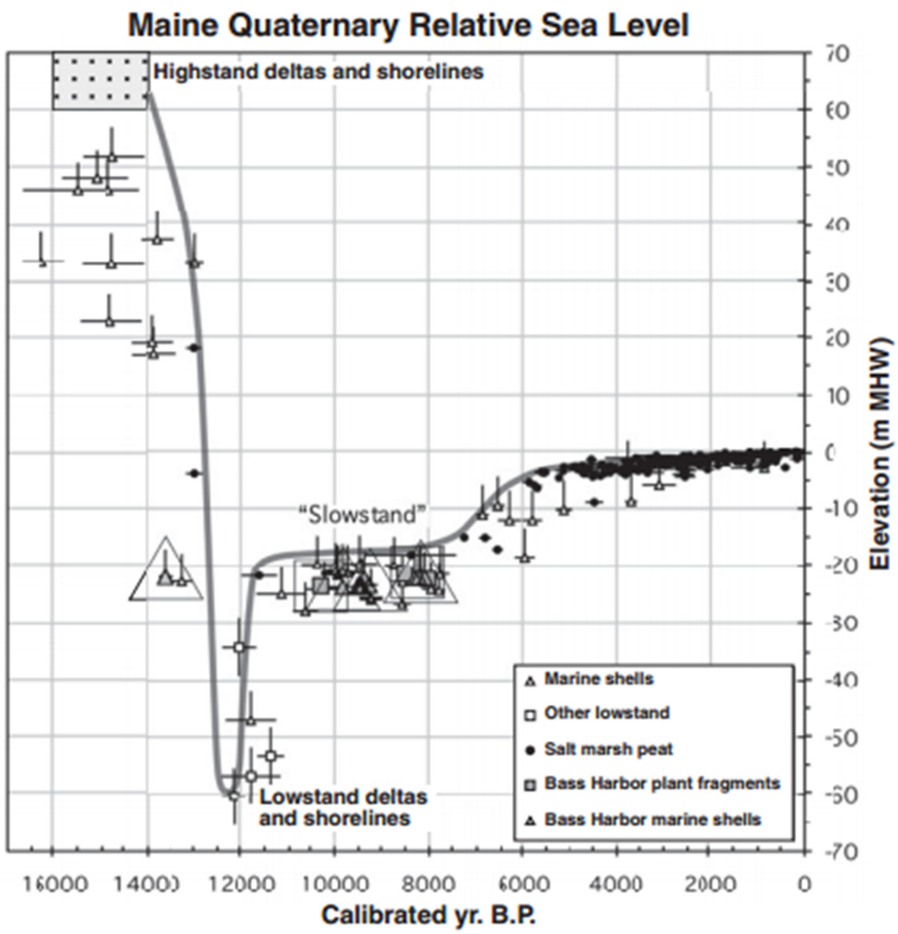

Figure 2-2: Sea-level curve for Maine from 16,000 cal. B.P. to present based on radiocarbon dates (MHW is mean high water) (Kelley et al., 2010).

Present Sea-Level

Tide gauge records in NH have discontinuous data, however, the Portsmouth Harbor tide gauge (Seavey Island, Maine) was in operation from 1926 to 2001, and analysis of the data by NOAA indicates a rate of sea-level rise over that period of 1.76±0.30mm/yr (NOAA, 2016). This value is consistent with a rate of sea-level rise of 1.87±0.15mm/yr over the period 1912–2016, calculated at the Portland, Maine tide gauge, which was in continuous operation over that period (NOAA, 2013a). Because of the similarities between the gauge values and the longer record of the Portland gauge, the Portland gauge data was used for further analysis.

Monthly mean tidal elevation data for the period 1912 to 2016 (in meters relative to MSL) were downloaded from the NOAA Tides & Currents website for the Portland, Maine gauge (NOAA, 2013a), and linear trend lines for several time periods were applied using MATLAB (polyfit.m and polyval.m) (Figure 2-3). Trend lines were created for the periods 1912-2016, 1912-1950, 1950-1980, and 1980-2016. Results suggest that the rate of relative sea-level rise in Portland, Maine was stable at 1.7 to 1.8mm/yr from 1912-1980, but increased to 2.3mm/yr during the period 1980-2016. This is consistent with the reported rate of relative sea-level rise of 1.87±0.15mm/yr over the period 1912-2016 calculated by NOAA from the same data at Portland, Maine. However, the reported rate does not highlight the fact that relative sea-level rise in Portland, Maine has increased from 1.7 to 1.8mm/yr pre-1980 to 2.3mm/yr post-1980 (NOAA, 2013b).

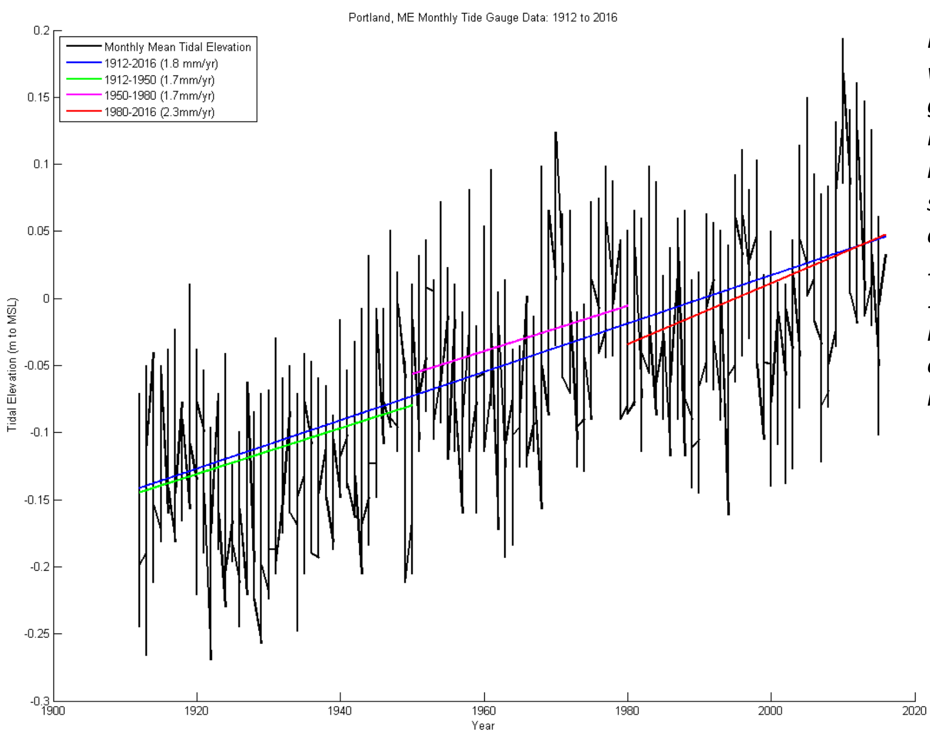

Figure 2-3: Monthly mean water levels from the tide gauge at Portland, Maine(station 8418150), located ~85 km north of the study area. Linear trends were computed for the periods 1912-2016, 1912-1950, and 1980-2016. The rate of sea-level rise for each period based on the analysis are given in the legend. (NOAA, 2013a).

Predicted Sea-Level Trends

Over the period 1900-2010, the rate of eustatic mean sea-level rise was 1.7±0.2mm/yr, however, that rate increased significantly during the period 1993-2010 to 3.2±0.4mm/yr (Figure 2-4) (IPCC, 2014). This increase was driven by ocean thermal expansion and inputs from terrestrial ice sheets and land water storage (IPCC, 2014). In addition, the IPCC (2014) has predicted that the rate of eustatic mean sea-level rise will increase significantly in the coming century due to climate change and anthropogenic greenhouse gas emissions. Eustatic mean sea-level rise for the most extreme scenario is expected to reach a rate of 8-16mm/yr for the period 2081-2100 (IPCC, 2014). However, relative sea-level rise in many regions will be more or less severe than eustatic sea-level rise, with 70% of coastlines projected to experience ±20% of the eustatic mean sea-level change due to fluctuations in ocean circulation, the pathways of CO_2 emissions, and regional tectonics (IPCC, 2014).

These changes, in addition to other climatic and oceanic changes, will bring increased risk of severe river and coastal flooding to many regions (IPCC, 2014). The NH coast has experienced a relatively slow rate of sea-level rise for the past ~4,000 years, however, an acceleration of sea-level rise and increased storm intensity may dramatically change the stability of the coast, leading to erosion, flooding, and/or shoreline retreat (Ward and Adams, 2001; Wake et al., 2011; Krishen et al., 2014).

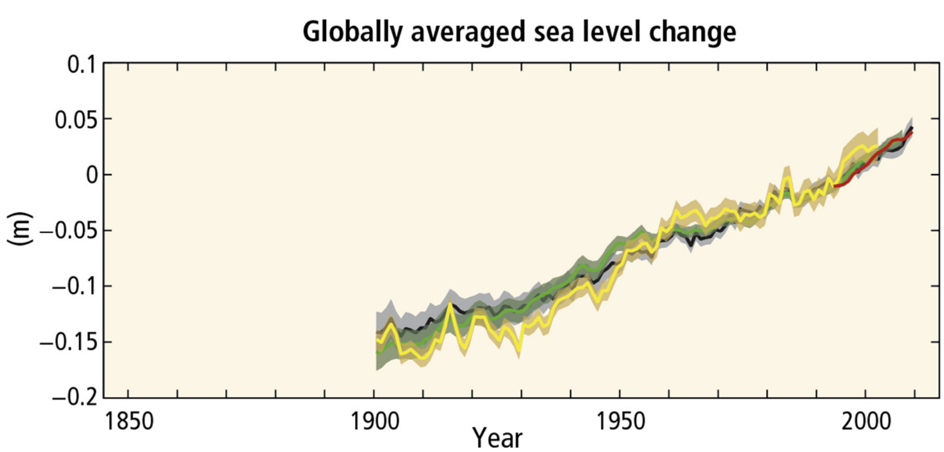

Figure 2-4: Eustatic mean sea-level change from 1900-2010. From IPCC, 2014.

STUDY AREA

The coast of NH includes small, narrow, discontinuous barrier beaches or pocket beaches composed of sand, mixed sand and gravel, or gravel, dominated by wave processes with tidal influences (Tuttle, 1960; Novotny, 1969; Hayes, 1979; Fitzgerald and Van Heteren, 1999; Kelley, 2004). The NH coast has semidiurnal tides with strong diurnal components (NOAA, 2013c). Mean tidal range (measured at the Fort Point tidal gauge, Portsmouth Harbor) in NH was 2.63m for the period 1976–2016 (Figure 1-2) (NOAA, 2013c). Mean monthly water temperature at 1m depth on the WGOM shelf ranged from 18.3˚C (August) to 3.7˚C (March) for the period 2001-2016, from Buoy B01, 27km northeast of Portsmouth, NH (NERACOOS, 2016). Mean monthly significant wave heights for the period 1982-2008 in the WGOM (6km offshore of Portland, Maine) ranged from 0.7m to 1.1m, with an annual average of 0.9m (NDBC, 2009b). Maximum significant wave heights at the same station over the same period ranged from 2.6m to 9.6m (NDBC, 2009b). Alongshore currents have not been well studied in NH.

<u>Climate</u>

The NH coastal region has warm, temperate summers (June–September) and cold, snowy winters (December–March). Mean monthly air temperatures recorded at the Isle of Shoals (Figure 1-1) meteorological station (IOSN3, located 11km offshore of the NH coast) for the period 1996–2008 ranged from 1.7°C to 19.3°C, with an annual average of 8.9°C (NDBC, 2009a). Monthly average wind speeds at the IOSN3 station for the same period ranged from 20–31km/hr, with an annual average of 25km/hr (NDBC, 2009a). The annual average precipitation in southern NH (including the coastal region) was 110.54cm/yr for the period 1901-2000 (NOAA NCEI, 2016).

Mean annual precipitation in NH increased 10% from 1895 to 2011 (~12.7cm) (Krishen et al., 2014). Extreme annual precipitation increased substantially from 1901 to 2012, including an increase of 50% in extreme storm events (Krishen et al., 2014). Both mean annual precipitation and extreme precipitation events in NH are projected to increase as much as 20% for the period 2071-2099 due to climate change (Krishen et al., 2014). Global extreme precipitation events are also predicted to become more intense and frequent during the 21st century in all IPCC CO_2 emission scenarios (IPCC, 2014), increasing the vulnerability of coastlines to erosion during storms.

The coast of New England is greatly impacted by storms, and coastal processes are controlled primarily by extratropical cyclones ("nor'easters") and tropical cyclones (Niederoda et al., 1985; Krishen et al., 2014). Local coastal fronts are common in New England during the fall and winter (Nielson, 1989). A study of winter storms on the New England continental shelf found that winter storms have intense winds that dominate shelf circulation and net flow (Beardsley and Butman, 1974). Strong storms have the potential to rework sediment and overtop barrier islands, creating overwash fans (Donnelly et al., 2001). At least five intense hurricanes have made landfall in New England since the early 1600's, leaving records of major sediment reworking in overwash fan deposits (Donnelly et al., 2001). Previous work in Maine found that frontal passages and southwest storms tended to bring sediment towards the shore, and northeast storms tended to remove sediment from the beach (Hill et al., 2004). No clear changes in extratropical storm intensity in the NH region due to climate change is clear, as storm intensity is based on storm speed, storm area, coastal bathymetry and topography, and angle of approach to the coast (Krishen et al., 2014). However, as extratropical storms account for the majority of storms in NH, changes in frequency or intensity are of great concern (Krishen et al., 2014).

Coastal Engineering

The NH coastline has been extensively modified with a variety of coastal engineering structures (including seawalls, rip rap, gravel berms, groins, and jetties) (Figure 2-5) (Blondin, 2016), and has undergone at least twelve recorded episodes of beach nourishment between 1935 and 2012 at Wallis Sands, Hampton Beach, and Seabrook Beach (Table 2-1) (Haddad and Pilkey, 1998; Olson and

Chormann, 2016; U.S. Army Corps of Engineers, 2016a, 2016b). Only a minor portion of the NH coast has been left without engineering structures, including the southern ~600m of Hampton Beach, which is a State Park, and the southern ~1500m of Seabrook Beach, which features an extensive dune system (Figure 2-5).

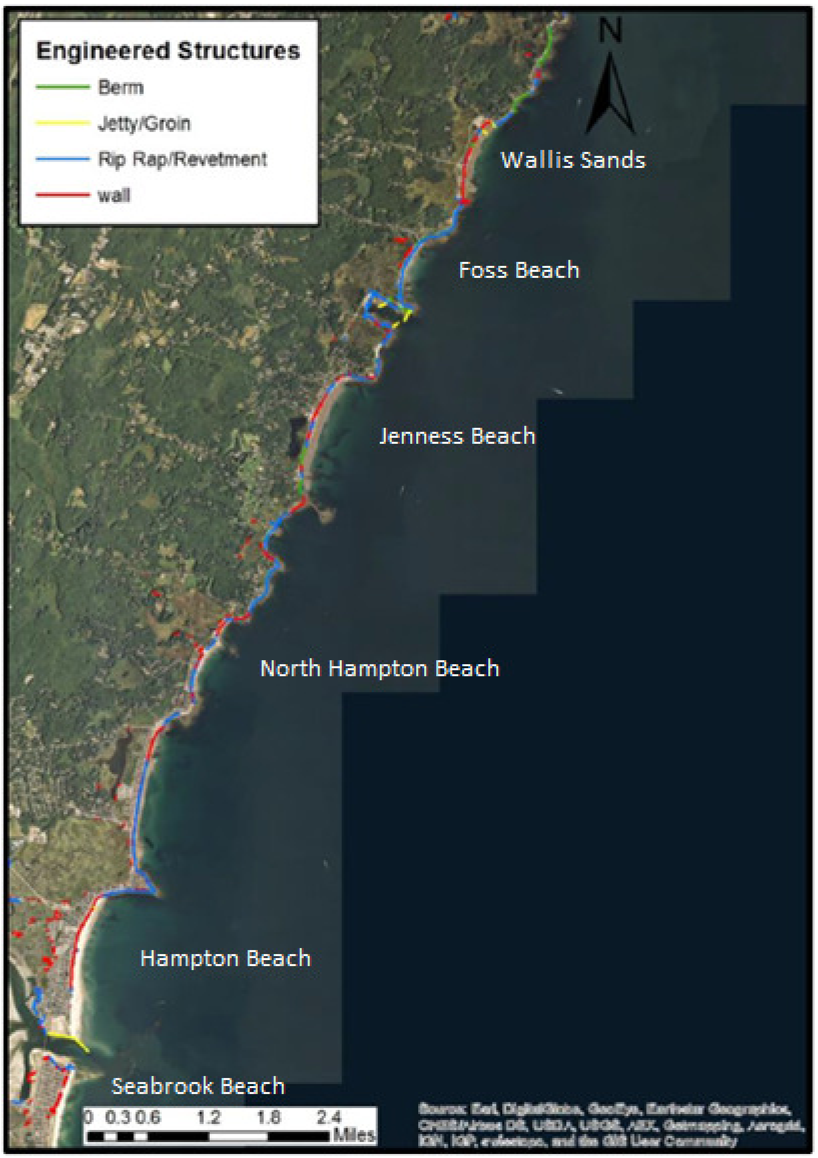

Figure 2-5: Map of New Hampshire coastal engineering structures. Structures in coastal NH are primarily hard structures, and include berms, jetties/groins, rip rap, and seawalls. Beaches included in this study are labelled in white. Modified from Blondin, 2016.

Table 2-1: Summary of known NH beach nourishment projects. (Haddad and Pilkey, 1998; Olson and Chormann, 2016; U.S. Army Corps of Engineers, 2016a; U.S. Army Corps of Engineers, 2016b.)

Location	Organization	Date	Nourishment (cubic meters)	Structure	Other
Wallis Sands	USACE NH Shore and Bank Protection Projects (NHSBPP)	1963	153,000	107m stone groin emplaced	Widened northernmost 244m of beach to 46m width
Wallis Sands	USACE NHSBPP	1973	7,700		Groin repaired
Wallis Sands	Unknown	1983	Unknown volume		
Wallis Sands	Unknown	2001	30,500		
Hampton Beach	State of NH	1935	765,000		
Hampton Beach	USACE NHSBPP	1955	306,000		Widened northern 1981m of beach
Hampton Beach	USACE NHSBPP	1965	130,000	58m stone groin emplaced	Widened northern 671m of beach with Hampton Harbor dredge material
Hampton Beach	USACE	1973	313,000		
Hampton Beach	Unknown	1987	16,000		
Hampton Beach	Unknown	2012	40,000		
Seabrook Beach	Unknown	2005	Unknown volume		
Seabrook Beach	Unknown	2012	92,000		

PREVIOUS WORK

The United States Geologic Survey ranked the New England coastline as low risk for coastal vulnerability during the National Assessment of Coastal Vulnerability (Thieler and Hammar-Klose, 1999). This assessment was based on risk variables such as coastal geomorphology, coastal slope, relative sea-level rise, mean tidal range, mean wave height, and coastal erosion/accretion rate. However, long-term (1800's to 2000's) and short-term (25 to 30 years) shoreline change rates for northern New England (Cape Ann, Massachusetts to northern Maine) determined by the National Assessment of Shoreline

Change vary greatly (Hapke et al., 2010). Between northern Maine and Cape Ann, Massachusetts, long-term shoreline change rates average 0.2m/yr of erosion, with 41% of beaches between northern Maine and Cape Ann eroding (Hapke et al., 2010). However, short-term shoreline change rates at individual beaches are often much more severe than this average suggests. For example, at Plum Island, Massachusetts (located ~10km south of the present study area) (Figure 1-1, Figure 1-2), the long-term (1800's to 2000's) shoreline change rate is over 3m/yr of erosion (Hapke et al., 2010). Castle Neck Beach, Massachusetts (located ~25km south of the Seabrook Beach) has the highest short-term (25 to 30 years) rates of both erosion and accretion in New England at 4.9 m/yr and 9.4m/yr, respectively, at the northern and southern end of a rapidly migrating barrier spit (Hapke et al., 2010).

The first systematic study of beach morphology and sedimentology in NH was conducted by Leo (2000). The study involved measuring elevation changes in the profiles of two beaches in southern Maine (Seapoint Beach and Crescent Beach) and three beaches in NH (Jenness Beach, North Beach, and Hampton Beach (Figure 1-2)) from September 1997 to September 1998. The study examined the reactions of two different beach types (small, mixed sediment barriers with little engineering and longer, more fortified beaches) of varying orientation to twenty-eight storm events of differing intensities and directions (Leo, 2000). The study found that Jenness Beach was eroded fairly steadily throughout the study period, with no major erosional events (Leo, 2000). Hampton Beach was greatly eroded by storms, but recovered quickly (Leo, 2000). The study concluded that a maximum erosional downcut limit was reached at Jenness Beach, but not at Hampton Beach, likely due to the large sand volume of Hampton Beach (Leo, 2000). A downcut limit of erosion on a beach is a critical elevation below which there is little to no vertical erosion (Nicholls and Orlando, 1993; Fucella and Dolan, 1996). This is evidenced by a decrease in erosion of a beach despite increasing or continued high wave energy as the stormy season progresses, and is determined by wave energy, beach profile shape, sediment grain size, and pre-existing beach sediment volume (Nicholls and Orlando, 1993; Fucella and Dolan, 1996).

Short-term (annual) and long-term (decadal) change in shoreline position, as well as volumetric sediment change between LIDAR surveys of NH beaches from the mid-1800's to 2014 were assessed using LIDAR data, historical charts, and orthophotography by Olson et al. (2016) and Olson and Chormann (2016). Results indicate that short-term variability and long-term sediment loss of varying scales exist on most NH beaches, with the exception of Hampton and Seabrook Beaches, which showed more gains than losses (Olson and Chormann, 2016; Olson et al., 2016). Similarly, the northern NH beaches showed minor net shoreward movement (erosion), while Hampton and Seabrook Beaches showed minor net seaward movement (accretion) (Olson and Chormann, 2016; Olson et al., 2016).

A study of potential flooding of the NH coast related to present sea-level and projected sea-level rise was conducted by Ward and Adams (2001). The high tide flooding plus storm surge from a 100-year storm event has the potential to drown some of the low-lying areas in the city of Portsmouth (Figure 1-2), and to completely flood the back-barrier marsh and lower barrier areas in Hampton Beach and Seabrook Beach (Ward and Adams, 2001). These same areas are projected to experience similar inundation on a long-term scale solely due to a hypothetical modeled sea-level rise of 0.6m by 2100 (Ward and Adams, 2001). These projections indicate significant amounts (34-100%) of land area in coastal NH will be below the 10-year and 100-year tidal flood levels, and in serious danger of storm-related flooding (Ward and Adams, 2001). Not only could coastal flooding cause severe damage, but will likely cause severe erosion to the beaches and/or change their locations.

A recent study by the Rockingham Planning Commission (2015) examined the vulnerability of coastal NH communities to inundation resulting from sea-level rise and storm surge. The study found that nearly 20,000 acres (81 km^2) of upland, fresh and tidal wetlands, conservation lands, wildlife habitats, and floodplain area would be inundated under the highest sea-level rise scenario (2m by 2100). Additionally, dozens of critical facilities (fire stations, hospitals, police stations, schools, etc), historical properties, and transportation structures would be endangered by sea-level rise and storm surge (Rockingham Planning Commission, 2015).

CHAPTER 3. METHODS

MONITORING NETWORK

Twenty-four monitoring stations were established on six NH beaches (Figure 3-1 and Table 3-1). At each beach, three to five stations (depending on beach length) were installed approximately equidistant along the length of the beach. At each station, station markers were created at the landward edge of the backshore of the beach, on a seawall or rip rap where possible. The positions of each station marker were measured with the GNSS system (see GNSS Rover Method, below). Stations were monitored over a fourteen-month period, from July 2015 to August 2016.

At twenty-one stations, three to five sediment samples (depending on beach width) were collected during the summer of 2015 to characterize the beach by sediment grain size. The beach profile (a measurement of the elevation of a shore-perpendicular cross-section of the beach) at each station was measured periodically (every 2-8 weeks) to capture seasonal geomorphologic changes. A subset of stations was chosen to be profiled in response to two storm events to capture the effects of and recovery from the storms.

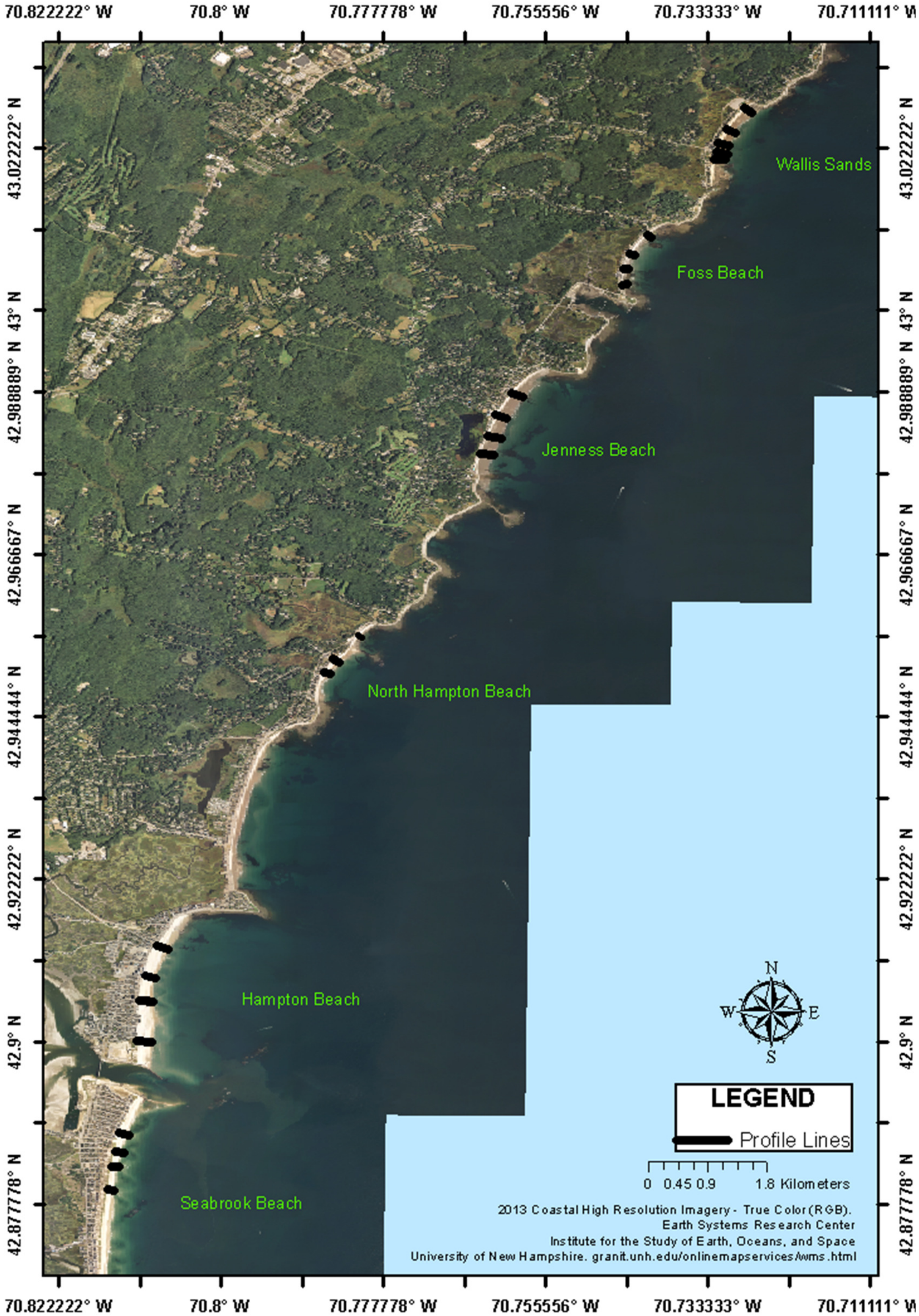

Figure 3-1: Map of profile locations. 2013 coastal 1-ft RBG imagery from NH Granit.

Table 3-1: List of monitoring station names and positions, organized by beach, arranged north to south. The position data refers to the station marker, the established starting point of each profile.

Beach	Station	WGS84 Longitude	WGS84 Latitude	Profile Azimuth (deg)
Wallis Sands	WS01	-70.728419	43.027700	134
	WS02	-70.730850	43.024808	119
	WS03	-70.731936	43.022896	110
	WS04	-70.732358	43.021686	103
	WS05	-70.732485	43.020683	93
Foss Beach	FO01	-70.741658	43.010410	129
	FO02	-70.440804	43.077705	115
	FO03	-70.745054	43.003529	97
	FO04	-70.745096	43.003530	81
Jenness Beach	JN01	-70.760201	42.988735	118
	JN02	-70.762426	42.985771	114
	JN03	-70.763513	42.982850	104
	JN04	-70.763513	42.982850	103
North Hampton Beach	NH01	-70.781288	42.955690	123
	NH02	-70.784663	42.952303	127
	NH03	-70.785804	42.950581	113
Hampton Beach	HA01	-70.808816	42.913074	113
	HA02	-70.810574	42.909014	103
	HA03	-70.811219	42.905535	112
	HA04	-70.811491	42.900153	98
Seabrook Beach	SE01	-70.814044	42.887581	110
	SE02	-70.814486	42.884924	100
	SE03	-70.814054	42.882809	99
	SE04	-70.815567	42.879816	104

BEACH PROFILING

A Global Navigation Satellite System (GNSS) was used to measure beach elevations and construct beach profiles at each station. Each profile measurement was conducted beginning at the station reference marker and extending to the low water line within two hours of low tide, perpendicular to the shoreline. Perpendicularity was maintained during profiling by lining up the reference marker with an established marker (such as a telephone pole) behind the reference point. In total, 133 profiles were measured at the twenty-four stations between July 2015 and August 2016.

GNSS Rover Method

The GNSS rover method utilized an Ashtech ProFlex 500 GNSS receiver recording at 1Hz continuously throughout the survey day. The ProFlex 500 was mounted in a water-proof hard case on a three-wheeled aluminum cart (hereafter referred to as "the rover") (Figure 3-2). An Ashtech Marine Antenna III L1/L2 (PN:700700C, SN: MA16854) was mounted on a fixed aluminum pole on the rover at 1.84m above the ground. Profiles were measured by lining up the antenna pole and the front rover tire with the profile line, with the handle of the rover against the station marker or as close to the marker as possible. The rover was walked at a steady pace from the reference point to the water line, recording the start and end time. The starting and ending point of each profile were recorded using the Garmin GPSMap 76Csx unit (accuracy <10m) to double-check the GNSS profile positions and to relocate stations in the field. The GNSS data was post-processed to reduce position and elevation errors. Subsequently, the profiles were extracted from the day's data (see GNSS Data Post-Processing, below, and a detailed explanation of GNSS Data Post-Processing in Appendix 2).

Figure 3-2: A beach profile being measured using the GNSS rover method at Wallis Sands on 08/03/15.

Storm Response

To assess the impacts of storms, two beaches were monitored before, during, and/or after the passage of storms. Hampton Beach and Seabrook Beach were monitored because they had large sand volumes, and any storm-related changes to the beach were likely to be larger than the uncertainty value (see CHAPTER 4. UNCERTAINTY ANALYSIS). The two storms were chosen because they were two of the few storms that occurred during the study period and they were powerful enough to significantly increase wave heights in the WGOM.

SEDIMENT SAMPLING

Sediment samples were collected for grain size analysis during summer (accretional) conditions along the profile line of twenty-one of the monitoring stations. Samples were taken at three to five locations (depending on beach width) along each profile, extending from the backshore to the low tide swash zone. Three of the samples were taken equidistant from each other, at approximately 25%, 50%, and 75% of the distance along the profile, as determined by pacing. If warranted by the width of the beach or the presence of aeolian dunes, a fourth and/or a fifth sample were taken in the dunes and/or near the seawall. In total, seventy-two sediment samples were collected during summer 2015 and analyzed for grain size statistics. The locations of each sample are given in Appendix 1.

The sediment samples were collected using an 8x20cm graduated PVC pipe to a depth of 10±2cm (or to the level of the underlying gravel, if present). Samples were placed in labeled WhirlPak or Ziploc bags and stored at 5°C until analyzed. Sediment sampling locations were recorded with the handheld Garmin 76SCx GPS unit.

This sampling procedure worked well for the unimodal sandy beaches, however, many NH beaches are bimodal and are composed of sand and gravel (including granules, pebbles, and cobbles). The sampling method likely under-sampled the gravel fraction of the beach sediments. Therefore, results presented here represent the beaches during summer accretional sandy conditions, which vary greatly from winter erosional conditions.

GRAIN SIZE ANALYSIS

Sediment samples were prepared for grain size analysis with a treatment of 30ml of 30% hydrogen peroxide over several days to dissolve any organic material. Samples were then rinsed with deionized water to remove remaining hydrogen peroxide and any salts. Calgon dispersant (sodium hexametaphosphate) was added to each sample to prevent flocculation. Grain size analysis was then conducted using standard sieving and pipetting methods (Folk, 1980). Grain size classification and statistics were determined using the Gradistat Grain Size Analysis Program (v 8.0) (Blott and Pye, 2001). Organic content was estimated by calculating loss on ignition (LOI). Each sample was subsampled, dried in a 50˚C oven overnight, weighed, heated to 450˚C oven for four hours, and then reweighed. Percent LOI for all samples was less than 0.6% by weight, was deemed inconsequential, and are not discussed further. Grain size statistics and LOI value tables are located in Appendix 1.

DATA PROCESSING

<u>*GNSS Data Post-Processing*</u>

A summary of the post-processing procedure for the GNSS data collected during this study is given below. A detailed description is given in Appendix 2.

Differential corrections for the raw GNSS data were obtained from the National Geodetic Survey Continuously Operating Reference Stations (CORS) (National Geodetic Survey, 2016a). The station located in Salisbury, Massachusetts (MASA) was primarily used due to its proximity to the NH coast. When MASA data was not available, the station located at the University of New Hampshire (NHUN) was used. The raw GNSS data were post-processed with the CORS differential correction data using Ashtech's Precise Differential Surveying and Navigation (PNAV) software (Ashtech, 1998). The post-processed data were imported into MATLAB and ArcGIS for analysis (*ArcGIS*, 2014; MathWorks, Inc., 2014).

Development of Beach Profiles

Beach profiles were developed by extracting post-processed position and elevation data from the GNSS file for each station using the start and end times recorded at each station during data collection. The horizontal position data (latitude and longitude) for each profile were imported into ArcGIS for preliminary analysis. These position analyses revealed that the paths of each profile measurement were typically not perfectly straight due to slight variations in the walking path and/or due to the uncertainty of the GNSS data (Figure 3-3). Though these errors tended to be small (<5m), when the cumulative distance (along profile) was calculated, these errors caused the beach profile shape to become distorted, leading to errors in profile analysis. Therefore, each profile line was straightened by generating a vector of evenly spaced (1m) points between chosen starting and ending points for each station, creating an idealized, straight profile line that is perpendicular to the shore (Figure 3-3). Every profile at a station is corrected to the same start and end point, ensuring that the profile lines overlie. The elevations at these new positions were interpolated in MATLAB (Figure 3-4). The corrected position data was then plotted against the interpolated elevation data at 5x vertical exaggeration to create beach profiles. A detailed explanation of these methods is given in Appendix 2, and comparisons of uncorrected and corrected (interpolated) profiles are located in Appendix 3.

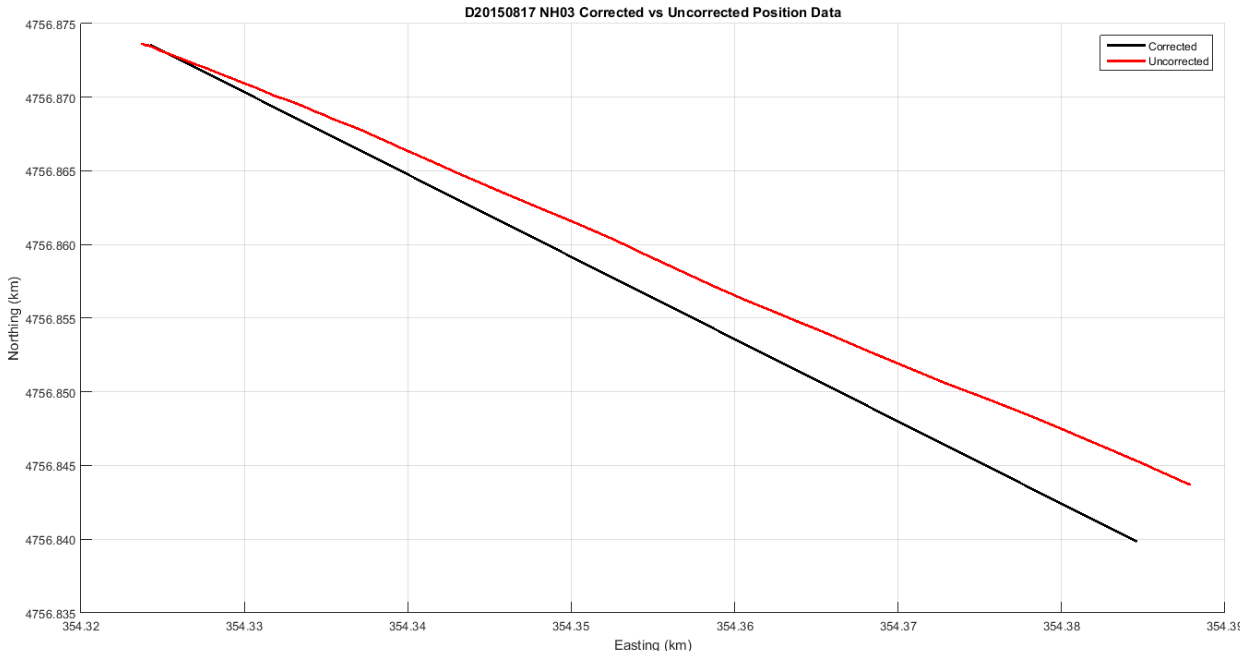

Figure 3-3: Comparison of uncorrected and corrected (interpolated) profile position data from 08/17/15 at North Hampton station NH03. Note that the raw profile position data deviated from the straight profile line by several meters near the end of the profile.

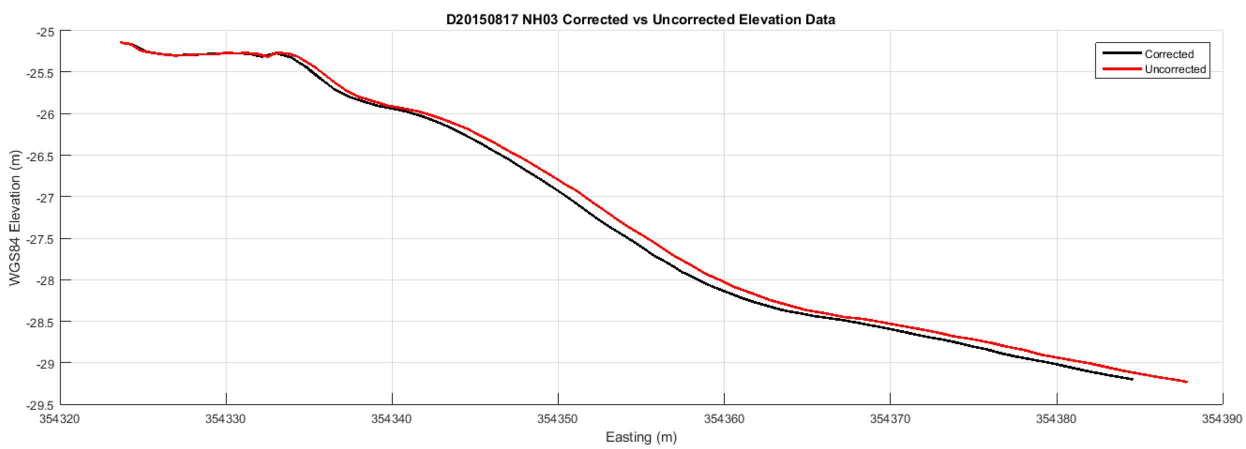

Figure 3-4: Comparison of uncorrected and corrected (interpolated) profile elevation data from 08/17/15 at North Hampton station NH03. Note that the several meter deviation in profile path seen above led to an error in profile elevation and morphology.

Volumetric Changes

The volume of sediment gained or lost (accreted or eroded) from each station between surveys was determined by calculating the area under each beach profile (between the profile and the x-axis, or 0m WGS84 ellipsoidal height). The area under each profile was calculated in MATLAB using the trapezoid method of integration (trapz.m). This method approximates the definite integral of the graph of a function by creating a series of equal width trapezoids under the curve, with each trapezoid extending from the curve to the x-axis (0m WGS84 ellipsoidal height). The area for each trapezoid was calculated, then the area of all the trapezoids were summed, resulting in an approximation of the area under the curve. The area under one beach profile was subtracted from the area of the previous profile taken at that station. The change in area was then multiplied by a 1m width, resulting in a volume change between profile measurements. The volume changes at each station were summed, resulting in the net sediment volume change for each station for the entire study period (July 2015–August 2016).

Due to the fact that profiles measured at each station differed in length by date (due to the height of the tide at the time of profiling), the volume change calculations were limited to the length of the shortest profile measured during the study period at each station.

In order to compare net sediment volume changes between beaches of different widths, sediment volume change values were normalized. The normalized net sediment volume change was calculated by dividing the net sediment volume change at each station by the width of the beach over which that station's profiles were integrated, resulting in values of average volume change per meter of beach width.

CHAPTER 4. UNCERTAINTY ANALYSIS

The uncertainty of using GNSS for beach profiling and measuring the positions and elevations of station markers was evaluated for this study. This examination of uncertainties was done to determine the magnitude and sources of potential errors, so that real changes in field surveys could be accurately identified. This uncertainty analysis was composed of the following:

- Comparison of measured and reported positions and elevations of a geodetic control point;
- Stationary GNSS rover test;
- Mobile GNSS rover test;
- Comparison of three GNSS data processing methods;

For this study, any data that lost satellite coverage, had high RMS errors, or had high PDOP values (poor satellite geometry) was discarded (see GNSS Data Post-Processing).

RESULTS OF ANALYSES

Comparison to Geodetic Control Point

In order to assess the accuracy of the GNSS surveying method and post-processing procedure, the position and elevation of a National Geodetic Survey (NGS) geodetic control point (AB2631) in Portsmouth, NH (Figure 1-2) was measured on 08/09/16 (National Geodetic Survey, 2014). The Ashtech ProFlex 500 and Ashtech Marine Antenna III were used, but the antenna was mounted on a tripod, rather than the rover, to increase stability. The GNSS setup was left stationary over the geodetic control point for two hours. It was assumed for this study that the NGS reported position of the geodetic control point was accurate and absolute.

The measured position data for the two-hour survey was processed as usual (see GNSS Data Post-Processing, above), with the exception that the elevation and position data were converted to NAD83 in VDatum (NOAA, 2015), resulting in latitude, longitude, and ellipsoidal height for comparison with the NGS reported position and elevation.

The mean and standard deviation of the elevation differences between the Ashtech measured elevation and the NGS reported elevation were 11.3±6.8cm for the two-hour period. The mean and standard deviation of the position differences between the Ashtech measured position and the NGS reported position were 108.8±3.1cm. The large uncertainty in the measured position is likely to due to a discontinuity in the receiver's lock on a satellite's signal (cycle slip), visible in Figure 4-1 as several groups of points.

The raw RINEX file of the GNSS data collected during the survey was also submitted to NOAA's Online Positioning User Service (OPUS) (National Geodetic Survey, 2016b). OPUS uses the NGS CORS network to compute high-accuracy National Spatial Reference System coordinates. The horizontal position calculated by OPUS for the survey was within 2.3cm of the horizontal position data reported for the AB2631 control point, and the elevation data calculated by OPUS was within 5.4cm of the NGS reported elevation.

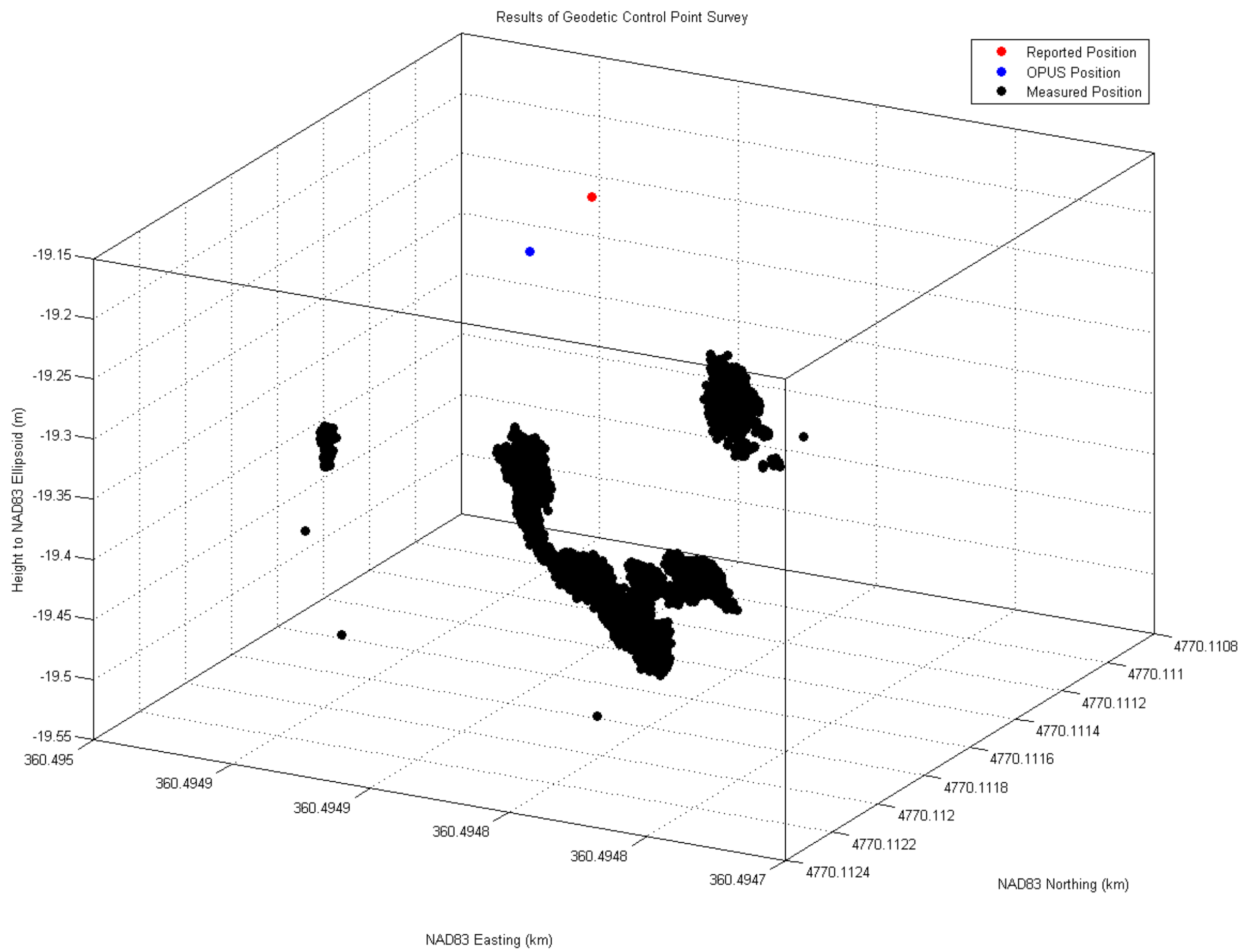

Figure 4-1: Results of the survey of the geodetic control point for NGS control point AB2631 (Portsmouth, NH), measured on 08/09/16 for two hours. Measured results computed by OPUS indicate horizontal position were within 2.3cm horizontally and within 5.4cm vertically of the position reported by NGS. The mean and standard deviation of the differences between the Ashtech measured elevations and the NGS reported elevation were 11.3±6.8cm. The mean and standard deviation of the differences between the Ashtech measured position and the NGS reported position were 108.8±3.1cm. This large uncertainty in position is likely due to cycle slips in the GNSS satellite data, visible as several groups of points.

<u>*Stationary GNSS Test*</u>

The precision of the GNSS rover unit while stationary was evaluated by setting up the Ashtech ProFlex 500 and Ashtech Marine Antenna III on the rover, with the wheels of the rover secured in place by cinderblocks. The rover was left stationary in this configuration for four hours, interrupted only to change the battery in the Ashtech, but the rover itself was not moved during the battery change. The test was conducted at the University of New Hampshire Coastal and Ocean Mapping facility on 05/07/16. The survey data was post-processed with the UNH CORS (NHUN) station data in PNAV. The

NHUN station was used due to its proximity to the testing site. The only difference in the post-processing method from the rover survey processing method was that the stationary survey elevation data was not converted to MLLW in VDatum, but left relative to the WGS84 ellipsoid.

The uncertainty in the position measurements was determined by calculating the difference in position of each data point from the mean position during the survey (Figure 4-2). The mean WGS84 position was calculated in MATLAB (meanm.m). Both the mean WGS84 position and the measured WGS84 positions were converted to UTM Northing and Easting coordinates (wgs2utm.m) (Schimel, 2011). Then, the distance of each data point from the mean position was calculated using the Pythagorean Theorem, then plotted against the survey time (Figure 4-2). The mean and standard deviation of the distance of each data point from the mean measured position was 0.78±0.6cm over the four-hour period.

The precision in the elevation measurements was determined by calculating the mean and standard deviation of the differences in the elevation data from the mean elevation in MATLAB. The mean and standard deviation of the elevation differences from the mean were 10.2±9.5cm (Figure 4-3). However, the mean elevation drifted -2.2cm (as determined by a linear regression line) over the four-hour period.

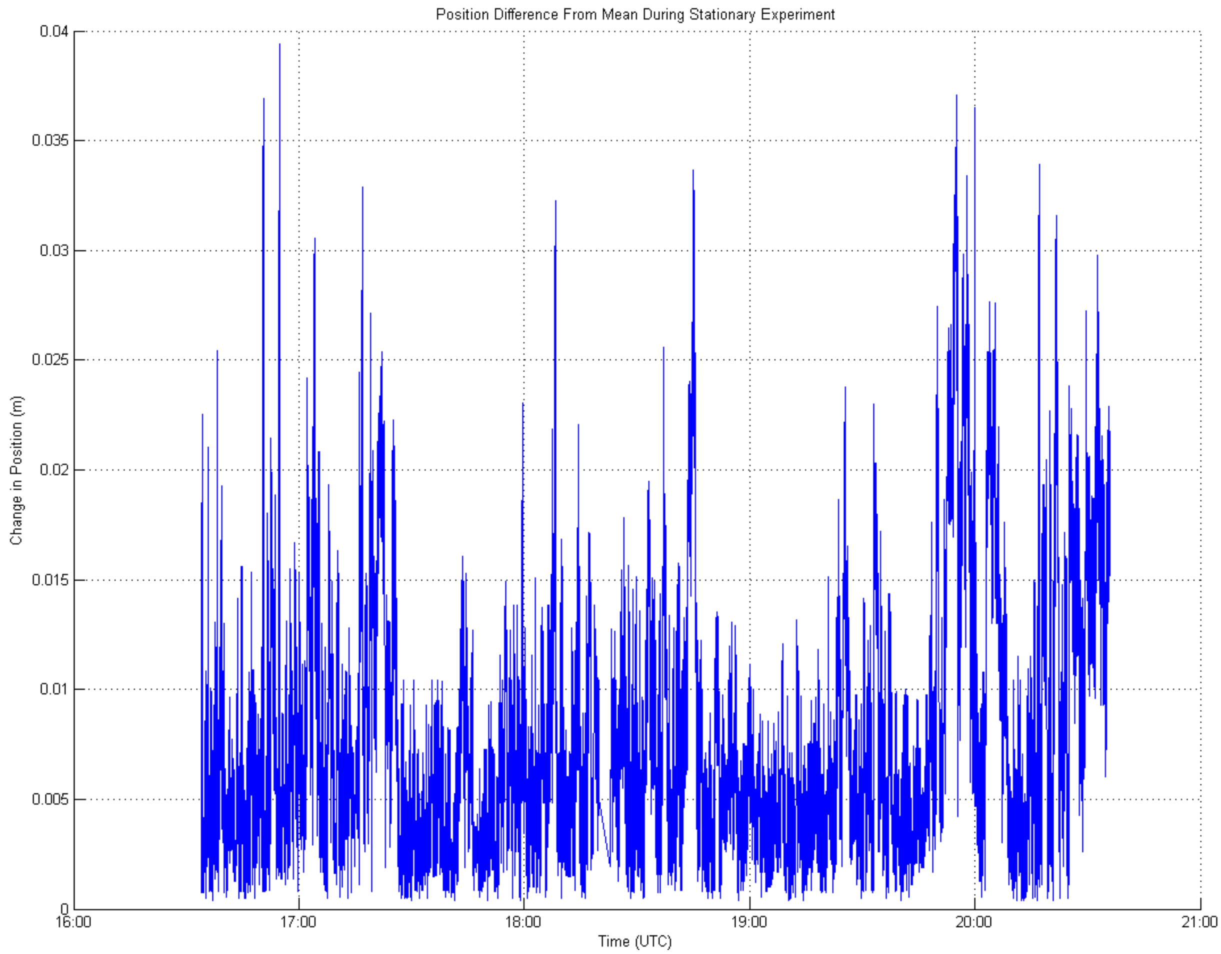

Figure 4-2: Rover position over the four-hour stationary test plotted as position change of each data point from the mean position (WGS84 latitude and longitude) during the four-hour stationary GNSS test. The mean and standard deviation in the differences in horizontal position from the mean position were 0.78±0.6cm over the four-hour period.

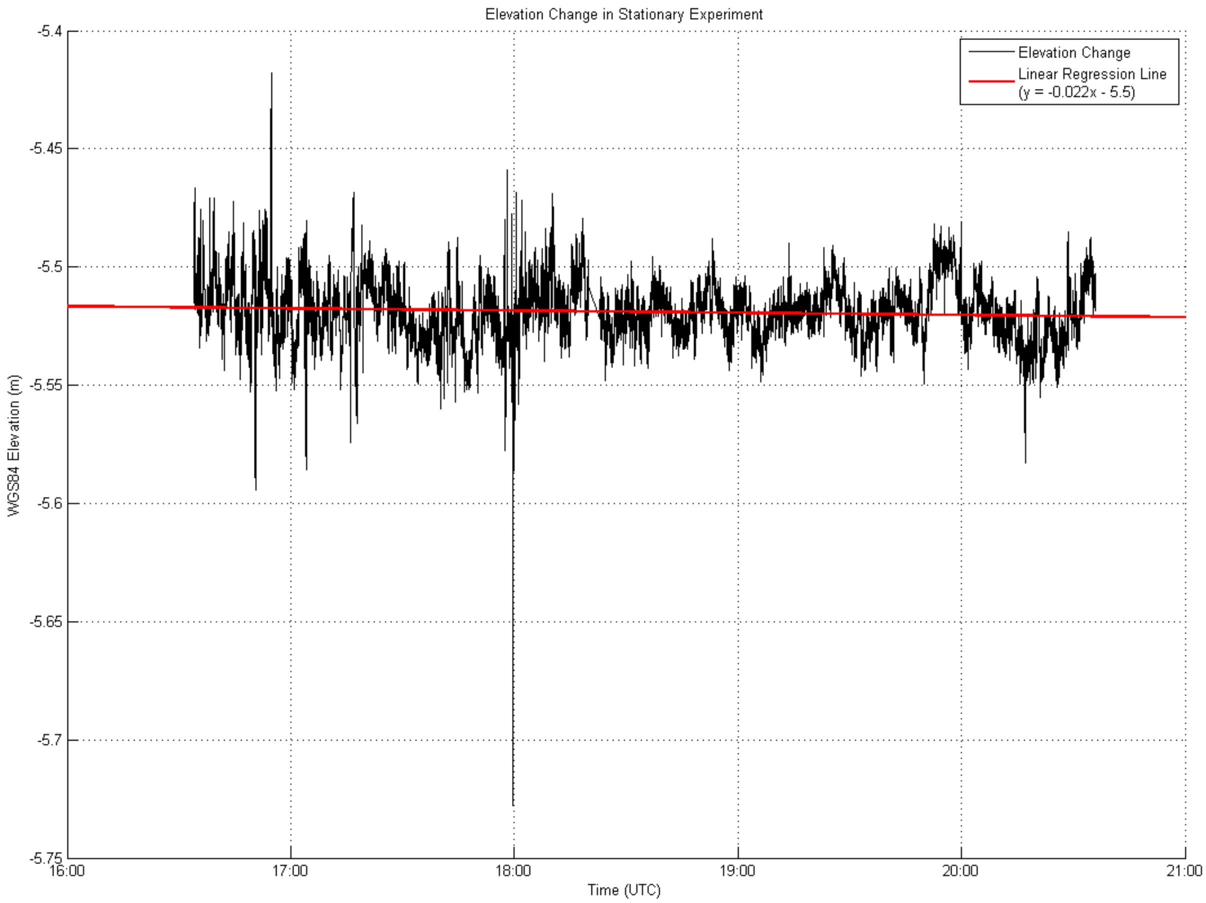

Figure 4-3: Rover elevation over the four-hour stationary test, (relative to the WGS84 ellipsoid) during the stationary GNSS test. The mean and standard deviation in the differences in the measured elevations from the mean elevation were 10.2±9.5cm plus a drift of -2.2cm over the four-hour period.

Mobile GNSS Test

The precision of the position and elevation measurements of the GNSS rover unit while in motion was tested by surveying the same section of an asphalt road located on the University of New Hampshire campus on three different days (05/07/16, 05/11/16, and 05/13/16). The rover was used to survey the yellow dividing line in the center of the road, ensuring that the survey was conducted on a hard, stable surface along the same line each day. Due to the slight differences in walking speeds between surveys, each survey measured different points along the line. This prevented a statistical analysis of the mean and standard deviation of each point in each survey, therefore, a visual assessment of the precision in position and elevation was performed using a random subset of approximately 20 points.

The position data for each of the three surveys were converted from WGS84 latitude and longitude to UTM Easting and Northing coordinates in MATLAB (Figure 4-4). The visual evaluation of the position data suggests that no data point was greater than 10cm from the others perpendicular to the direction of travel. As a conservative estimate, 20cm was chosen as the horizontal uncertainty.

The elevation data for each of the three surveys was not converted to MLLW, but left relative to the WGS84 ellipsoid. The cumulative distance traveled during each survey was plotted against the elevation data for visual comparison (Figure 4-5). The visual evaluation of the data suggests that no data point was more than 15cm different in elevation in any given area.

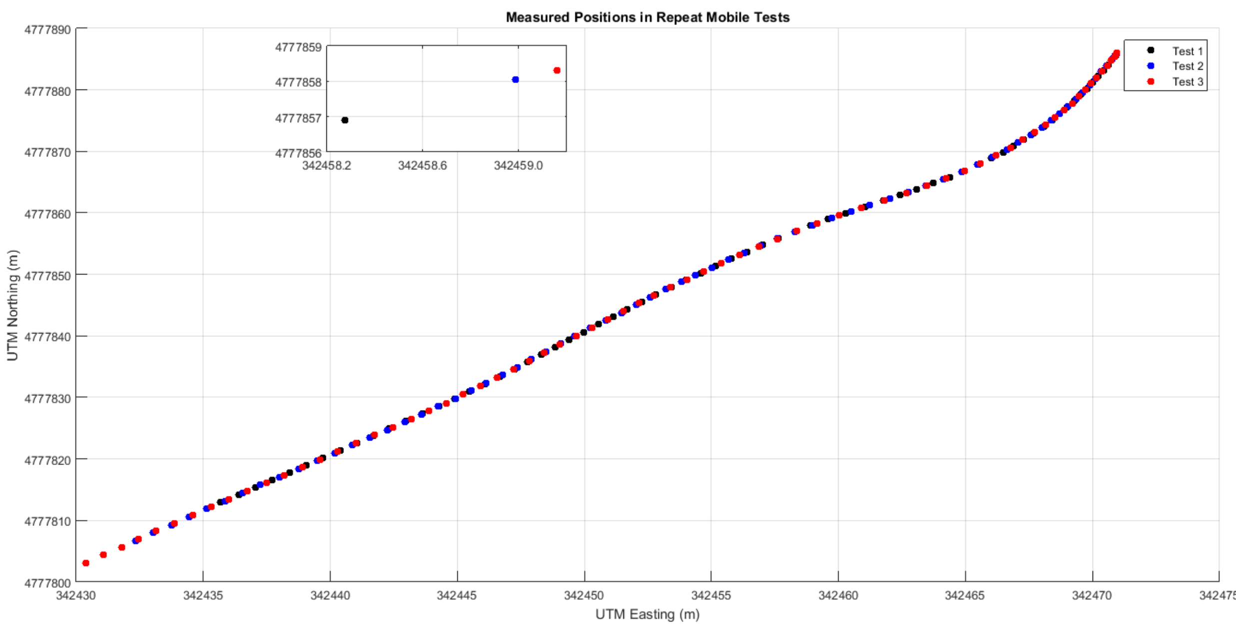

Figure 4-4: Position of the rover during the mobile test. The test indicates that while in motion, the precision in the horizontal position was ±20cm. Inset is same lines, zoomed in.

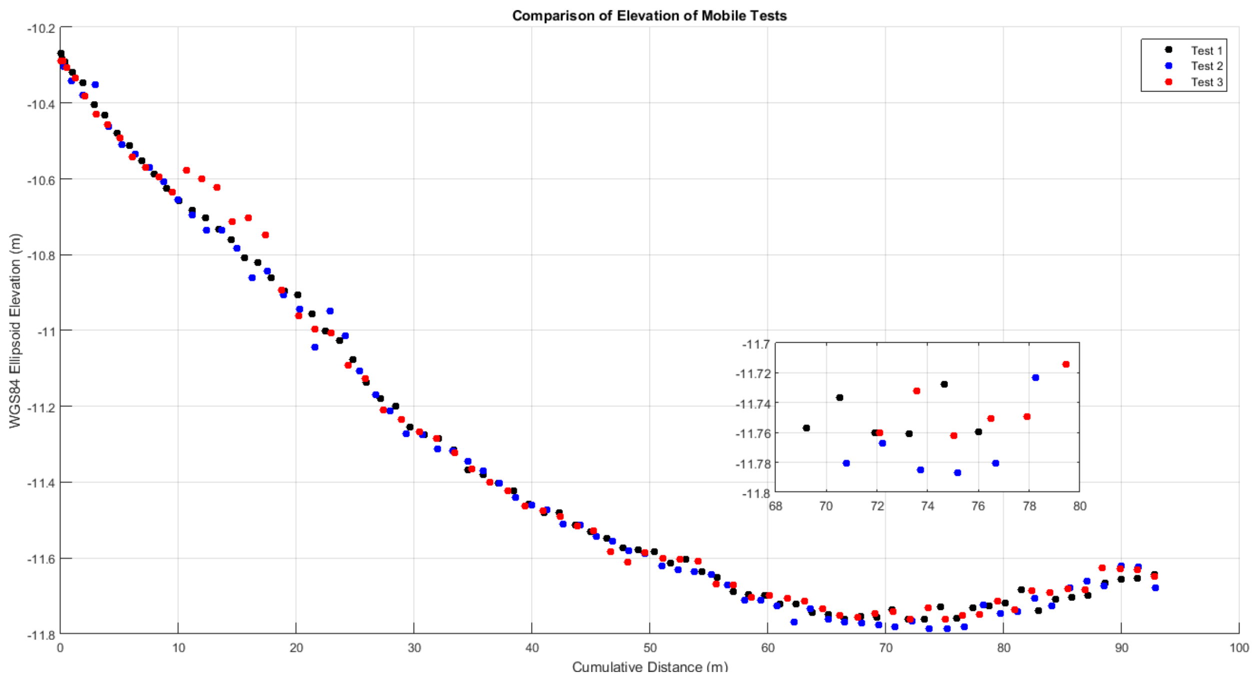

Figure 4-5: Elevation of the rover during the mobile test. The test indicated that while in motion, the precision in the elevation was ±15cm. Inset is same lines, zoomed in.

<u>Comparison of GNSS Data Processing Methods</u>

Three different methods of processing the GNSS data were compared to determine the most precise and efficient processing method. The comparison included a Real-Time Kinematic (RTK) correction method (Networked Transport of RTCM via Internet Protocol [NTRIP] streaming method) (Federal Agency for Cartography and Geodesy of Germany, 2005), and two post-processing methods (setting up a local base station and using the MASA CORS station).

The tests were conducted at Wallis Sands (WS01) on 07/06/15, and Hampton Beach (HA01) on 07/07/15. The profile for each station was measured using the Ashtech ProFlex 500 and Ashtech Marine antenna III mounted on the rover. The local base station was a Trimble 5700 GPS receiver, mounted on a tripod, and left recording for the entire survey (~4 hours). The raw GNSS data was corrected in real-time using the RTK NTRIP method, and post-processed in PNAV with the MASA CORS data and the Trimble base station data.

When comparing the three GNSS processing methods, it was assumed that the local Trimble base station-corrected measurements were the most accurate, as that base station was the closest to the field site. The MASA CORS station is located in Salisbury, Massachusetts, ~9km from Hampton Beach and ~23km from Wallis Sands. The Trimble base station was set up directly behind the station reference marker at each beach, within 200m of the rover during the surveys.

The mean and standard deviation of the elevation differences at each point between the CORS post-processed data and the Trimble post-processed data, and between the NTRIP RTK-processed data and the Trimble post-processed data were calculated in MATLAB.

The mean and standard deviation of the elevation differences between the CORS post-processed data and Trimble post-processed data for the Wallis Sands test were 2.48±0.5cm, and the mean and standard deviation of these elevation differences between the NTRIP RTK-processed data and the Trimble post-processed data at Wallis Sands were 195±86cm. The huge error in the NTRIP data is the result of a loss of cell reception during the survey, causing a loss of differential GNSS corrections data (Figure 4-6).

The mean and standard deviation of the elevation differences between the CORS post-processed data and the Trimble post-processed data for the Hampton Beach test were 5.26±5.0cm, and the mean and standard deviation of the elevation differences between the NTRIP RTK-processed data and the Trimble post-processed data at Hampton Beach were 3.91±11.7cm. The large standard deviation in the NTRIP data was of unknown origin, but is visible in Figure 4-7 as a divergence of the NTRIP elevation data from the Trimble and CORS elevation data along the steep beach face.

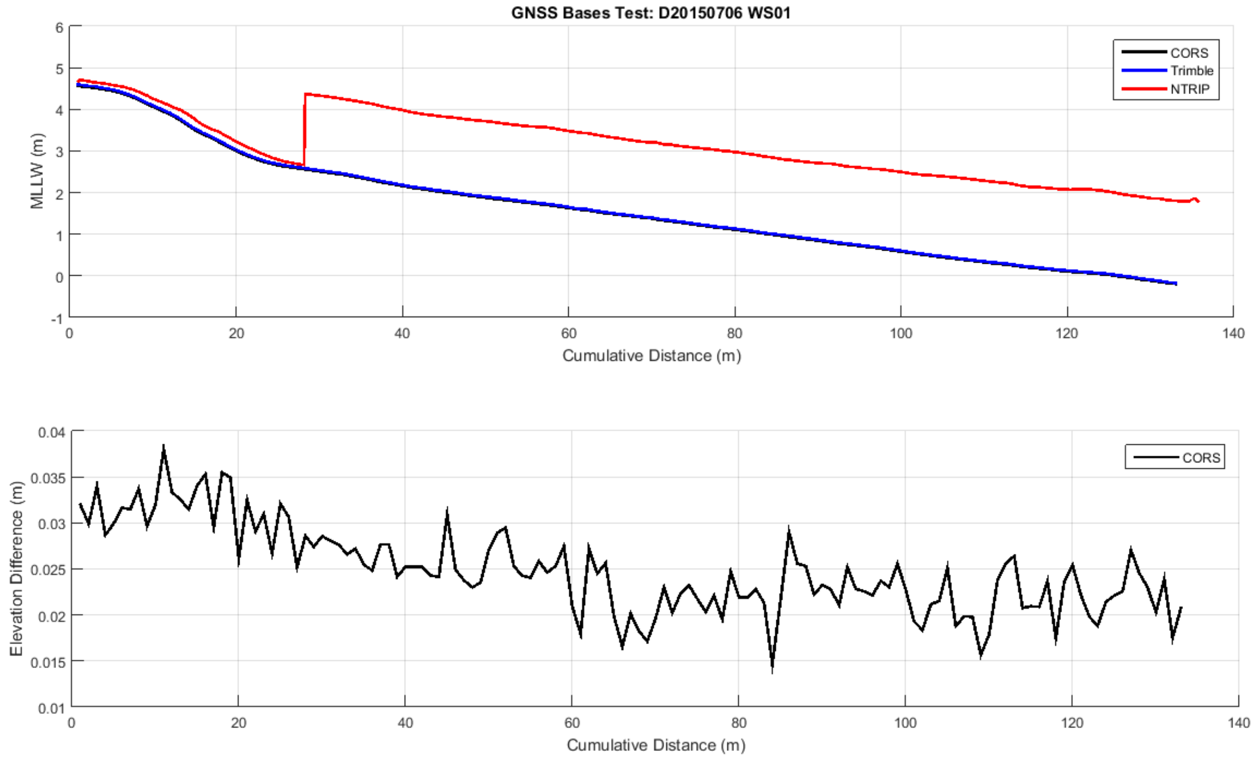

Figure 4-6: Comparison of the precision of the three GNSS processing techniques (post-processed with CORS base station, post-processed with the local Trimble base station, and RTK processed with NTRIP software) at Wallis Sands WS01 on 07/06/15. Top panel is the plot of cumulative distance vs elevation for each measured profile, bottom panel is the difference in elevation of the CORS method from the Trimble method (NTRIP method was removed due to huge error). The mean and standard deviation of the elevation differences between the CORS method and the Trimble method were 2.48±0.5cm, and 195±86cm between the NTRIP method and the Trimble method.

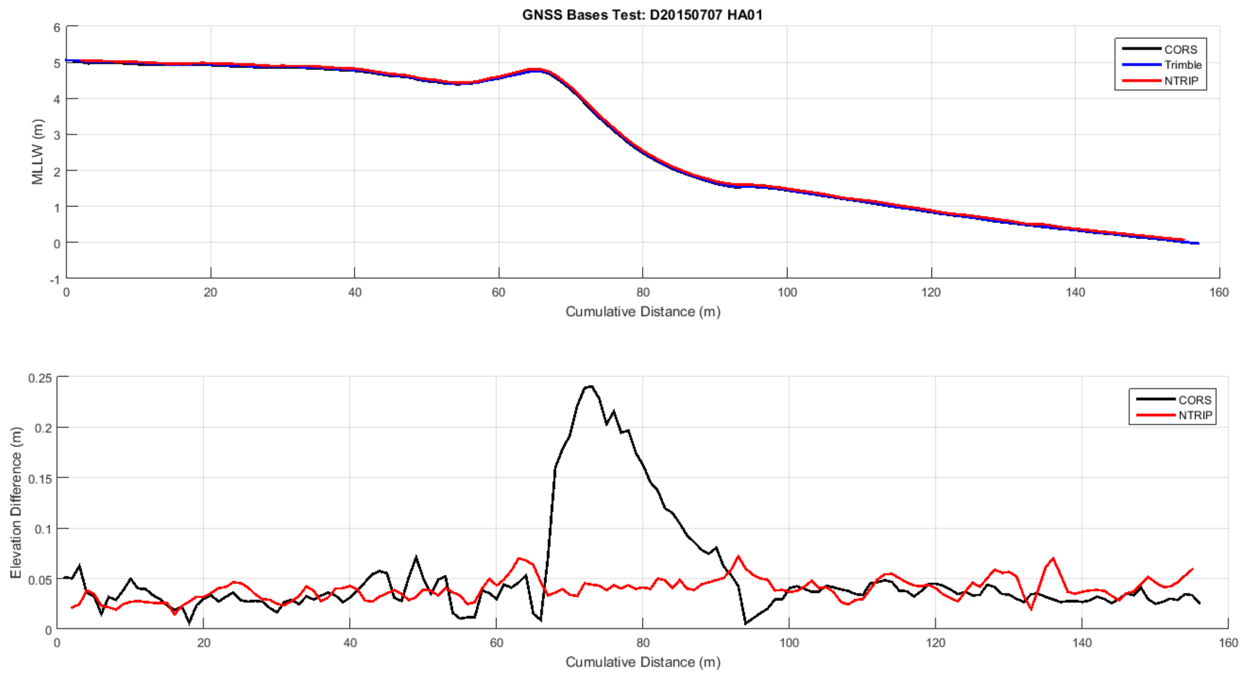

Figure 4-7: Comparison of the precision of the three GNSS processing techniques (post-processed with CORS base station, post-processed with the local Trimble base station, and RTK processed with NTRIP software) at Hampton Beach HA01 on 07/07/15. Top panel is the plot of cumulative distance vs elevation for each measured profile, bottom panel is the difference in elevation of the CORS and NTRIP methods from the Trimble method. The mean and standard deviation of the elevation differences between the CORS method and the Trimble method were 5.26±5.0cm, and 3.91±11.7cm between the NTRIP method and the Trimble method.

UNCERTAINTY IN VDATUM CONVERSIONS

In addition to errors associated with the use and processing of the GNSS data, there was uncertainty introduced by the coordinate transformations and calculations. The National Ocean Service (NOS) reports that transformations between ellipsoidal and NAD83 coordinate systems using the GEOID12A model in VDatum, from NAD83 to Mean Sea-level (MSL), from MSL to Mean Lower Low Water (MLLW) in the Gulf of Maine region results in a maximum cumulative uncertainty of 13.4cm (NOAA, 2015).

SUMMARY

The tested GNSS data post-processing methods included one Real-Time Kinematic method and two post-processing methods. The RTK method (NTRIP) was prone to errors due to loss of cell phone reception. The local Trimble base method was assumed to be the most accurate, but the amount of equipment required by this method significantly complicated field work logistics. Therefore, the GNSS data was post-processed using CORS base stations for this study.

The results of the uncertainty analysis indicated that elevation is measurable within ±15cm and that horizontal position is measurable within ±20cm. These values are the horizontal and vertical uncertainty assessed during the mobile rover test. These values were chosen because the mobile rover test most closely represents the measurements made in the field. For the most part, the results of the other tests support this assumption and these values. The horizontal uncertainty measured during the comparison to the geodetic control point (108.8±3.1cm) suggests that the loss of satellite coverage could cause horizontal uncertainty over 100cm, however, the interpolation method used during post-process would correct such errors. Overall, the uncertainty in the data was within the acceptable limits for the purposes of this research (Table 4-1).

Sediment volume changes between surveys were determined by calculating the change in area under two profiles, which were then multiplied by 1m (width), resulting in a sediment volume. The resulting sediment volumes are directly affected by the vertical uncertainty of each profile measurement (±15cm). To account for the vertical uncertainty in the sediment volume calculations, the vertical uncertainty (±15cm) was multiplied by the average profile length of 100m and the 1m sediment volume width, resulting in an uncertainty in the sediment volume calculations of ±15m^3. Therefore, any sediment volume change less than ±15m^3 was considered to be within the limits of the uncertainty, and is not considered a measurable change. Only sediment volume changes greater than ±15m^3 are considered to be true, measurable changes. In order to compare net sediment volume changes between beaches of different widths, net sediment volume change values were normalized by the width of the beach at each station, resulting in an average volume change for every meter of beach width. Given that the uncertainty in sediment volume changes is $15m^3$, the normalized sediment volume change uncertainty is this value divided by the average beach width of 100m, resulting in a normalized volume change uncertainty threshold of $\pm 0.15m^3/m$ for normalized sediment volume change values.

Table 4-1: Summary of uncertainties in horizontal and vertical positions from the uncertainty analysis tests, conversions, and measurements.

Uncertainty Test/Type	Uncertainty in Horizontal Position (cm)	Uncertainty in Vertical Position (cm)
Comparison of measured and reported positions of geodetic control point	2.3 (reported vs OPUS) 108.8±3.1 (reported vs measured)	5.4 (reported vs OPUS) 11.3±6.8 (reported vs measured)
Stationary GNSS rover test	0.78±0.6	10.2±9.5 -2.2 (downward drift)
Mobile GNSS rover test	±20	±15
Comparison of GNSS data processing methods (Wallis Sands)		2.48±0.5 (CORS vs Trimble) 195±86 (NTRIP vs Trimble)
Comparison of GNSS data processing methods (Hampton Beach)		5.26±5.0 (CORS vs Trimble) 3.91±11.7 (NTRIP vs Trimble)
VDatum conversions		13.4 (National Ocean Service, 2016)

CHAPTER 5. RESULTS

The results of the study are organized by beach, moving from north to south (Figure 1-2, Table 3-1). Reported results include a simplified beach type classification, measured beach profiles, sediment grain size distributions, net volumetric sediment changes at each station over the survey period, and wind and wave data during two storm events (see STORM RESPONSE for analysis of storm effects). Full grain size statistics for each sediment sample and detailed analyses of beach morphology are given in Appendices 1 and 4, respectively.

Beaches were classified based on beach morphology and surf zone dynamics, after Wright and Short (1984). The Wright and Short classification categorizes beaches into three basic types: reflective, intermediate, and dissipative, and identified several trends relating profile shape to grain size and wave energy. Dissipative beaches have flat to concave beach profiles that cause decay of wave energy over a wide swash zone. Dissipative profiles are generally found on beaches with high wave energy and fine-grained sediments (sandy), and are comparable to storm or winter profiles on seasonal beaches. Intermediate beaches have steeper profiles than dissipative beaches, but less well-developed berms than reflective beaches, or can be beaches which are reflective at high tide and dissipative at low tide. Intermediate profiles generally have the most mobility, and are related to changeable wave energy, medium-grained sediments, and meager sediment supplies. Reflective profiles are found on beaches with low-steepness waves (surging and collapsing breakers) and coarse-grained sediments (sand and gravel). Reflective beaches often have large beach cusps, or a high straight berm with a steep beach face under low energy conditions (Wright and Short, 1984).

Beaches were further classified based on the Wentworth grain size scale for sediment samples (Wentworth, 1922). Full grain size analyses were conducted on summer 2015 samples (which were collected once at several locations along 22 profiles), while visual field observations and photographs supplemented classification during the fall and winter of 2015, and the spring and summer of 2016.

WALLIS SANDS

Wallis Sands is approximately 1.3km in length and 0.13km in width at low tide. The beach is protected by bedrock headlands at both ends and by bedrock outcrops offshore and is backed by an extensive salt marsh system, suggesting that it is a welded barrier (Figure 1-2, Figure 5-1, Figure 5-2). A ~100m stone groin separates the northernmost station (WS01) from the southern four stations (WS02–WS05).

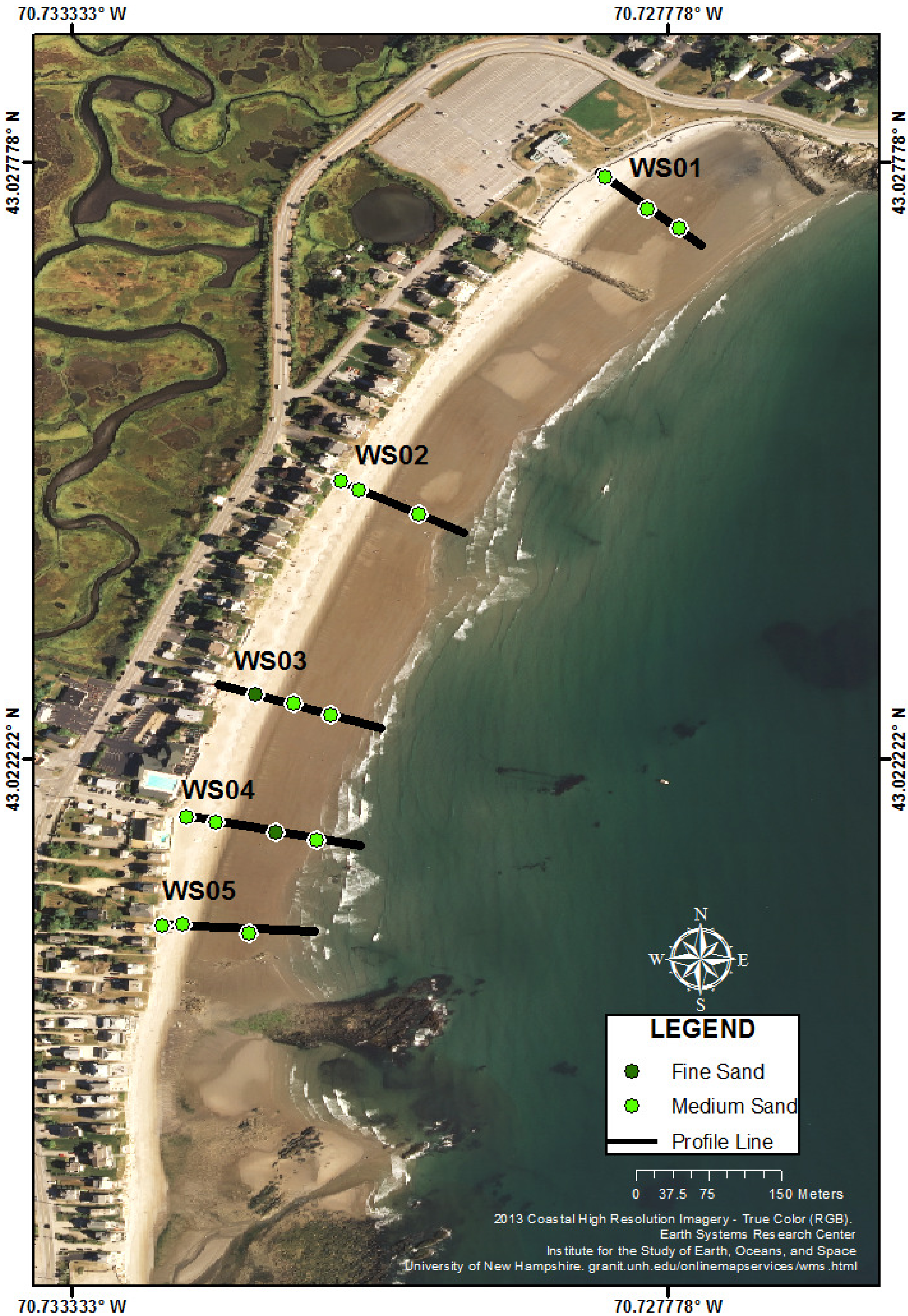

Figure 5-1: Location map of stations on Wallis Sands, New Hampshire. Black lines are the profile locations while dots represent summer 2015 sediment sample locations. Sediment size classification (after Wentworth, 1922) are shown by dot color.

Figure 5-2: Photos of Wallis Sands taken on 06/20/15 (top) and 01/14/16 (bottom) at station WS02, facing south. Note the loss of the small berm and the presence of gravel in January.

Beach Profiles

Beach profiles measured during the study period reveal a complexity in erosion and accretion patterns, both temporally and spatially (Figure 5-3 and Figure 5-4). However, some clear trends became apparent throughout the study. For example, stations WS01, WS03, and WS05 accreted vertically between 07/06/15 and 10/25/15, then eroded between 10/25/15 and 04/02/16. Additionally, the northern central station (WS02) and the southern central station (WS04) had well developed berms during July and August of 2015, which eroded entirely by 10/25/15. The northernmost station (WS01) experienced nearly 1m of vertical erosion between 01/14/16 and 04/02/16, while the other stations experienced much less erosion during the same period. In general, after 10/25/15, the entire beach became concave without a berm. The profile morphology changed very little until 07/22/16. At this time, the beach began to show signs of recovery, including the rebuilding of the berm at the northernmost (WS01), central (WS03), south central (WS04), and southernmost (WS05) stations. Most of the profiles (except WS02) accreted between 04/02/16 and 07/22/16, although only the southernmost station exceeded its summer 2015 elevation level.

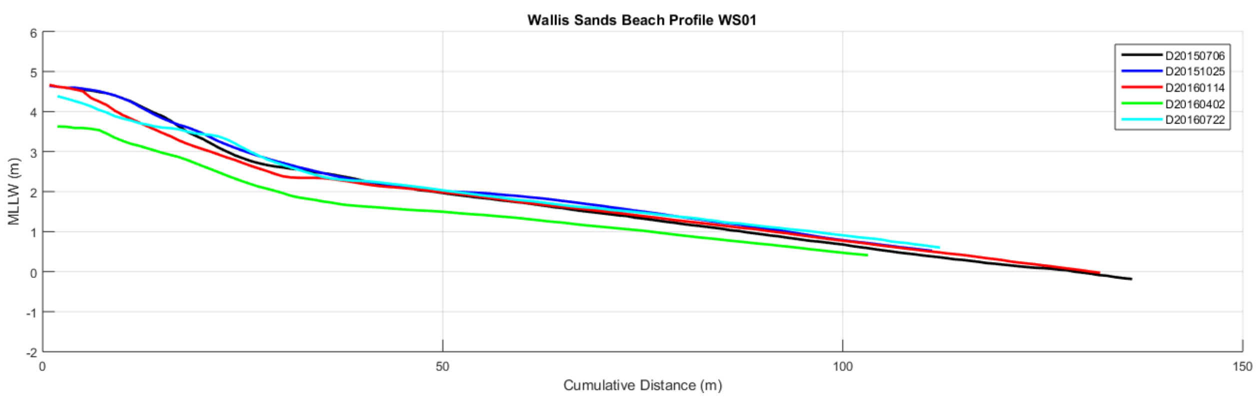

Figure 5-3: Beach profiles at the northernmost station on Wallis Sands. Survey dates for each profile are displayed in the legend, with dates formatted as "D"YYYYMMDD. Profile color corresponds with date of survey.

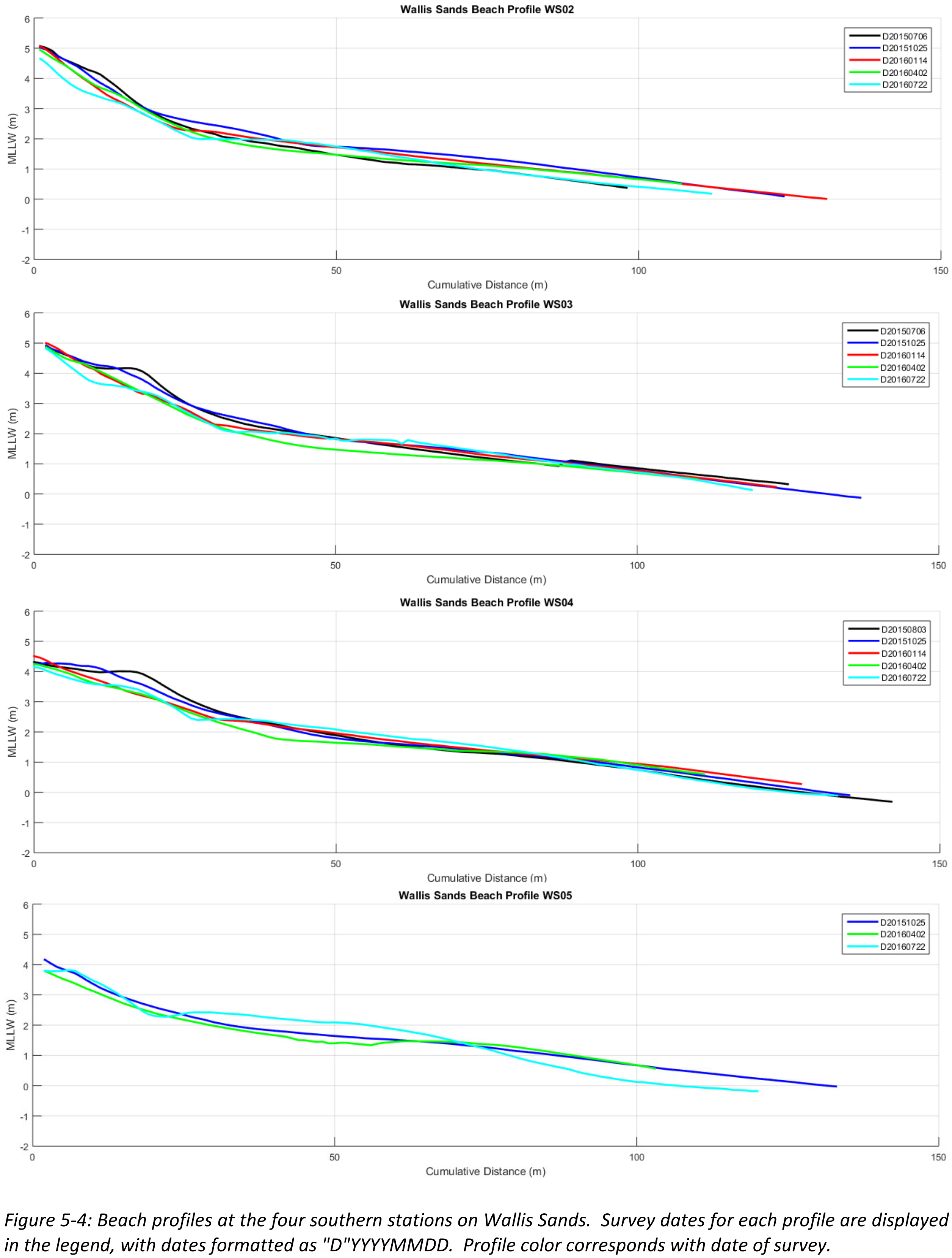

Figure 5-4: Beach profiles at the four southern stations on Wallis Sands. Survey dates for each profile are displayed in the legend, with dates formatted as "D"YYYYMMDD. Profile color corresponds with date of survey.

<u>*Sediment Volume Change*</u>

Over the study period, all five Wallis Sands stations had net volume changes within the uncertainty threshold (Figure 5-5). However, station volume changes between individual surveys was often much greater than net volume changes suggested. For example, the northernmost station (WS01) underwent only small sediment volume changes (<20m^3) between 07/06/15 and 01/14/16, but experienced 50.5m^3 of erosion between 01/14/16 and 04/02/16, and then accreted 55.9m^3 of sediment between 04/02/16 and 07/22/16, resulting in nearly no net volume change over the whole study period (Appendix 4).

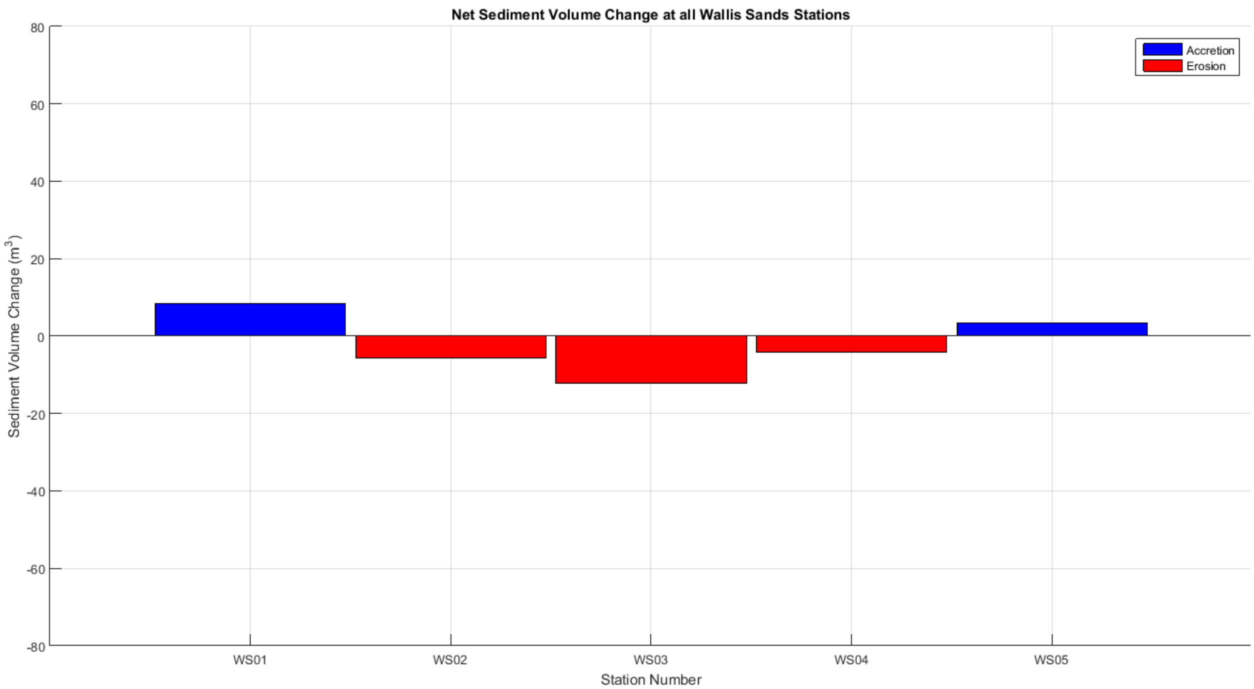

Figure 5-5: Net sediment volume change at the five Wallis Sands stations from July 2015 – July 2016. Blue bars represent accretion and red bars represent erosion.

<u>*Sediment Grain Size*</u>

Sediment samples were collected from three to four sites along every profile at Wallis Sands between June and August of 2015 (Table 5-1, Appendix 1). Most samples were unimodal and moderately to moderately well sorted, with the southern three stations (WS03, WS04, and WS05) more well sorted than the northern two stations. Most samples were composed of slightly granular fine or medium sand, however there were no clear trends in grain size along or across the beach during summer conditions

(Table 5-1). During the fall and winter of 2015, field observations suggest a coarsening of sediment grain size and an increase in gravel population along the lower beach (Figure 5-2).

Table 5-1: Location, textural group, sediment name, and sorting of samples from Wallis Sands, collected summer 2015. Abbreviations include Sl. For Slightly and Mod. for Moderately.

Sample Number	Latitude	Longitude	Sample Collected	Textural Group %GSM from Gradistat	Sediment Name %GSM and Mode in Wentworth Scale	Classification Mean Phi Size	Sorting from Gradistat
WS01A	43.027650	-70.728350	20150610	Sl. Gravelly Sand	Sl. Granular Fine Sand	Medium Sand	Poorly Sorted
WS01B	43.027350	-70.727967	20150610	Sl. Gravelly Sand	Sl. Granular Medium Sand	Medium Sand	Mod. Sorted
WS01C	43.027167	-70.727667	20150610	Sl. Gravelly Sand	Sl. Granular Fine Sand	Medium Sand	Mod. Sorted
WS02A	43.024817	-70.730817	20150610	Sl. Gravelly Sand	Sl. Granular Medium Sand	Medium Sand	Mod. Well Sorted
WS02B	43.024733	-70.730650	20150610	Sl. Gravelly Sand	Sl. Granular Coarse Sand	Medium Sand	Mod. Well Sorted
WS02C	43.024500	-70.730100	20150610	Sl. Gravelly Sand	Sl. Granular Medium Sand	Medium Sand	Mod. Sorted
WS03A	43.022817	-70.731617	20150706	Sl. Gravelly Sand	Sl. Granular Fine Sand	Fine Sand	Mod. Well Sorted
WS03B	43.022733	-70.731267	20150706	Sl. Gravelly Sand	Sl. Granular Medium Sand	Medium Sand	Mod. Sorted
WS03C	43.022633	-70.730917	20150706	Sl. Gravelly Sand	Sl. Granular Fine Sand	Medium Sand	Mod. Well Sorted
WS04A	43.021633	-70.731983	20150803	Sl. Gravelly Sand	Sl. Granular Medium Sand	Medium Sand	Mod. Well Sorted
WS04B	43.021533	-70.731433	20150803	Sl. Gravelly Sand	Sl. Granular Fine Sand	Fine Sand	Mod. Well Sorted
WS04C	43.021467	-70.731050	20150803	Sl. Gravelly Sand	Sl. Granular Medium Sand	Medium Sand	Mod. Well Sorted
WS04D	43.021683	-70.732267	20150803	Sl. Gravelly Sand	Sl Pebbly Medium Sand	Medium Sand	Mod. Well Sorted
WS05A	43.020667	-70.732483	20150610	Sand	Medium Sand	Medium Sand	Mod. Well Sorted
WS05B	43.020683	-70.732300	20150610	Sl. Gravelly Sand	Sl. Granular Medium Sand	Medium Sand	Mod. Well Sorted
WS05C	43.020600	-70.731683	20150610	Sl. Gravelly Sand	Sl. Granular Medium Sand	Medium Sand	Mod. Well Sorted

FOSS BEACH

Foss Beach is a narrow, welded barrier beach separated from a back-barrier marshland by a large (~5m high) anthropogenic berm composed of gravel and fronted by riprap (Figure 5-6 and Figure 5-7). Foss Beach is bound by headlands to the north and south, and bedrock outcrops are visible offshore in aerial photographs. The beach is often completely covered by water during high tides and storms, and waves frequently break directly on the riprap.

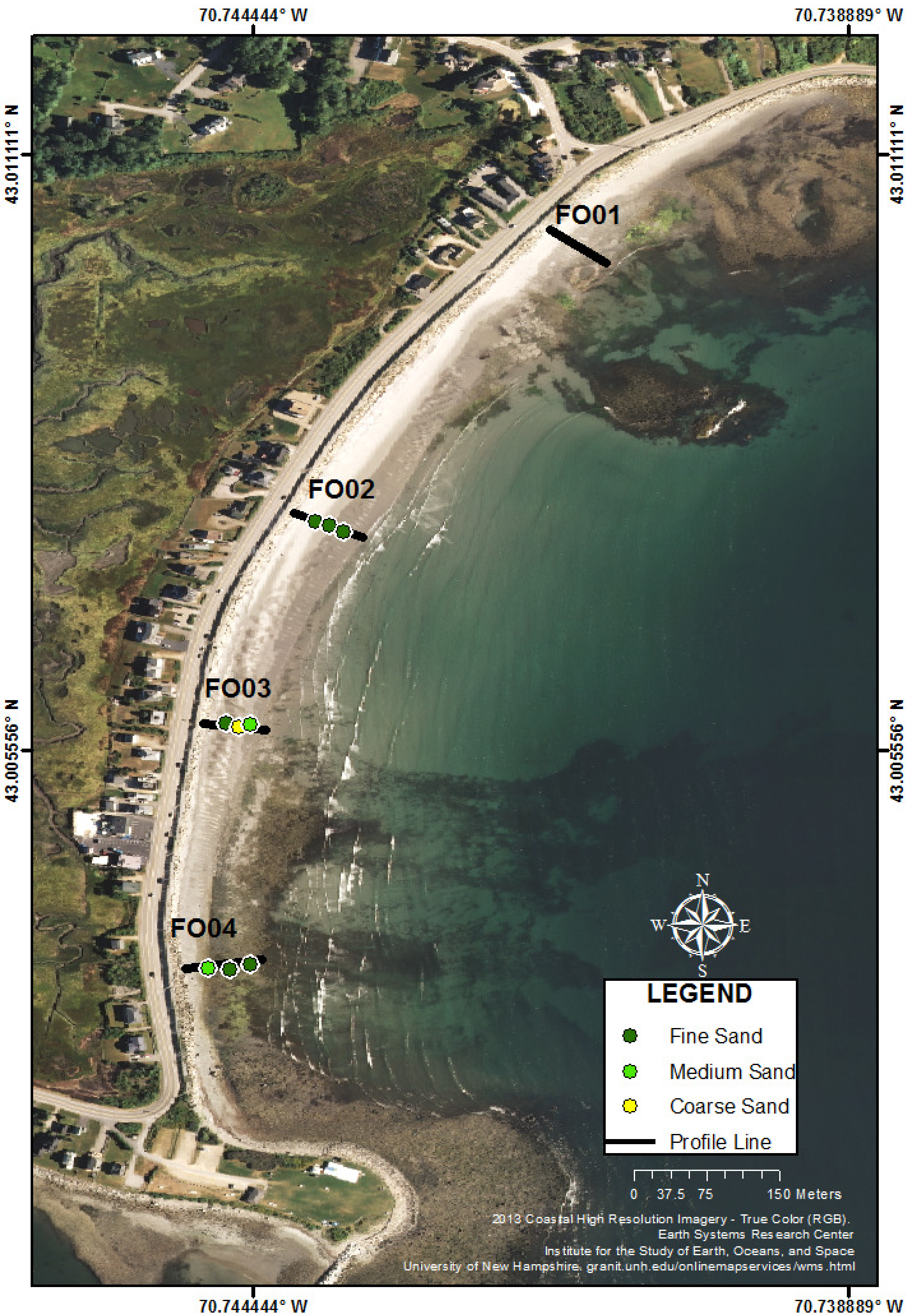

Figure 5-6: Location map of stations on Foss Beach, New Hampshire. Black lines are the profile locations while dots represent summer 2015 sediment sample locations. Sediment size classification (after Wentworth, 1922) is shown by dot color. The profile line without sediment information was established after the summer 2015 sediment sampling.

Figure 5-7: Photos of Foss Beach at station FO02, looking south on 07/18/15 (top) and on 11/08/15 (bottom). Note the large gravel and riprap berm on the upper beach, the sandy lower beach, and the high gravel population on 11/08/15 on the lower beach.

Beach Profiles

Foss Beach underwent major changes in elevation and sediment volume over the study period. Foss Beach tended to transition from a higher-elevation flat beach during the summer to a lower-elevation concave beach during the fall, winter, and spring (Figure 5-8 and Figure 5-9). The two northern stations experienced major vertical erosion (40-90cm) between 08/18/15 and 11/08/15. After these erosional events, a gravel ramp composed primarily of pebbles and cobbles formed on the upper beach at the southern three stations (FO02, FO03, and FO04) (this gravel ramp was not included in elevation or volume change calculations). The ramp was pushed up against the riprap at all stations and buried several of the station reference markers. From 11/08/15 to 02/07/16, the entire beach accreted between 30–90cm, then experienced minor erosion (10-20cm) between 02/07/16 and 04/09/16. The northern half of the beach accreted significantly (70-110cm) between 04/09/16 and 08/09/16, while the southern central station (FO03) accreted 40cm, and the southernmost station eroded 40cm. Overall, Foss Beach underwent significant vertical elevation change, but rebuilt by the end of the study period.

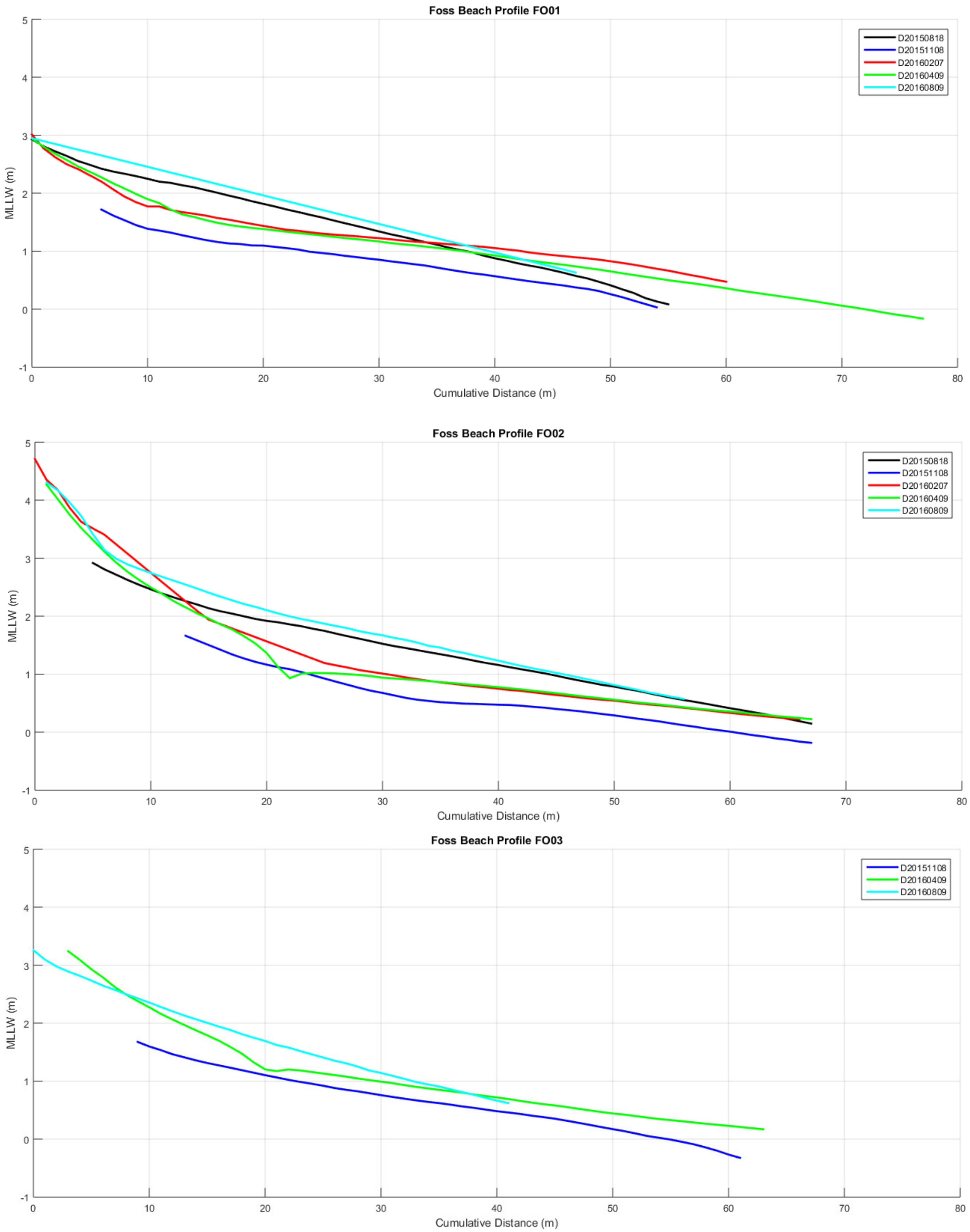

Figure 5-8: Beach profiles at the three northern stations on Foss Beach. Survey dates for each profile are displayed in the legend, with dates formatted as "D"YYYYMMDD. Profile color corresponds with date of survey.

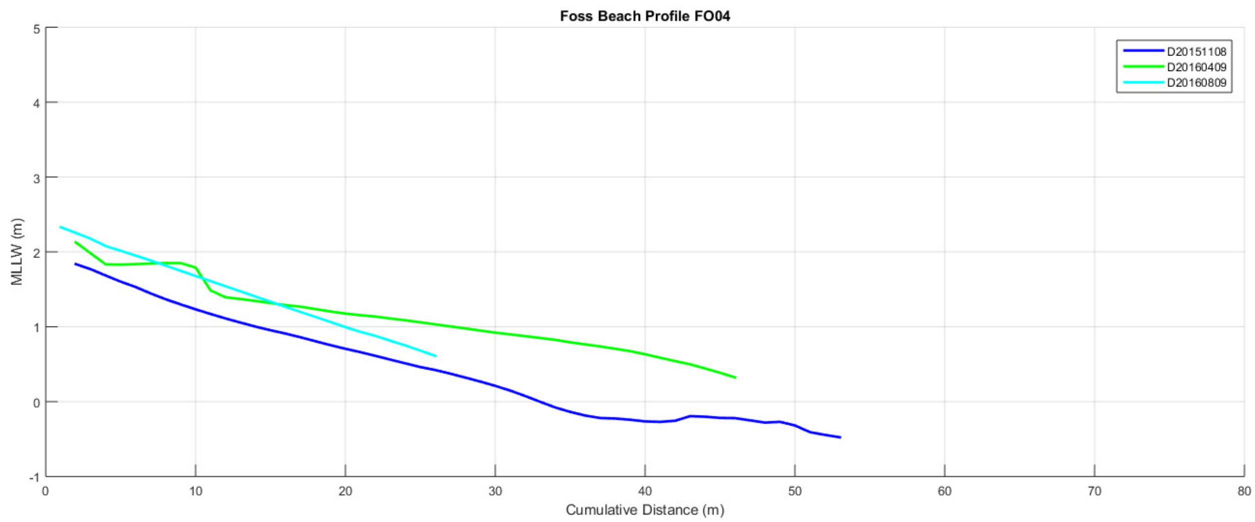

Figure 5-9: Beach profiles at the southernmost station on Foss Beach. Survey dates for each profile are displayed in the legend, with dates formatted as "D"YYYYMMDD. Profile color corresponds with date of survey.

<u>*Sediment Volume Change*</u>

Net sediment volume changes at the northernmost and southernmost stations on Foss Beach (FO01 and FO04) were below that of the uncertainty limit of 15m^3 (Figure 5-10). However, these stations often underwent large volume changes between surveys (e.g. -26.8m^3 at FO01) (Appendix 4). In contrast, the northern central station (FO02) accreted 43.4m^3 over the study period. This station also underwent large sediment volume changes between surveys (Appendix 4). For example, FO02 eroded 29.4m^3 between 08/18/15 and 11/08/15, and accreted 61.2m^3 of sediment from 04/09/16 to 08/09/16.

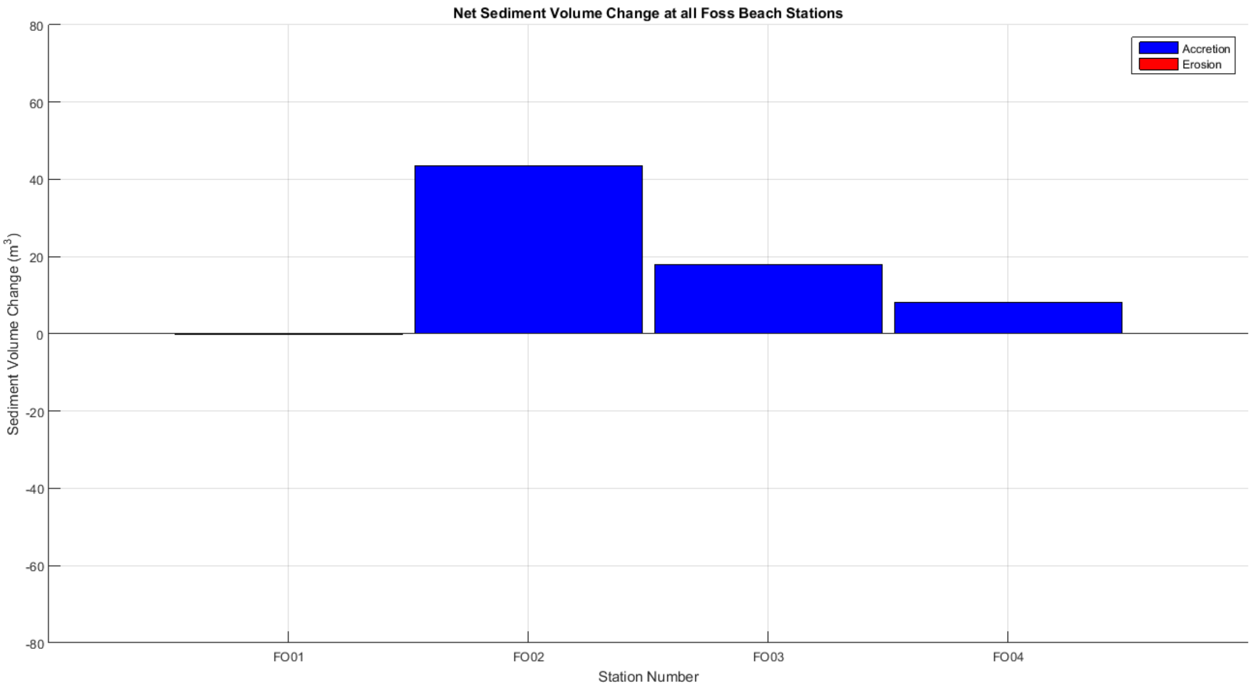

Figure 5-10: Sediment volume change at the four Foss Beach stations from July 2015–August 2016. Blue bars represent accretion and red bars represent erosion.

<u>*Sediment Grain Size*</u>

Foss Beach is highly bimodal, with sand and gravel deposits. For much of the study period, the upper beach was dominated by a gravel (pebble and cobble) ramp, which covered the lower parts of the riprap berm (Figure 5-7). During summer 2015, the lower beach was mainly composed of well sorted slightly granular fine sand and poorly sorted pebbly fine sand (Table 5-2 and Appendix 1). The southernmost station (FO04) was composed of unimodal, very well sorted fine sand. During the winter of 2015, field observations suggest that the beach was considerably coarser for much of the winter and spring (Figure 5-7).

Table 5-2: Location, textural group, sediment name, and sorting of samples from Foss Beach, collected summer 2015. Abbreviations include Sl. For Slightly and Mod. for Moderately.

Sample Number	Latitude	Longitude	Sample Collected	Textural Group %GSM from Gradistat	Sediment Name %GSM and Mode in Wentworth Scale	Classification Mean Phi Size	Sorting from Gradistat
FO02A	43.00769	-70.74386	20150718	Sl. Gravelly Sand	Sl. Granular Fine Sand	Fine Sand	Well Sorted
FO02B	43.00765	-70.74373	20150718	Sand	Fine Sand	Fine Sand	Well Sorted
FO02C	43.00759	-70.74360	20150718	Sl. Gravelly Sand	Sl. Granular Fine Sand	Fine Sand	Well Sorted
FO03A	43.00580	-70.74470	20150718	Gravelly Sand	Pebbly fine Sand	Fine Sand	Mod. Sorted
FO03B	43.00577	-70.74458	20150718	Gravelly Sand	Pebbly fine Sand	Coarse Sand	Poorly Sorted
FO03C	43.00579	-70.74447	20150718	Gravelly Sand	Pebbly fine Sand	Medium Sand	Poorly Sorted
FO04A	43.00352	-70.74486	20150718	Gravelly Sand	Pebbly fine Sand	Medium Sand	Poorly Sorted
FO04B	43.00351	-70.74466	20150718	Sand	Fine Sand	Fine Sand	Very Well Sorted
FO04C	43.00355	-70.74447	20150718	Sand	Fine Sand	Fine Sand	Very Well Sorted

JENNESS BEACH

Jenness Beach is a wide, flat, featureless beach bounded by headlands to the north and south, and extensive bedrock outcrops in the intertidal and offshore (Figure 5-11 and Figure 5-12). The beach separates a lagoon from the ocean, suggesting that it is a welded barrier beach, a hypothesis supported by Tuttle (1960). The northern half of the beach is backed by small seawalls and infrastructure, while the southern half of the beach is backed by a large riprap and gravel berm.

Figure 5-11: Location map of stations on Jenness Beach, New Hampshire. Black lines are the profile locations while dots represent summer 2015 sediment sample locations. Sediment size classification (after Wentworth, 1922) is shown by dot color.

Figure 5-12: Photos of Jenness Beach at station JN02, looking north, on 06/11/15 (top) and on 04/03/16 (bottom). Note the loss of the small berm through the winter, and the high gravel population on the lower beach on 04/03/16.

Beach Profiles

Beach profile measurements indicate that Jenness Beach eroded small but consistent amounts (~10-40cm) between every survey (~2-3 months) over the study period (Figure 5-13 and Figure 5-14). The northern two stations (JN01 and JN02) began the study with small berms (09/29/15), which were eroded by 11/21/15 and did not rebuild. From 11/21/15 to 04/06/16, the entire beach was flat and featureless. There was major erosion between 04/03/16 and 07/25/16, in which the entire beach eroded 40-60cm. There was evidence of some rebuilding of the beach by 07/25/16, as evidenced by small ridge and runnel systems at the northern three stations (JN01–JN03).

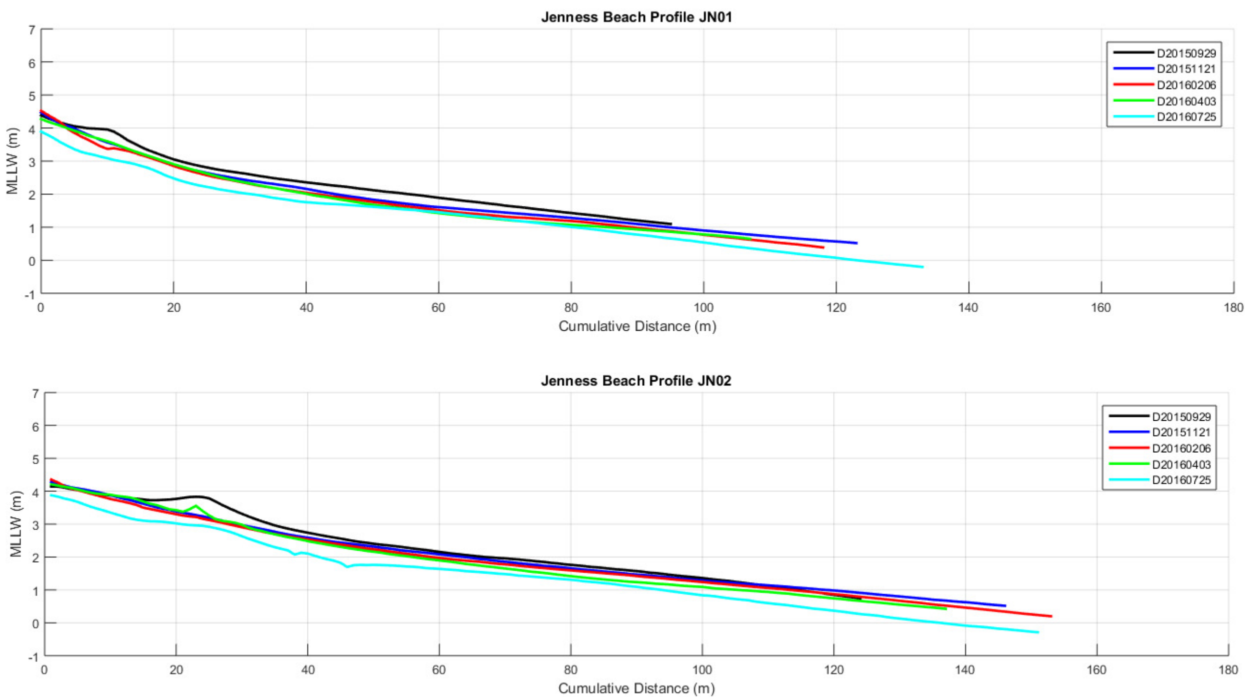

Figure 5-13: Beach profiles at the two northern stations on Jenness Beach. Survey dates for each profile are displayed in the legend, with dates formatted as "D"YYYYMMDD. Profile color corresponds with date of survey.

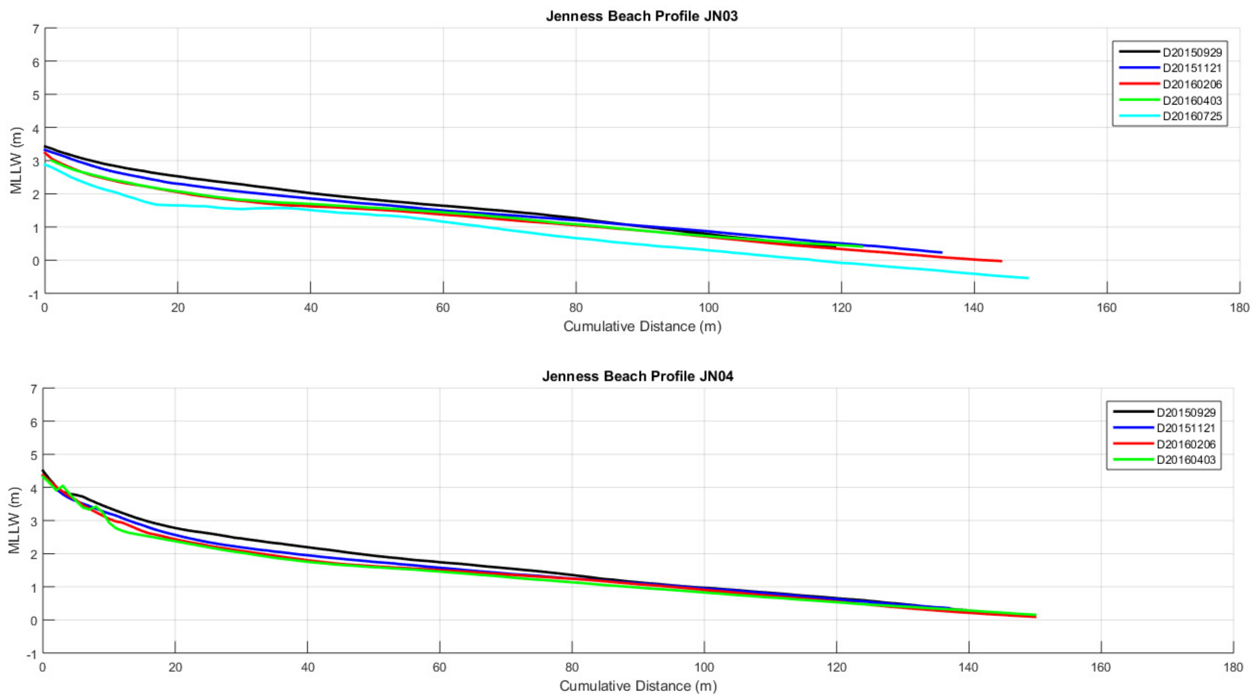

Figure 5-14: Beach profiles at the two southern stations on Jenness Beach. Survey dates for each profile are displayed in the legend, with dates formatted as "D"YYYYMMDD. Profile color corresponds with date of survey.

<u>*Sediment Volume Change*</u>

Over much of the study period, Jenness Beach tended to erode small sediment volumes consistently between surveys (10-20 m^3) (Appendix 4). The exception to this trend was during the period 04/03/16 to 07/25/16, where JN02 and JN03 eroded 39.0m^3 and 38.8m^3, respectively. Overall, all four stations on Jenness Beach experienced major net erosion over the study period, on the scale of 30-70m^3 eroded (Figure 5-15).

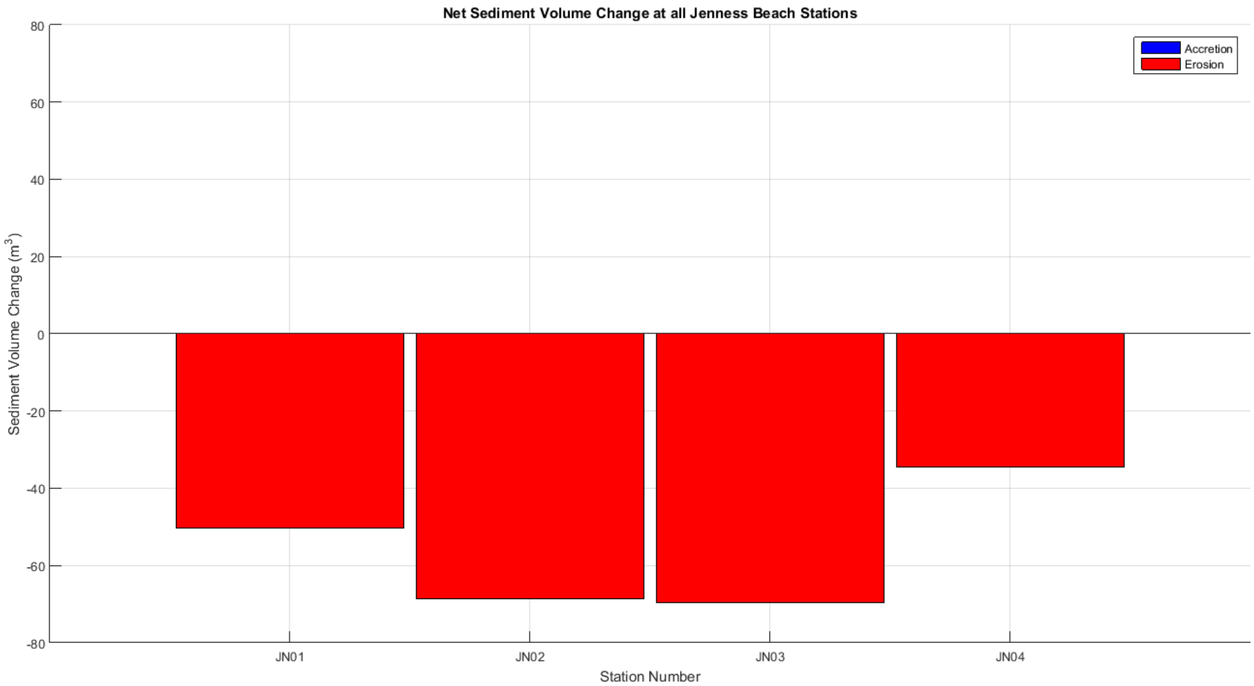

Figure 5-15: Sediment volume change at the four Jenness Beach stations from July 2015–July 2016. Blue bars represent accretion and red bars represent erosion.

__Sediment Grain Size__

Sediment samples collected during summer 2015 indicated that the beach is highly bimodal and that a large range of grain sizes were present on Jenness Beach (Table 5-3 and Appendix 1). Sediments included sandy pebbly gravel, sandy granular gravel, slightly granular medium sand, and slightly granular fine sand. There was also a range of sample sorting from very poorly sorted to well sorted. Field observations suggest that during the fall, winter, and spring, there was a significant increase in the presence of gravel along the entire beach, especially on the lower and mid-beach (Figure 5-12). During summer 2016, field observations suggest that the gravel population decreased considerably.

Table 5-3: Location, textural group, sediment name, and sorting of samples from Jenness Beach, collected summer 2015. Abbreviations include Sl. For Slightly and Mod. for Moderately.

Sample Number	Latitude	Longitude	Sample Collected	Textural Group %GSM from Gradistat	Sediment Name %GSM and Mode in Wentworth Scale	Classification Mean Phi Size	Sorting from Gradistat
JN01A	42.988683	-70.760167	20150611	Sl. Gravelly Sand	Sl. Granular Medium Sand	Medium Sand	Mod. Well Sorted
JN01B	42.988550	-70.759850	20150611	Sandy Gravel	Sandy Granular Gravel	Very Coarse Sand	Poorly Sorted
JN01C	42.988350	-70.759433	20150611	Sl. Gravelly Sand	Sl. Pebbly Fine Sand	Fine Sand	Poorly Sorted
JN02A	42.985750	-70.762333	20150611	Sl. Gravelly Sand	Sl. Granular Fine Sand	Fine Sand	Well Sorted
JN02B	42.985617	-70.761900	20150611	Sandy Gravel	Sandy Pebbly Gravel	Coarse Sand	Poorly Sorted
JN02C	42.985467	-70.761367	20150611	Sl. Gravelly Sand	Sl. Granular Fine Sand	Fine Sand	Mod. Sorted
JN03A	42.982833	-70.763433	20150611	Sandy Gravel	Sandy Pebbly Gravel	Granular Gravel	Very Poorly Sorted
JN03B	42.982717	-70.762767	20150611	Sl. Gravelly Sand	Sl. Granular Fine Sand	Fine Sand	Well Sorted
JN03C	42.982567	-70.762250	20150611	Sl. Gravelly Sand	Sl. Pebbly Fine Sand	Medium Sand	Poorly Sorted
JN04A	42.980433	-70.764167	20150803	Sl. Gravelly Sand	Sl. Granular Fine Sand	Fine Sand	Mod. Well Sorted
JN04B	42.980333	-70.763600	20150803	Sl. Gravelly Sand	Sl. Pebbly Fine Sand	Fine Sand	Mod. Well Sorted
JN04C	42.980267	-70.763183	20150803	Sl. Gravelly Sand	Sl. Pebbly Fine Sand	Fine Sand	Well Sorted
JN04D	42.980467	-70.764517	20150803	Gravelly sand	Pebbly Fine Sand	Medium sand	Poorly Sorted

NORTH HAMPTON BEACH

North Hampton Beach is a narrow but dynamic beach bounded by small headlands to the north and south (Figure 5-16 and Figure 5-17). The beach is backed by a marsh system, suggesting that North Hampton Beach formed as a welded barrier beach. A nearshore bedrock or glacial feature has led to the formation of a tombolo on the northern central part of the beach. Other outcrops are visible in the intertidal and offshore (Figure 5-16).

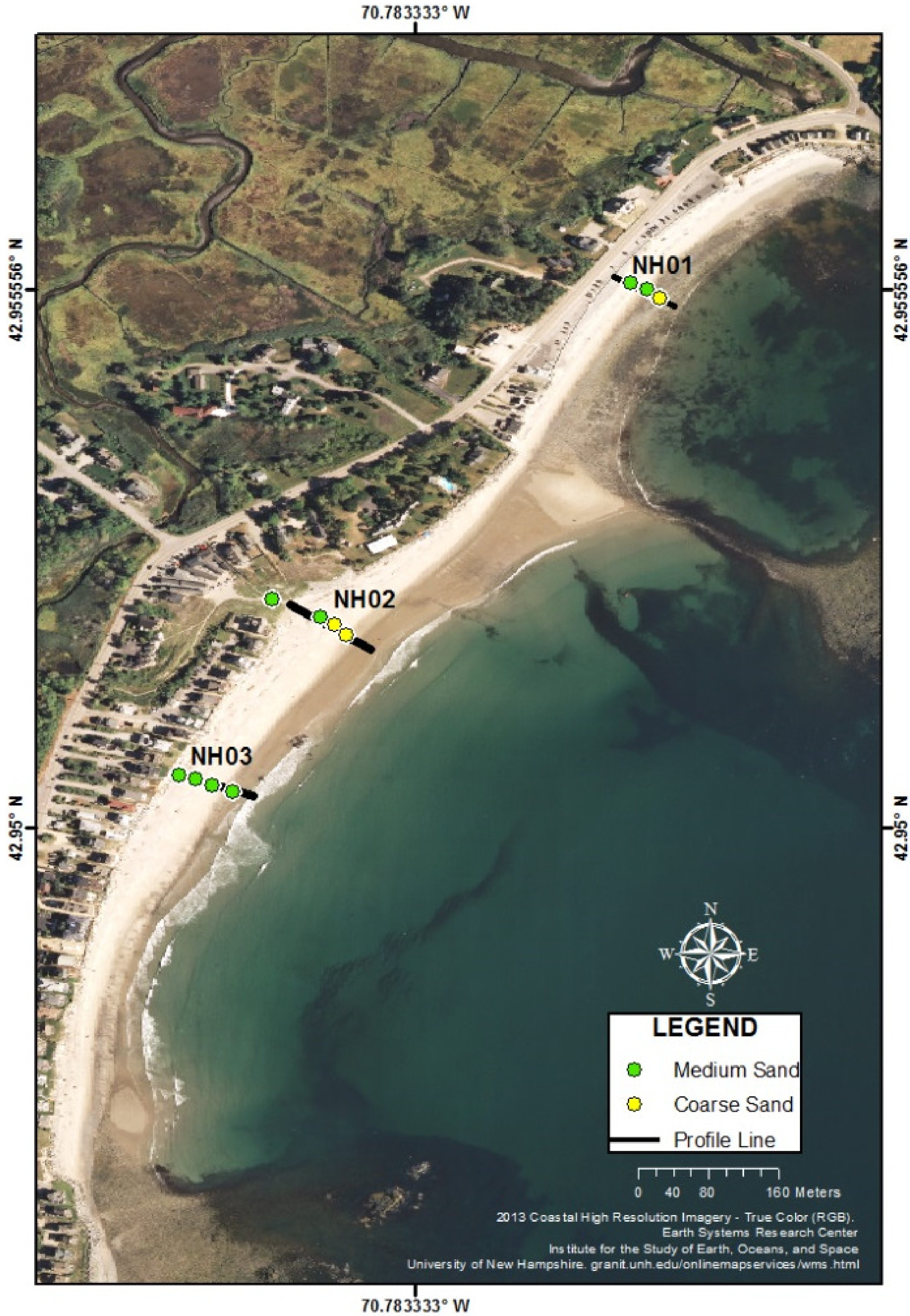

Figure 5-16: Location map of stations on North Hampton Beach, New Hampshire. Black lines are the profile locations while dots represent summer 2015 sediment sample locations. Sediment size classification (after Wentworth, 1922) is shown by dot color.

Figure 5-17: Photos of North Hampton Beach, looking north from station NH03, on 08/17/15 (top) and 02/21/16 (bottom). Note loss of the small berm and presence of gravel and pebbles in February.

Beach Profiles

North Hampton Beach underwent major changes in morphology and elevation over the study period (Figure 5-18 and Figure 5-19). On 08/17/15, the entire beach had a large, well-developed berm, which had eroded 40-80cm by 11/07/15, and had completely eroded by 01/15/16 (an additional 40-50cm of erosion). Vertical erosion was most severe at the central (and widest) station (NH02) during this time period. Interestingly, while the upper beach and berm experienced severe erosion between 11/07/15 and 01/15/16, the lower beach accreted 80-100cm at each station, which suggests that the sediment eroded from the upper beach was deposited on the lower beach, or was removed from the beach completely and was subsequently redeposited. After 01/15/16, the whole beach then took on a flat, dissipative morphology, which continued until 04/17/16. By 08/08/16, the beach had accreted considerably and rebuilt a large part of the berm, although the lower beach was much lower in elevation compared to the previous August.

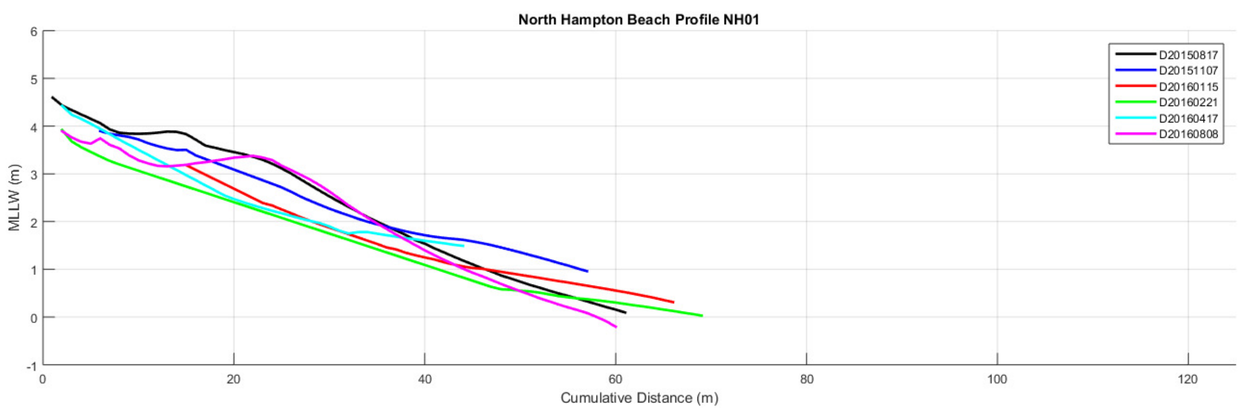

Figure 5-18: Beach profiles at the northernmost station on North Hampton Beach. Survey dates for each profile are displayed in the legend, with dates formatted as "D"YYYYMMDD. Profile color corresponds with date of survey.

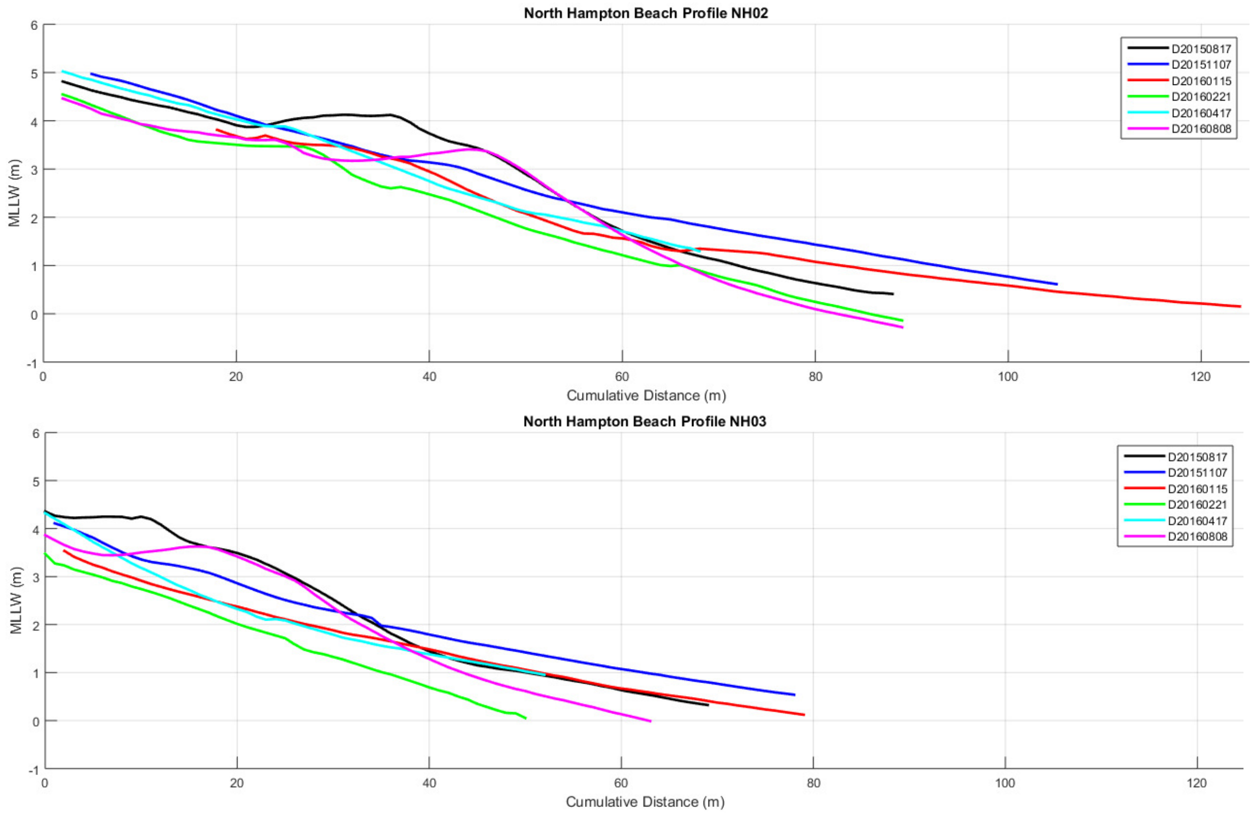

Figure 5-19: Beach profiles at the two southern stations on North Hampton Beach. Survey dates for each profile are displayed in the legend, with dates formatted as "D"YYYYMMDD. Profile color corresponds with date of survey.

<u>Sediment Volume Change</u>

North Hampton Beach tended to erode and accrete small volumes of sediment between surveys (<20m^3) at the northern end of the beach (NH01), but eroded and accreted larger volumes of sediment (20-50m^3) between surveys at the southern two stations (NH02 and NH03) (Appendix 4). The northern station also eroded the most between 08/17/15 and 11/07/15, then experienced slow erosion until 02/21/16, after which the beach began to slowly accrete through the end of the study period (08/08/16). In contrast, the southern two stations (NH02 and NH03) experienced the most erosion in the fall and winter (11/07/15 to 02/21/16), then accreted significantly between 02/21/16 and 04/17/16, with the southernmost station undergoing additional accretion between 04/17/16 and 08/08/16. Overall, North Hampton Beach ended the study period with minor net erosion (Figure 5-20).

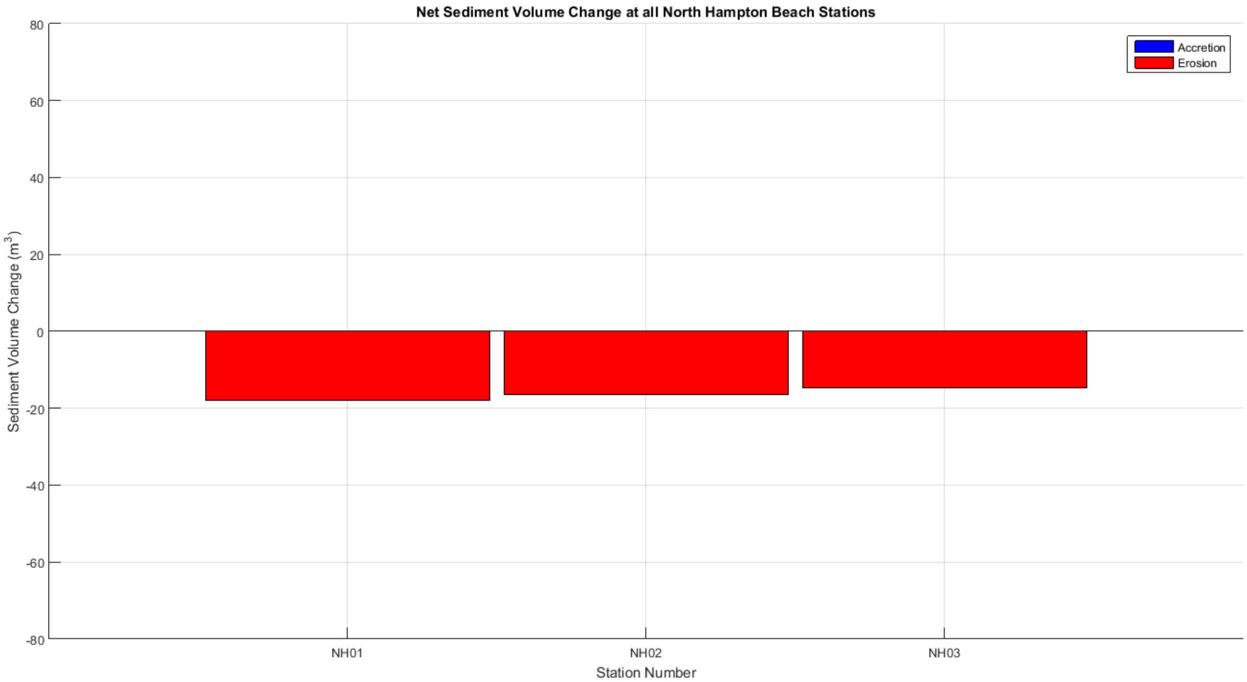

Figure 5-20: Sediment volume change at the three North Hampton Beach stations from July 2015 – August 2016. Blue bars represent accretion and red bars represent erosion.

<u>Sediment Grain Size</u>

Sediment samples collected on North Hampton Beach during summer 2015 were composed of a variety of sizes, including pebbly and slightly pebbly medium sand, granular and slightly granular medium sand, and medium sand (Table 5-4 and Appendix 1). Samples ranged from well sorted to poorly sorted. The less well sorted, more gravelly sediments tended to be located on the lower to mid-beach, while the more well sorted, sandy sediments tended to be located on the upper beach and in the dunes (NH02). Field observations indicated that during the fall and winter, the entire beach became more gravelly, with very little sand remaining at the northern station (NH01) (Figure 5-17).

Table 5-4: Location, textural group, sediment name, and sorting of samples from North Hampton Beach, collected summer 2015. Abbreviations include Sl. For Slightly and Mod. for Moderately.

Sample Number	Latitude	Longitude	Sample Collected	Textural Group %GSM from Gradistat	Sediment Name %GSM and Mode in Wentworth Scale	Classification Mean Phi Size	Sorting from Gradistat
NH01A	42.955620	-70.781110	20150817	Sand	Medium Sand	Medium Sand	Well Sorted
NH01B	42.955560	-70.780940	20150817	Sand	Medium Sand	Medium Sand	Mod. Sorted
NH01C	42.955470	-70.780810	20150817	Gravelly Sand	Pebbly Medium Sand	Coarse Sand	Poorly Sorted
NH02A	42.950500	-70.785600	20150817	Sl. Gravelly Sand	Sl. Pebbly Medium Sand	Medium Sand	Well Sorted
NH02B	42.950440	-70.785440	20150817	Sl. Gravelly Sand	Sl. Granular Medium Sand	Medium Sand	Mod. Sorted
NH02C	42.950370	-70.785220	20150817	Sl. Gravelly Sand	Sl. Granular Medium Sand	Medium Sand	Mod. Sorted
NH02D	42.950550	-70.785770	20150817	Sand	Medium Sand	Medium Sand	Mod. Well Sorted
NH03A	42.952170	-70.784310	20150817	Sand	Medium Sand	Medium Sand	Well Sorted
NH03B	42.952100	-70.784170	20150817	Gravelly Sand	Granular Medium Sand	Coarse Sand	Poorly Sorted
NH03C	42.951990	-70.784050	20150817	Gravelly Sand	Granular Medium Sand	Coarse Sand	Poorly Sorted
NH03D	42.952360	-70.784820	20150817	Sl. Gravelly Sand	Sl. Pebbly Medium Sand	Medium Sand	Mod. Well Sorted

HAMPTON BEACH

Hampton Beach, a popular tourist destination, is the second longest and the widest beach in New Hampshire (2.3km in length and 0.2km in width on the southern end of the beach at low tide) (Figure 5-21 and Figure 5-22). Hampton Beach is a barrier spit, attached at the northern end to Great Boar's Head, a glacial drumlin. Hampton Beach is separated from Seabrook Beach (a barrier island) to the south by Hampton Harbor Inlet, a tidal inlet that provides seawater access to the backbarrier, which is composed of an extensive channelized salt marsh system. Hampton Inlet is stabilized by ~400m of rip rap and a ~300m jetty that extends southeast from the southern tip of Hampton Beach. The southern end of Hampton Beach has a dune field approximately 400m long and 120m wide. The beach has been extensively developed with a continuous seawall along the northern ~1km of beach and a stone groin at the northern end of the beach. In the summer, the backshore is graded daily to accommodate tourists.

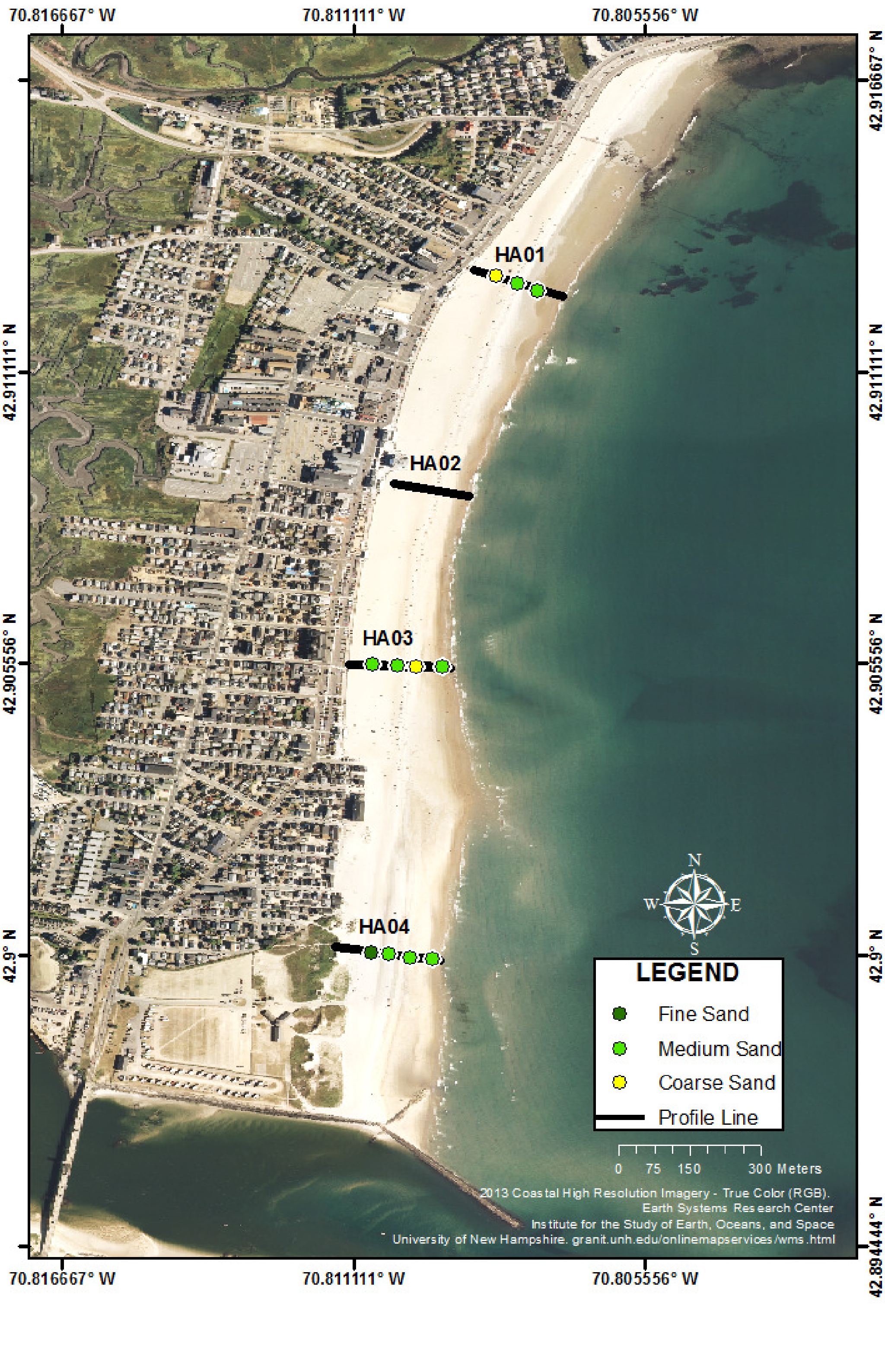

Figure 5-21: Location map of stations on Hampton Beach, New Hampshire. Black lines are the profile locations while dots represent summer 2015 sediment sample locations. Sediment size classification (after Wentworth, 1922) is shown by dot color. The profile without sediment information was established after the summer 2015 sediment sampling.

Figure 5-22: Photos of Hampton Beach from station HA01, looking south, on 06/18/15 (top) and 01/30/16 (bottom). Note the significant decrease in berm slope and the presence of several high tide swash lines behind the berm crest in January.

Beach Profiles

Hampton Beach was the most variable of the six New Hampshire beaches studied, experiencing major morphologic changes over the course of the study. A large, well-developed berm on the northern half of the beach underwent considerable vertical and horizontal changes (Figure 5-23 and Figure 5-24). For example, the berm crest at the northern two stations (HA01 and HA02) experienced ~20m of horizontal position change at between 07/07/15 and 02/20/16, while the berm crest at the southern central station (HA03) changed 32m horizontally between 07/07/16 and 02/20/16. In addition, the beach face was eroded 1.5m vertically at HA01. The southernmost Hampton Beach station (HA04) behaved much differently than the other three stations. HA04 had a small but distinctive berm on 10/03/15. However, the berm had completely eroded by 01/30/16, taking on a concave, dissipative profile until 04/16/16. The berm at station HA02 did not rebuild completely by 08/22/16. Overall, Hampton Beach began to erode in October of 2015, and did not fully recover by August of 2016. However, the extent of the bulldozers on the beach morphology and elevation of the northern three stations are unknown.

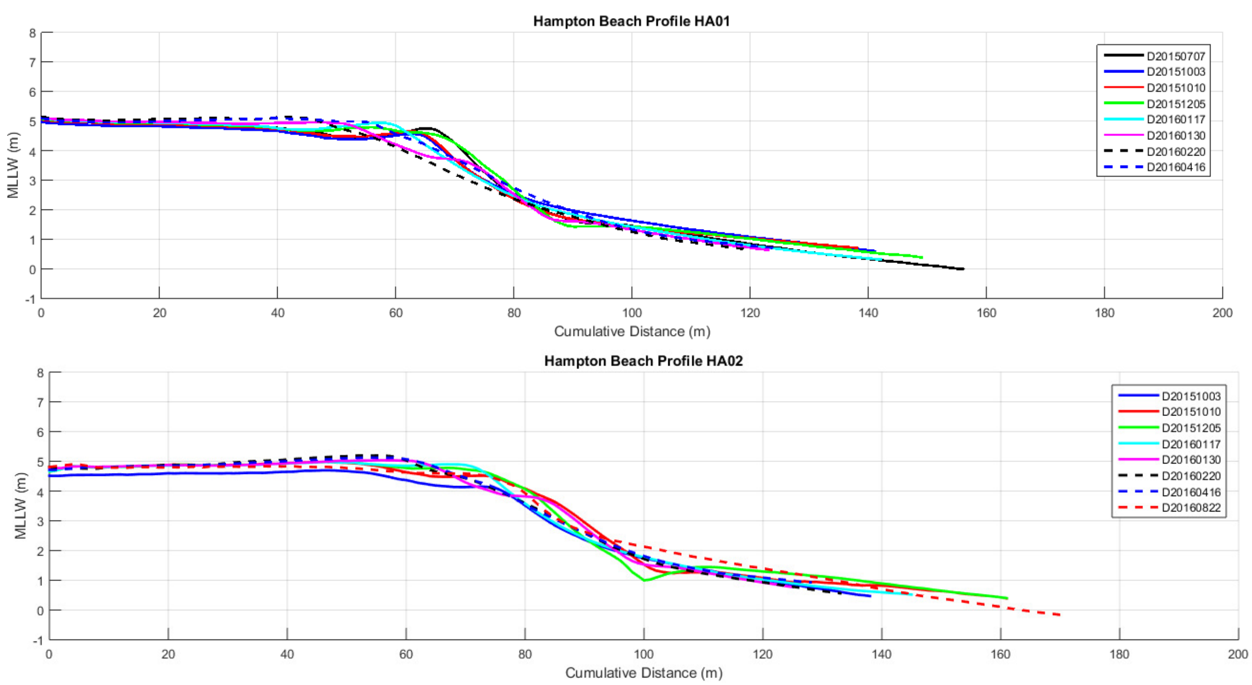

Figure 5-23: Beach profiles at the northern two stations on Hampton Beach. Survey dates for each profile are displayed in the legend, with dates formatted as "D"YYYYMMDD. Profile color corresponds with date of survey.

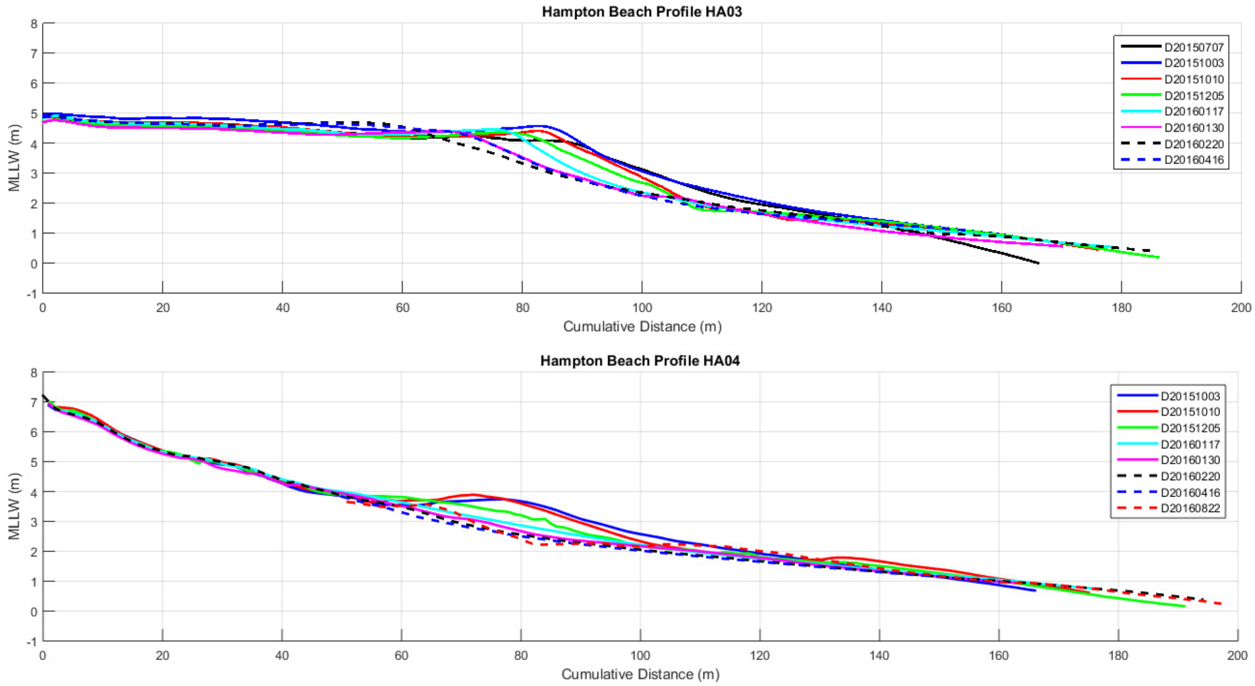

Figure 5-24: Beach profiles at the southern two stations on Hampton Beach. Survey dates for each profile are displayed in the legend, with dates formatted as "D"YYYYMMDD. Profile color corresponds with date of survey.

<u>*Sediment Volume Change*</u>

Despite large vertical and horizontal changes in the beach profiles at the four Hampton Beach stations, all four of the stations generally had small sediment volume changes between surveys (Appendix 4). Exceptions to this trend include the accretion of 53.2m^3 at station HA02 between 10/03/15 and 10/10/15, and the erosion of 52.1m^3 at station HA03 between 04/16/16 and 8/22/16. Overall, the northern half of the beach accreted during the study period, and the southern half of the beach slightly eroded or had no net change (Figure 5-25). However, profiles were only collected on 08/22/16 at stations HA02 and HA04 due to poor satellite data, therefore, the net sediment volume changes for HA01 and HA03 only extend through April 2016.

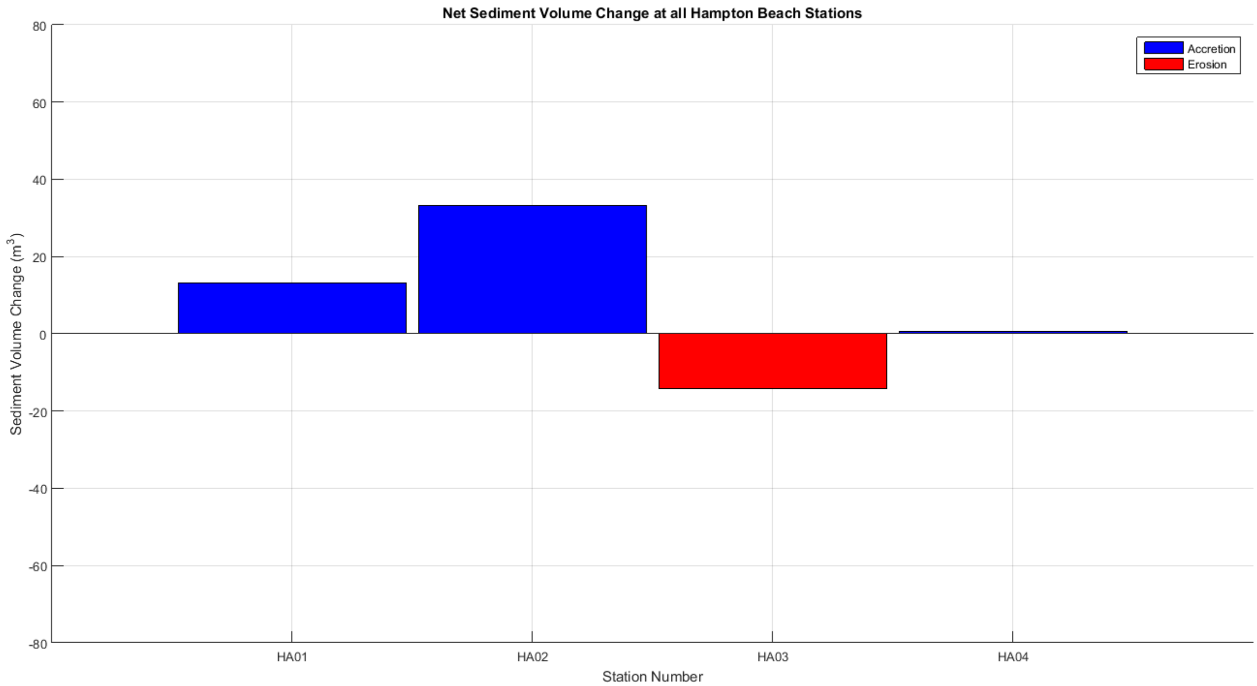

Figure 5-25: Sediment volume change at the four Hampton Beach stations from July 2015–August 2016. Blue bars represent accretion and red bars represent erosion.

<u>Sediment Grain Size</u>

Sediment samples were collected during the summer of 2015 at stations HA01, HA03, and HA04 (station HA02 had not yet been established). Samples were predominately composed of moderately to moderately well sorted, slightly granular medium and coarse sand, although three samples were composed of slightly granular fine sand or fine sand (Table 5-5 and Appendix 1). During the fall and winter, field observations suggest that sediments coarsened, with very coarse sand eroding out at the berm toe at the northern three stations. A lens of finer sand appeared to be present on the low tide terrace at all four stations in August of 2016.

Table 5-5: Location, textural group, sediment name, and sorting of samples from Hampton Beach, collected summer 2015. Abbreviations include Sl. For Slightly and Mod. for Moderately.

Sample Number	Latitude	Longitude	Sample Collected	Textural Group %GSM from Gradistat	Sediment Name %GSM and Mode in Wentworth Scale	Classification Mean Phi Size	Sorting from Gradistat
HA01A	42.912933	-70.808400	20150618	Sl. Gravelly Sand	Sl. Granular Coarse Sand	Coarse Sand	Mod. Sorted
HA01B	42.912800	-70.808000	20150618	Sl. Gravelly Sand	Sl. Granular Medium Sand	Medium Sand	Mod. Well Sorted
HA01C	42.912650	-70.807617	20150618	Sl. Gravelly Sand	Sl. Granular Fine Sand	Medium Sand	Mod. Sorted
HA03A	42.905483	-70.809417	20150618	Sl. Gravelly Sand	Sl. Granular Coarse Sand	Medium Sand	Poorly Sorted
HA03B	42.905500	-70.809917	20150618	Sl. Gravelly Sand	Sl. Granular Coarse Sand	Coarse sand	Mod. Sorted
HA03C	42.905517	-70.810283	20150618	Sl. Gravelly Sand	Sl. Granular Medium Sand	Medium Sand	Mod. Sorted
HA03D	42.905533	-70.810750	20150618	Sand	Medium Sand	Medium Sand	Mod. Well Sorted
HA04A	42.900000	-70.810450	20150707	Sl. Gravelly Sand	Sl. Granular Fine Sand	Medium Sand	Poorly Sorted
HA04B	42.899950	-70.810050	20150707	Sl. Gravelly Sand	Sl. Granular Medium Sand	Medium Sand	Mod. Sorted
HA04C	42.899917	-70.809617	20150707	Sl. Gravelly Sand	Sl. Granular Medium Sand	Medium Sand	Mod. Sorted
HA04D	42.900033	-70.810783	20150707	Sand	Fine Sand	Fine Sand	Well Sorted

SEABROOK BEACH

Seabrook Beach is the northern portion of a barrier island that extends ~8km from Hampton Inlet to the Merrimack River (Massachusetts) (Figure 1-1). The state border divides the barrier island into Seabrook Beach, NH, and Salisbury Beach, Massachusetts. Seabrook Beach is ~2.2km in length. The northern end of Seabrook Beach opens to Hampton Harbor Inlet, and is fortified by ~500m of riprap seawall and jetty (Figure 5-26). The northern third of the beach has had its dune system removed and infrastructure emplaced, and is periodically graded in the summer. The southern two-thirds of the beach has well-developed, 50-130m wide dune fields (Figure 5-27). Seabrook Beach has a narrow but well-defined berm on the northern half of the beach, and a less steep berm on the southern half of the beach.

Figure 5-26: Location map of stations on Seabrook Beach, New Hampshire. Black lines are the profile locations while dots represent summer 2015 sediment sample locations. Sediment size classification (after Wentworth, 1922) is shown by dot color. The profile line without sediment information was established after summer 2015 sediment sampling.

Figure 5-27: Photos of Seabrook Beach, looking south from station SE01, on 07/19/15 (top) and 01/31/16 (bottom). Note the major decrease in berm slope and coarsening of grain size on 01/31/16.

<u>*Beach Profiles*</u>

Beach profile changes on Seabrook Beach during the study were dominated by changes in the berm (Figure 5-28 and Figure 5-29). On 07/19/15 and 09/26/15, the berm was large and well-developed, with a steep berm face. The berm at the northern three stations experienced little change by 12/06/15, however, the berm at the southernmost station (SE04) had eroded 150cm vertically and the berm crest had retreated 13.5m landward. The berm and entire profile at every station was significantly eroded by 01/31/16, and was at the lowest elevation of the study period. By 04/10/16, the berm had rebuilt at all four stations, accreting between 60 and 170cm vertically. However, between 04/10/16 and 08/05/16, every station eroded 30-50cm vertically, especially the northern two stations (SE01 and SE02). Overall, the berm along Seabrook Beach eroded significantly during the study, and generally rebuilt to the same elevation by the end of the study period. However, due to the lack of infrastructure on which to place a station marker, Seabrook Beach profiles were interpolated over a 20m width, as opposed to a 10m width (Appendix 2), which may have had a slight effect on profile elevations.

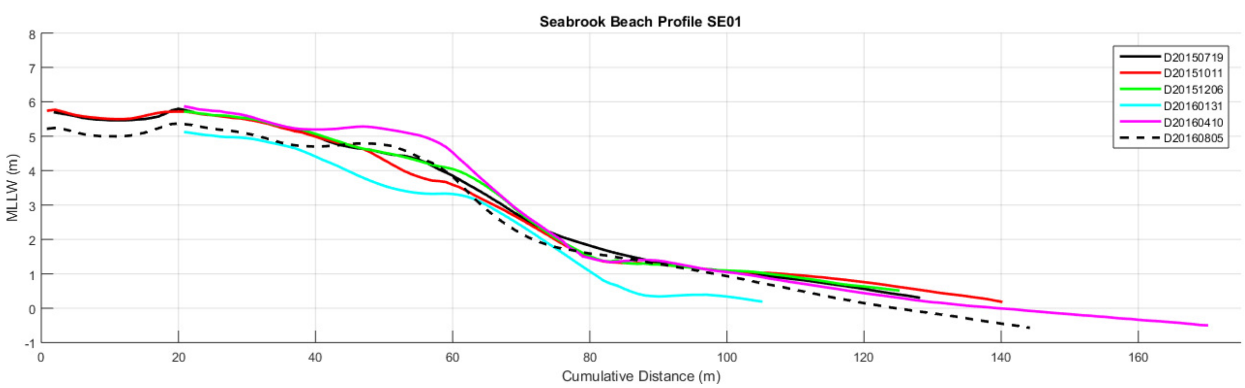

Figure 5-28: Beach profiles at the northernmost station on Seabrook Beach. Survey dates for each profile are displayed in the legend, with dates formatted as "D"YYYYMMDD. Profile color corresponds with date of survey.

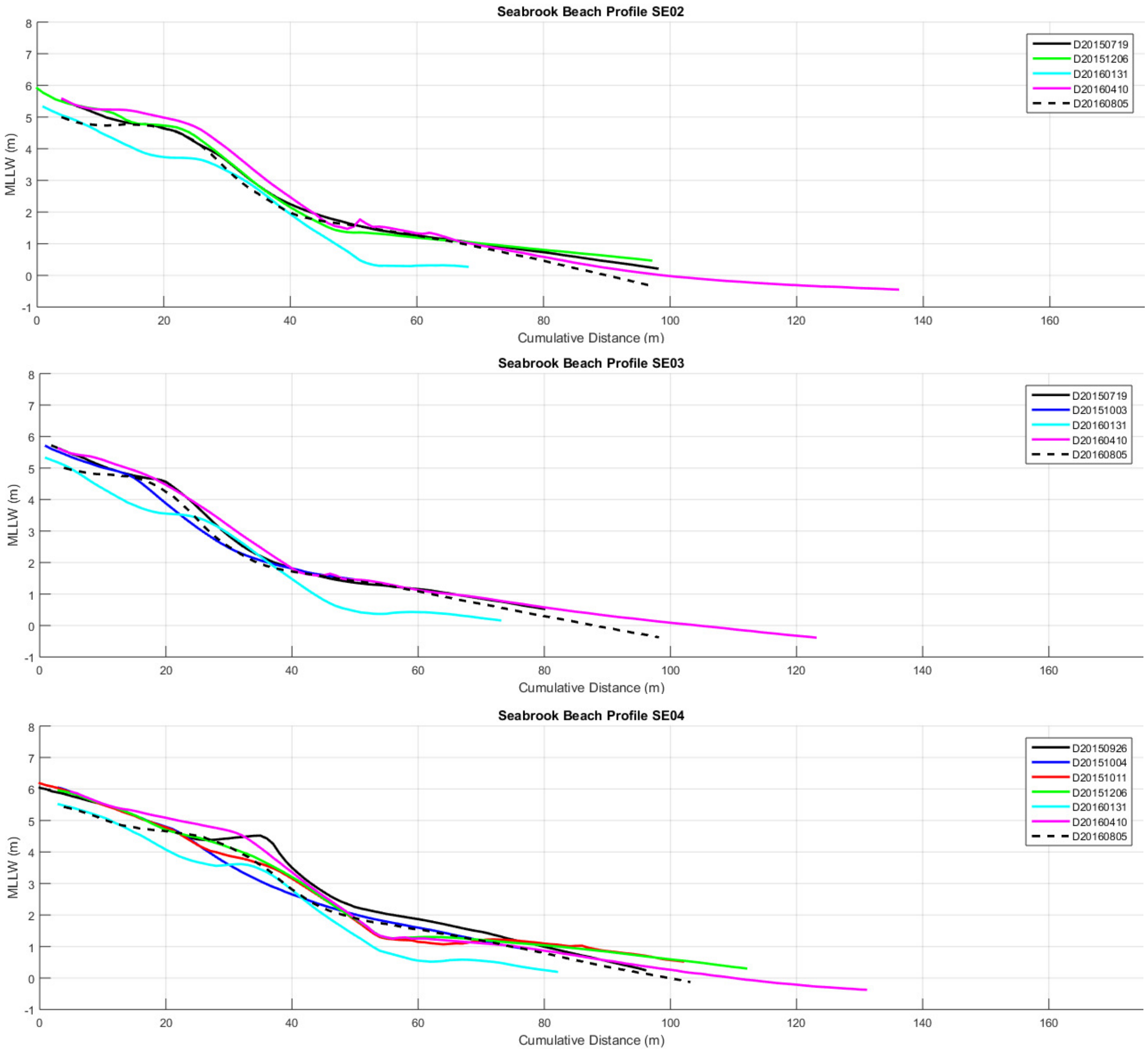

Figure 5-29: Beach profiles at the three southern stations on Seabrook Beach. Survey dates for each profile are displayed in the legend, with dates formatted as "D"YYYYMMDD. Profile color corresponds with date of survey.

<u>Sediment Volume Change</u>

The northern Seabrook Beach station (SE01) underwent the most extreme volumetric changes of any of the stations between surveys (-56.4m^3 between 12/06/15 and 01/31/16, and +71.2m^3 between 01/31/16 and 04/10/16) (Appendix 4). The southern three stations (SE02, SE03, and SE04) underwent less extreme changes between surveys (±20-40m^3), but all stations ended the study with net erosion (-

16.3 to -49.8m^3) or no net change (Figure 5-30). Over the study period, two of the northern stations (SE01 and SE03) had minor net erosion (-16.3 and -16.9m^3, respectively), while the southern station (SE04) experienced major net erosion (-49.8m^3). The major erosion seen at SE04 is due to the lack of rebuilding of the berm over the study period (Figure 5-29).

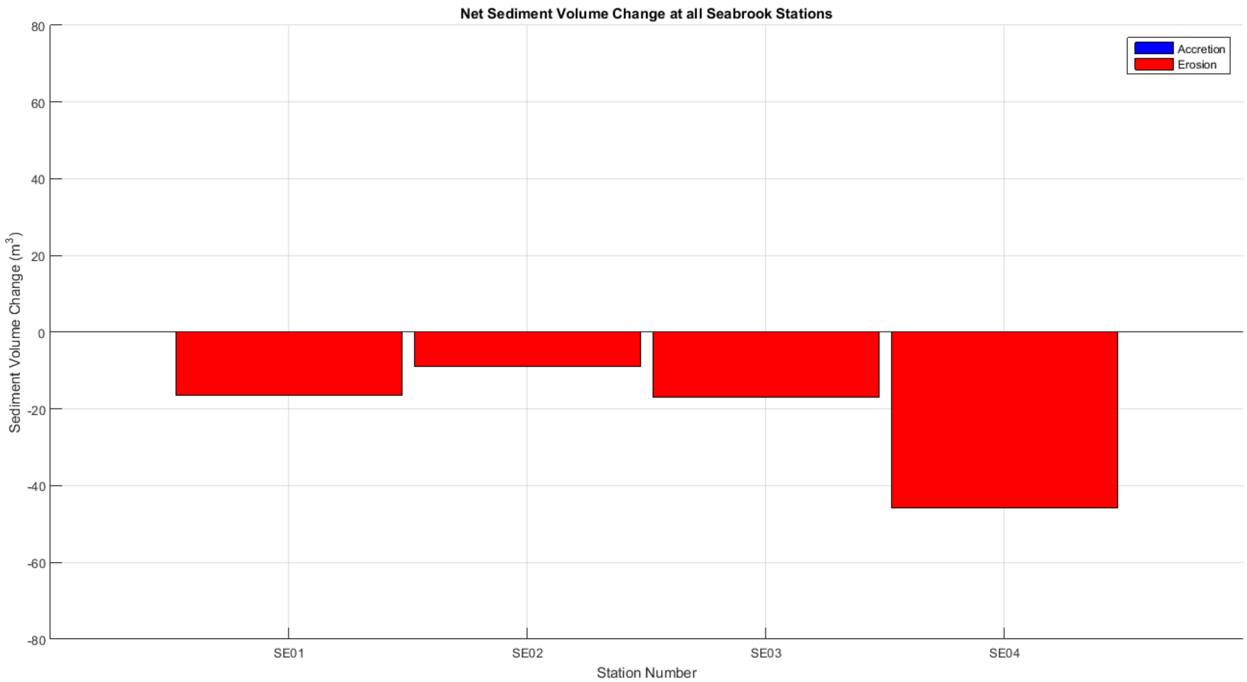

Figure 5-30: Sediment volume change at the four Seabrook Beach stations from July 2015–August 2016. Blue bars represent accretion and red bars represent erosion.

<u>*Sediment Grain Size*</u>

Sediment samples were collected from the northern three stations (SE01-SE03) during the summer 2015 sampling (SE04 was established after the sediment sampling). Summer sediments were composed mainly of moderately to moderately well sorted slightly granular medium to coarse sand (Table 5-6 and Appendix 1). Field observations suggest that sediments coarsened during the winter and spring (Figure 5-27).

Table 5-6: Location, textural group, sediment name, and sorting of samples from Seabrook Beach, collected summer 2015. Abbreviations include Sl. For Slightly and Mod. for Moderately.

Sample Number	Latitude	Longitude	Sample Collected	Textural Group %GSM from Gradistat	Sediment Name %GSM and Mode in Wentworth Scale	Classification Mean Phi Size	Sorting from Gradistat
SE01A	42.887483	-70.813650	20150719	Sand	Medium Sand	Medium Sand	Mod. Well Sorted
SE01B	42.887400	-70.813300	20150719	Sl. Gravelly Sand	Sl. Granular Medium Sand	Medium Sand	Mod. Well Sorted
SE01C	42.887333	-70.812967	20150719	Sl. Gravelly Sand	Sl. Granular Medium Sand	Medium Sand	Mod. Sorted
SE01D	42.887567	-70.814000	20150719	Sl. Gravelly Sand	Sl. Granular Medium Sand	Medium Sand	Mod. Sorted
SE02A	42.884833	-70.814233	20150719	Sl. Gravelly Sand	Sl. Granular Coarse Sand	Coarse Sand	Mod. Sorted
SE02B	42.884783	-70.813950	20150719	Sl. Gravelly Sand	Sl. Granular Fine Sand	Medium Sand	Mod. Sorted
SE02C	42.884750	-70.813633	20150719	Sl. Gravelly Sand	Sl. Granular Medium Sand	Medium Sand	Mod. Well Sorted
SE02D	42.884883	-70.814450	20150719	Sl. Gravelly Sand	Sl. Granular Coarse Sand	Coarse Sand	Mod. Well Sorted
SE03A	42.882917	-70.814683	20150719	Sl. Gravelly Sand	Sl. Granular Coarse Sand	Coarse Sand	Mod. Sorted
SE03B	42.882917	-70.814450	20150719	Sl. Gravelly Sand	Sl. Granular Fine Sand	Medium Sand	Poorly Sorted
SE03C	42.882883	-70.814200	20150719	Sl. Gravelly Sand	Sl. Granular Medium Sand	Medium Sand	Mod. Well Sorted
SE03D	42.882950	-70.814900	20150719	Sl. Gravelly Sand	Sl. Granular Coarse Sand	Coarse Sand	Mod. Well Sorted

STORM DATA

Two storm events occurred during the study period that impacted the NH coast, directly or indirectly. Joaquin achieved hurricane status in the Bahamas on 09/28/15, then moved northeast parallel to the east coast of the United States far offshore (~900km) (Berg, 2016). Joaquin was offshore of the northeastern United States between 10/04/15 and 10/07/15, only slightly impacting the WGOM, before moving further out into the Atlantic and losing hurricane status on 10/07/15 (Berg, 2016). The impact of the far-offshore storm was monitored at Hampton and southern Seabrook Beaches.

The blizzard of January 2016, also known as Winter Storm Jonas, incapacitated the northeastern United States from January 22-24, 2016 and was ranked a Category 4 ("Crippling") storm on the NOAA Northeast Snowfall Impact Scale (Kocin and Uccellini, 2004; O'Leary, 2016). Hampton Beach was monitored prior to and following the event to examine the impact of the event on the coast.

Joaquin

Wave heights (significant wave heights averaged for 20-minute sampling periods each hour) recorded at the Jeffreys Ledge buoy (54km offshore of Hampton Beach) for the period 09/27/15 to 10/15/15 ranged from 0.77 to 3.83m, while wave periods (average of all waves in 20-minute sampling period) ranged from 3.82 to 9.85 seconds (Figure 5-31) (NDBC, 2016). Shorter period waves are generally associated with local wind-generation, while longer period waves (swell) are generally formed by distant storms (Masselink et al., 2011). Peak wave heights at Jeffreys Ledge (10/02/15 to 10/05/15) were associated with shorter wave periods (~6 second) and correspond to local maximum wind speeds. This suggests that these largest waves were locally generated, likely unrelated directly to the storm event. Longer period waves (8-10 second) occurred between 10/06/15 and 10/09/15, and were likely swell related to the storm event. Wave direction was primarily from a southeasterly to easterly direction, consistent with a tropical cyclone moving north/northeast from the Caribbean (Figure 5-32). Wind speeds recorded at the Isle of Shoals meteorological station for the same period ranged from 1-20m/s and had no preferential direction (Figure 5-33 and Figure 5-34).

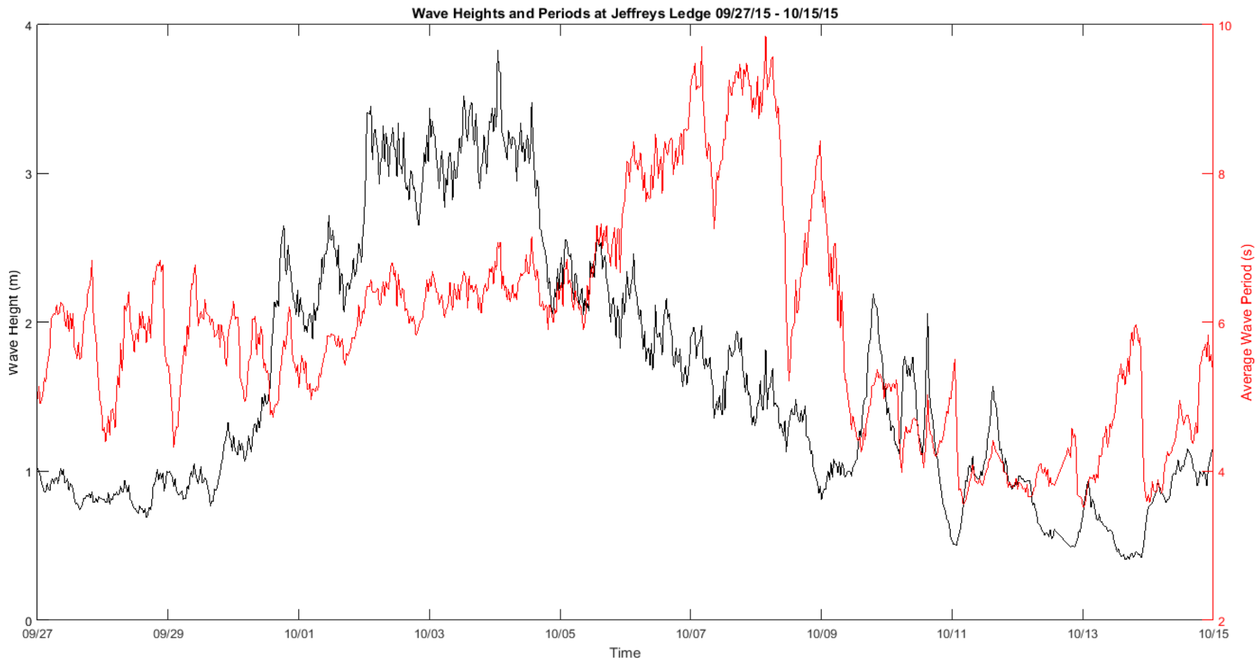

Figure 5-31: Wave heights and periods at the Jeffreys Ledge wave buoy from 09/27/15 to 10/15/15 (NDBC, 2016). Joaquin was offshore of the northeastern United States between 10/04/15 and 10/07/15. Note that wave height in the WGOM maximized before Joaquin passed the WGOM.

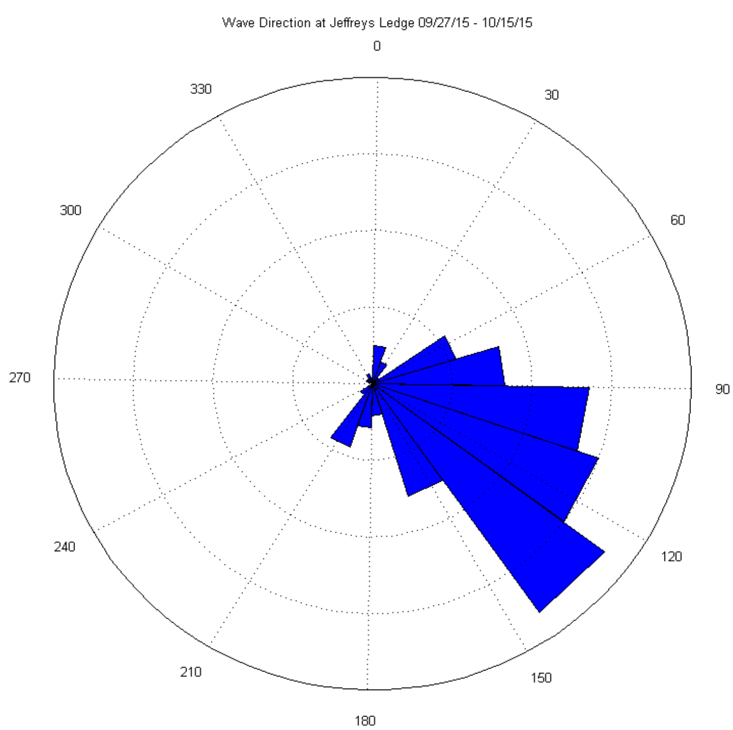

Figure 5-32: Wave directions at the Jeffreys Ledge wave buoy from 09/27/15 to 10/15/15 (NDBC, 2016).

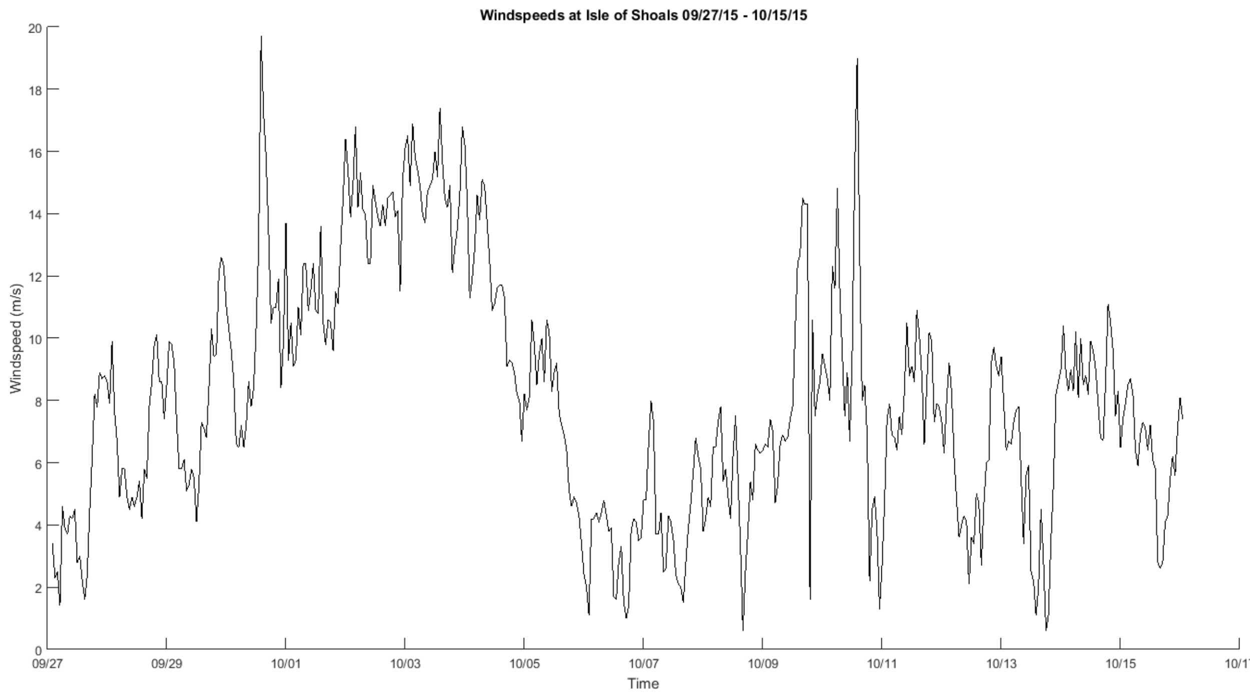

Figure 5-33: Wind speeds at Isle of Shoals from 09/27/15 to 10/15/15 ("Station IOSN3 - Isle of Shoals, NH," 2016). Note that maximum wind speeds correspond to maximum wave heights (Figure 5-31).

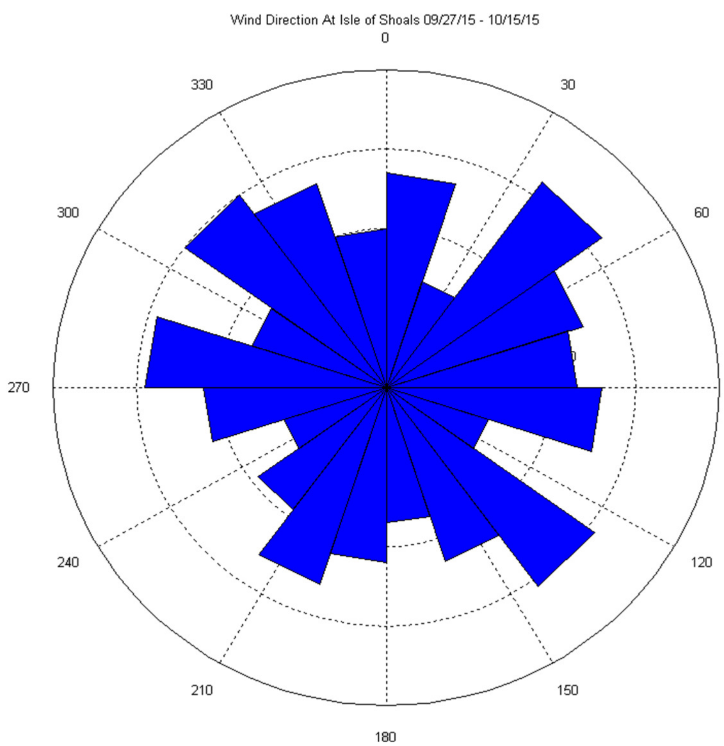

Figure 5-34: Wind directions at Isle of Shoals from 09/27/15 to 10/15/15 ("Station IOSN3 - Isle of Shoals, NH," 2016).

Profiles were measured at Hampton Beach (on 10/03/15 and 10/10/15), and at Seabrook Beach (on 09/26/15, 10/04/15, and 10/11/15) to examine the impact of the storm (Figure 5-35, Figure 5-36, and Figure 5-37). On Hampton Beach, there was 30cm of vertical erosion on the lower beach at the northernmost station (HA01) (Figure 5-35), though the southern central station (HA03) experienced 60cm of vertical erosion and 31.6m^3 of sediment volume loss between 10/03/15 and 10/10/15 (Figure 5-36 and Appendix 4). Conversely, there was 80cm of accretion on the berm face at the northern central station (HA02) during the same time period (Figure 5-36). The southernmost station (HA04) experienced little change as a result of the storm. Overall, the storm caused only minor erosion on Hampton Beach.

Southern Seabrook Beach experienced more significant erosion than Hampton Beach as a result of the storm. At the southernmost station (SE04), there was 150cm of vertical erosion on the berm and 39.5m^3 of sediment volume loss between 09/26/15 and 10/04/15 (Figure 5-37 and Appendix 4). During this time period, the berm at SE04 was completely eroded. From 10/04/15 to 10/11/15, SE04 lost 60cm of sediment from the base of the berm, but accreted 40cm on the berm face.

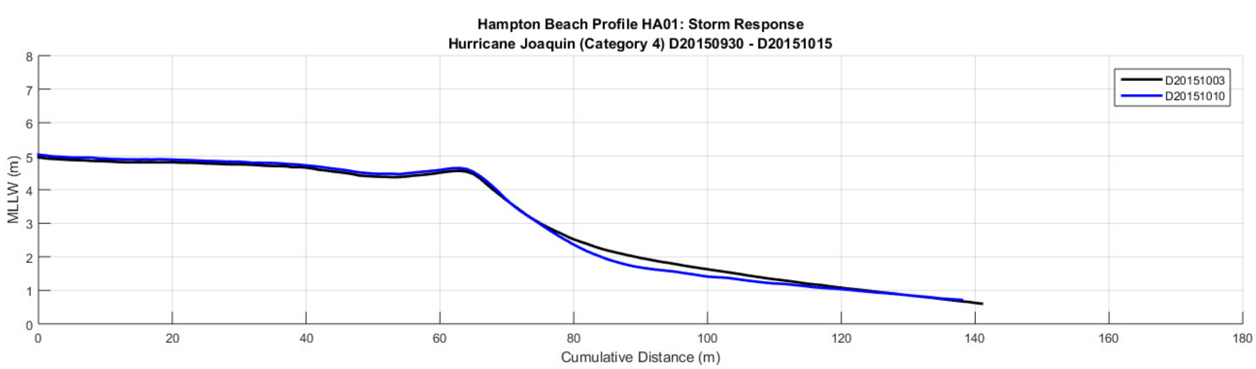

Figure 5-35: Joaquin storm response profile measurements of Hampton Beach (HA01) measured on 10/03/15 and 10/10/15 to monitor the impact of Joaquin (09/27/15–10/15/15).

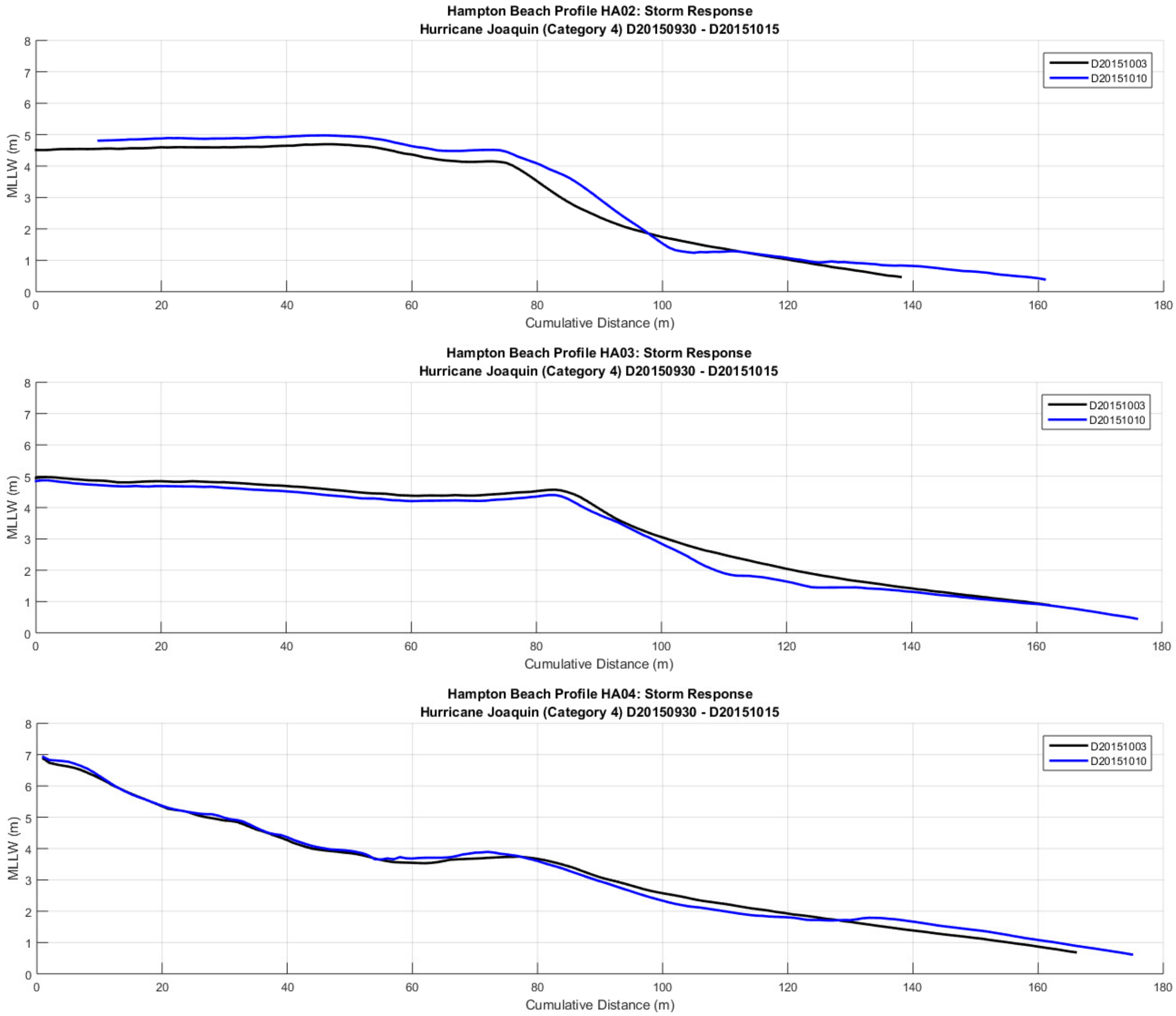

Figure 5-36: Joaquin storm response profile measurements of Hampton Beach (HA02-HA04) measured on 10/03/15 and 10/10/15 to monitor the impact of Joaquin (09/27/15–10/15/15).

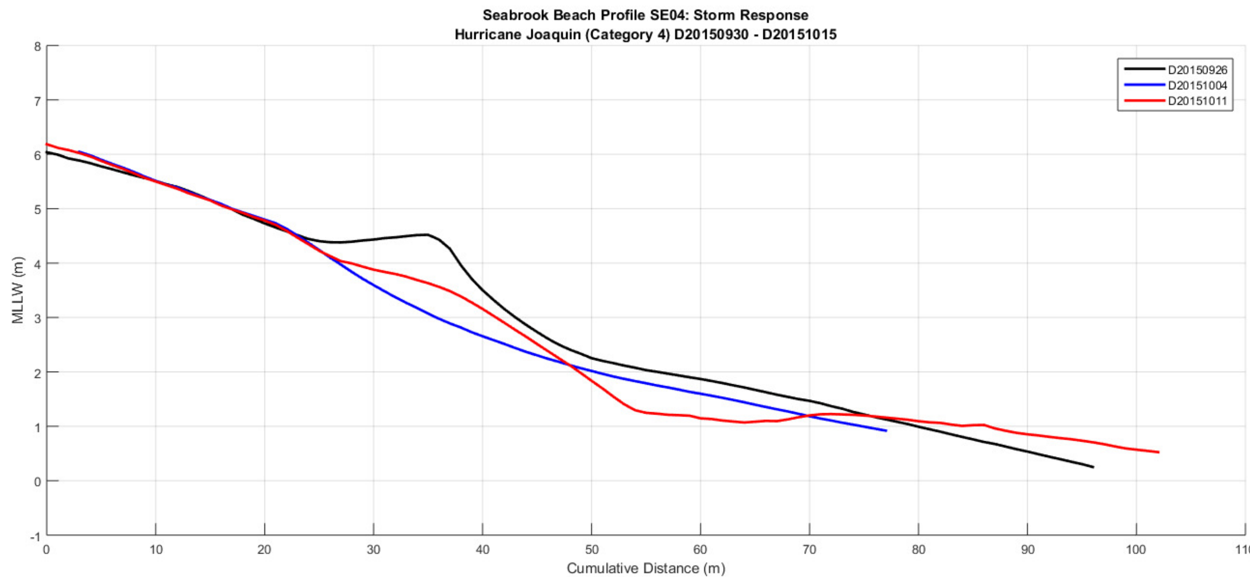

Figure 5-37: Joaquin storm response profile measurements of Seabrook Beach (SE04) measured on 09/26/15, 10/04/15, and 10/11/15 to monitor the impact of Joaquin (09/27/15–10/07/15).

<u>*Jonas*</u>

Wave heights (significant wave height averages for 20-minute sampling periods each hour) recorded at Jeffreys Ledge from 01/20/16 to 01/27/16 ranged from 0.82 to 5.43m, and wave periods (average of all waves in 20-minute sampling period) ranged from 3.53 to 10.04 seconds (Figure 5-38) (NDBC, 2016). Wave heights and periods were at the maximum from 01/24/16 to 01/25/16 (~5.43m and ~10 seconds, respectively). Wave direction during the period of maximum waves (01/23/16 – 01/25/16) was predominantly from the east southeast (Figure 5-39). Wind speeds recorded at the Isle of Shoals meteorological station for the same period ranged from ~0 to 20.0 m/s (Figure 5-40) and had no preferential direction (Figure 5-41). Wind speeds were at the maximum between 01/23/16 to 01/25/16, consistent with the storm event.

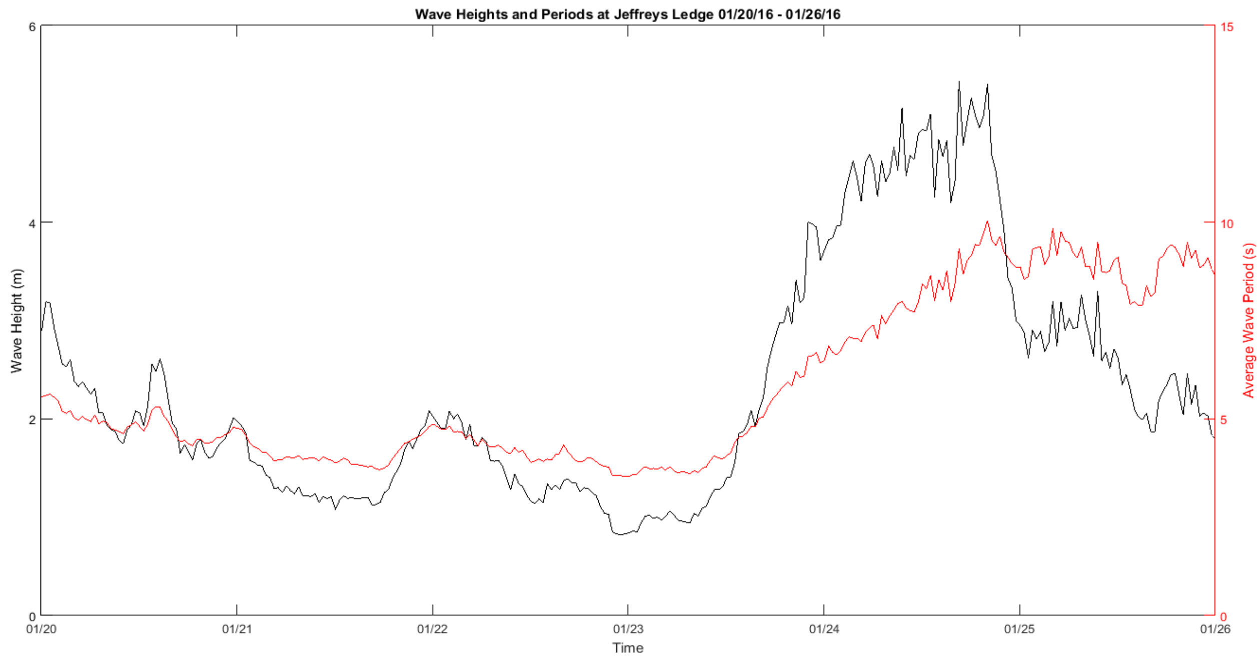

Figure 5-38: Wave heights and periods at the Jeffreys Ledge wave buoy for the period 01/20/16 to 01/26/16 ("Station 44098 - Jeffreys Ledge, NH (160)," 2016). Note that maximum wave height and period occurred during and after a period of maximum winds (Figure 5-40).

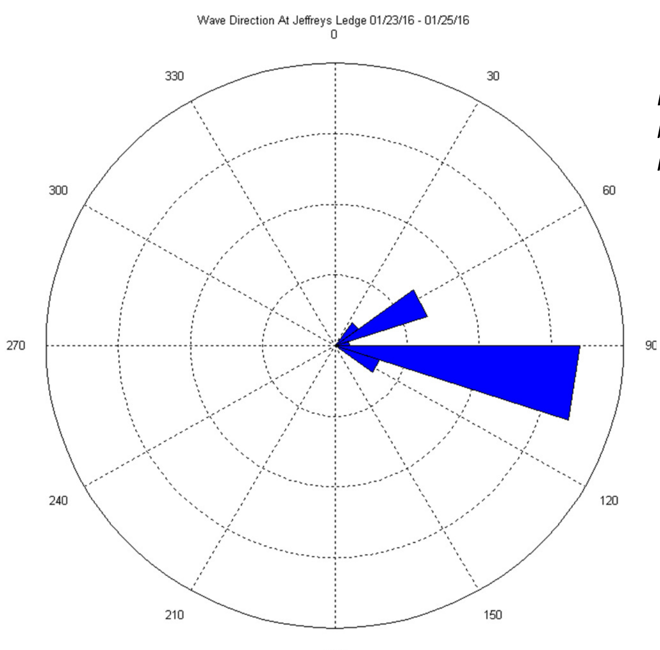

Figure 5-39: Wave directions at the Jeffreys Ledge wave buoy for the period 01/23/16 – 01/25/16, the period of maximum wave heights.

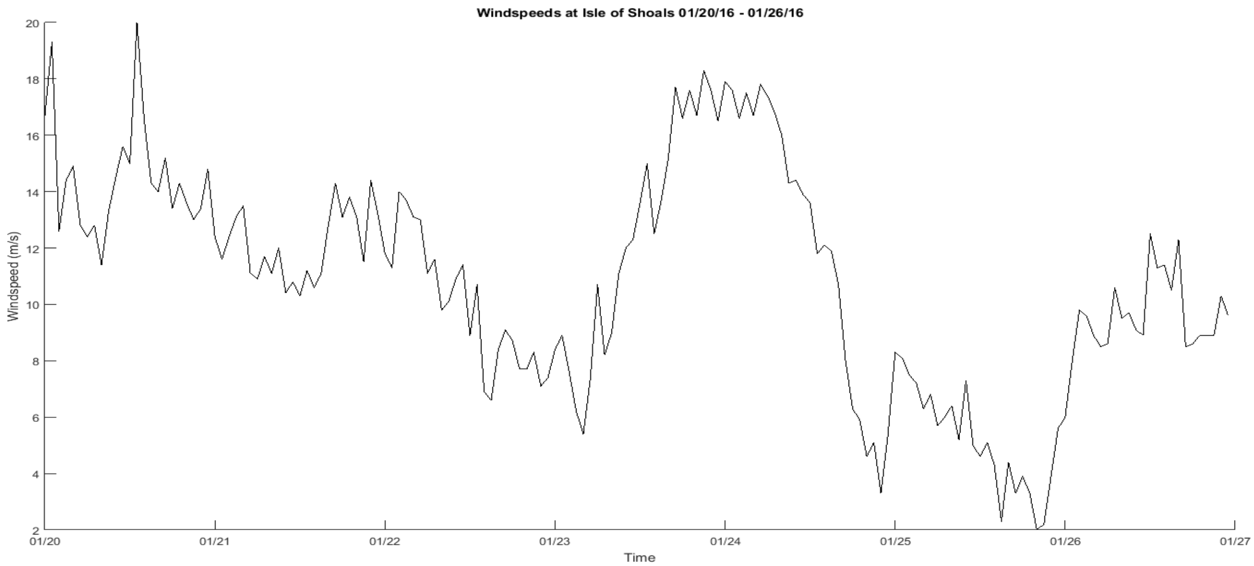

Figure 5-40: Wind speeds at Isle of Shoals for the period 01/20/16 to 01/27/16 ("Station IOSN3 - Isle of Shoals, NH," 2016).

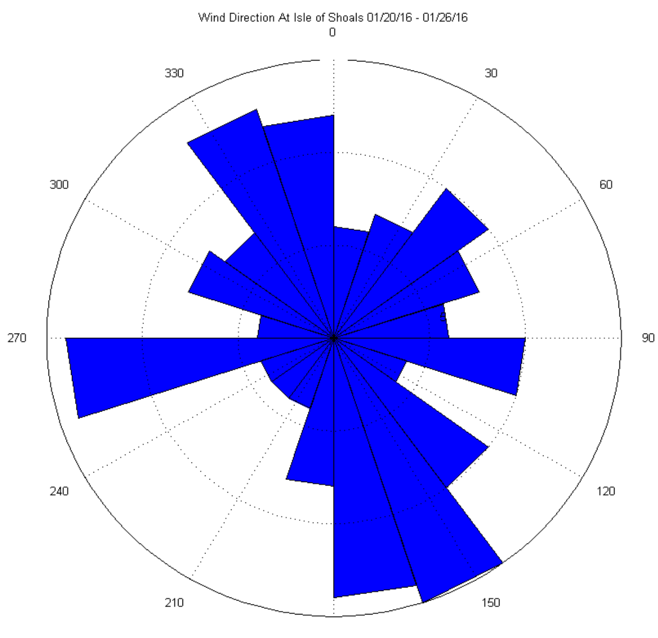

Figure 5-41: Wind directions at Isle of Shoals for the period 01/20/16 to 01/27/16 ("Station IOSN3 - Isle of Shoals, NH," 2016).

Profiles were measured at Hampton Beach two weeks apart (on 01/17/16 and 01/30/16) in order to characterize the response of the beach to Jonas (Figure 5-42). Hampton Beach experienced severe erosion (60-70cm) and major berm crest retreat (6-8m) at the northern three stations. At the northern two stations, a new berm developed at a lower elevation. The southernmost station experienced little erosion.

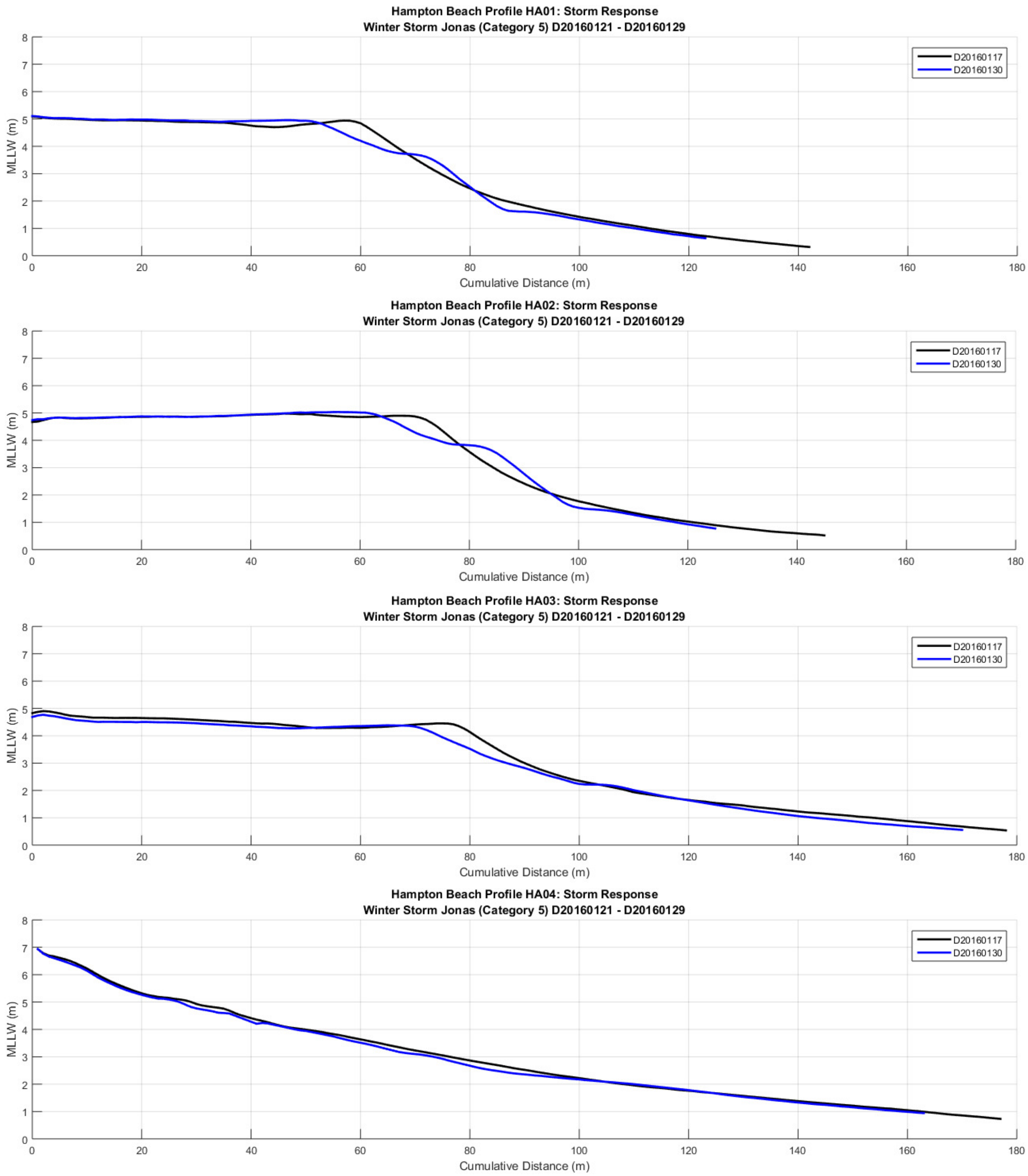

Figure 5-42: Jonas storm response profiles of Hampton Beach. Profile measurements of Hampton Beach taken before and after the impact of Jonas (01/22/16–01/24/16). Note the major berm retreat and erosion on northern Hampton Beach.

CHAPTER 6. DISCUSSION

MORPHOLOGIC TRENDS

<u>Erosion and Accretion</u>

Over the study period, northern NH beaches (Wallis Sands, Foss Beach, and Jenness Beach) tended to vertically erode or accrete small to moderate amounts (20-40cm) between surveys, while southern NH beaches (North Hampton Beach, Hampton Beach, and Seabrook Beach) tended to vertically erode or accrete significant amounts (30-70cm) between surveys (on the scale of weeks to months), and the beaches often underwent major morphologic changes, including erosion or retreat of the berm (Figure 6-1).

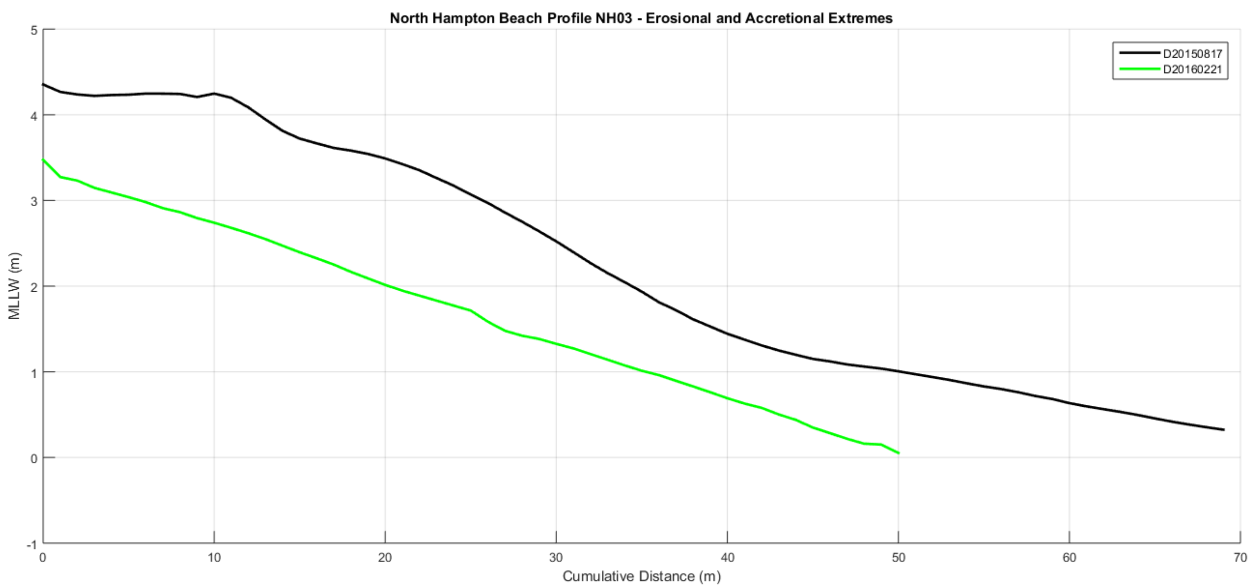

Figure 6-1: Morphologic extremes measured at North Hampton station NH03 during the study period, on 08/17/15 and 02/21/16. Note the significant vertical erosion, the total loss of the berm, and the change in morphology from a reflective profile to a dissipative profile.

Over the entire study period (fourteen months), the northern beaches had little morphologic change, but underwent moderate to major elevation changes. For example, Foss Beach significantly *increased* in elevation (20-50cm) between summer 2015 and summer 2016, with little change in morphology (Figure

6-2). In contrast, Jenness Beach significantly *decreased* in elevation (50-100cm) over the study period, with little morphologic change (Figure 6-3).

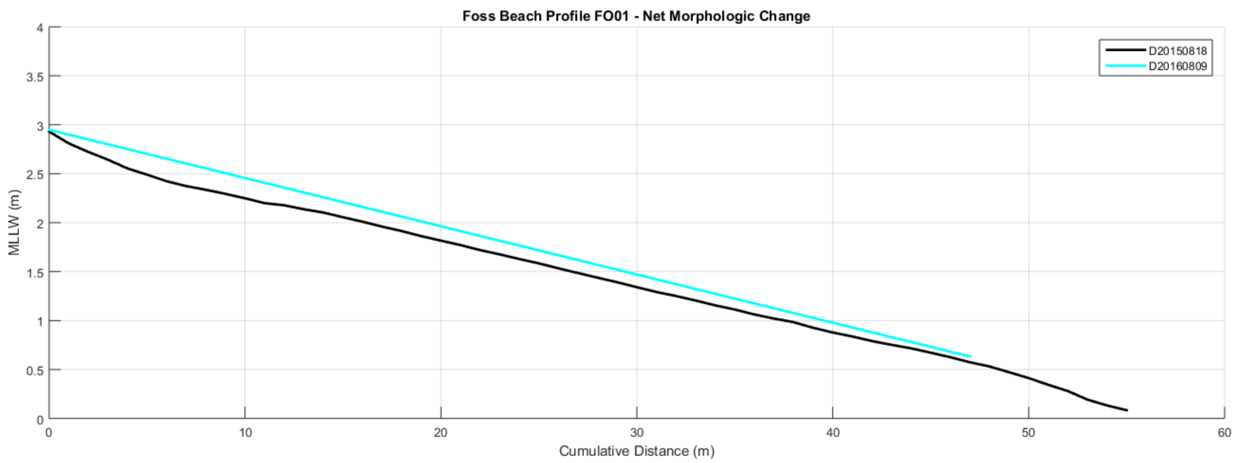

Figure 6-2: Net morphologic change at Foss Beach station FO01 over the study period. Note the vertical accretion along the entire profile.

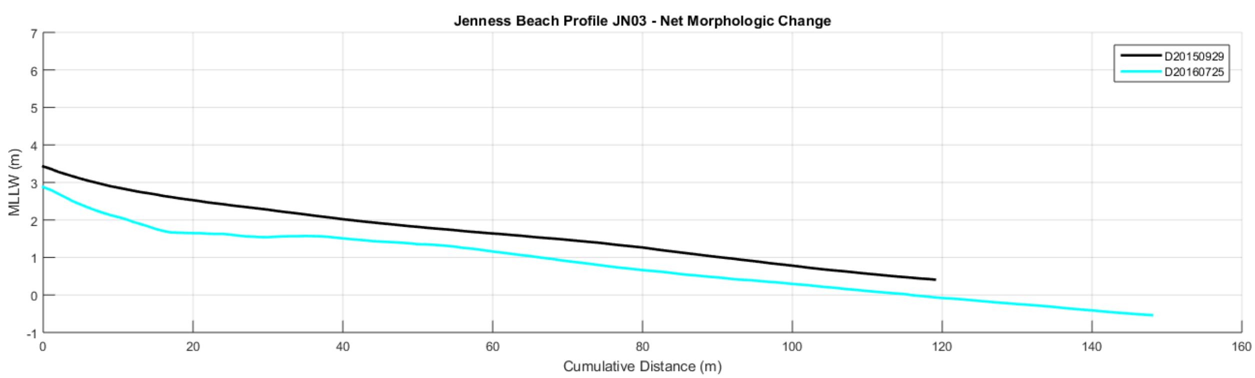

Figure 6-3: Net morphologic change at Jenness Beach station JN03 over the study period. Note the vertical erosion along the entire profile.

The southern beaches (North Hampton, Hampton, and Seabrook) tended to erode then rebuild to a similar elevation, but with a different morphology (Figure 6-4). This change in morphology was primarily seen at the berm, which generally experienced net landward retreat and/or did not fully rebuild over the study period.

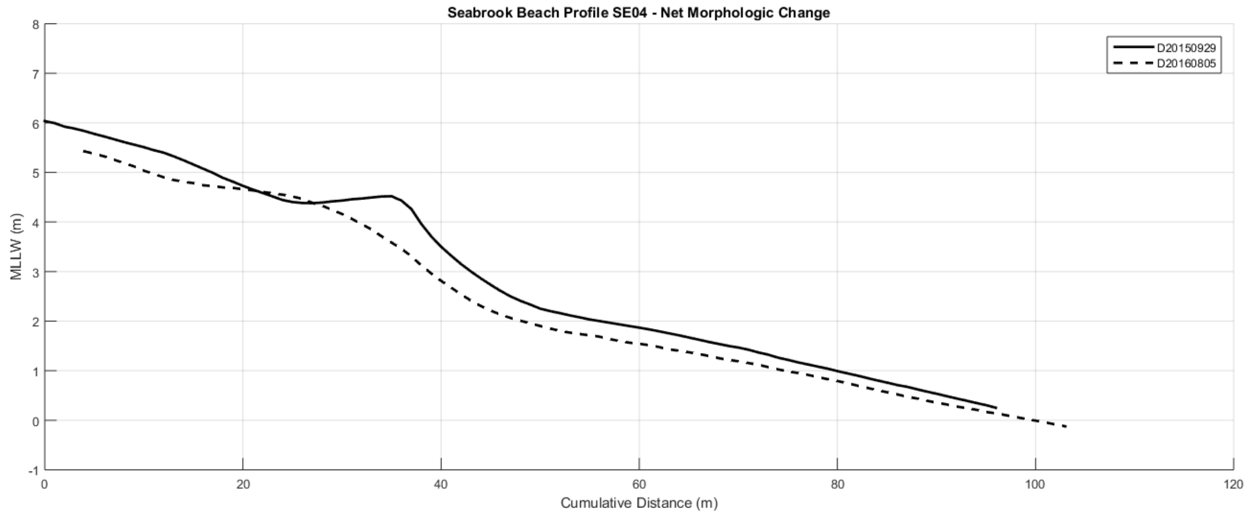

Figure 6-4: Net morphologic change at Seabrook Beach station SE04 over the study period. Note the change in berm steepness and morphology.

<u>*Berm Change*</u>

Berms are a dynamic and often ephemeral geomorphic feature of NH beaches. For example, all of the stations on Wallis Sands and Jenness Beach had small to moderately sized, well-defined berms. However, each of these stations lost their berms completely between September and December 2015, transitioning from reflective or intermediate profiles to dissipative profiles. After initial large erosional episodes (generally in September or November of 2015) in which the berms were eroded, these stations tended to experience much less erosion as winter and spring progressed (Figure 6-5). However, both Wallis Sands and Jenness Beach experienced 40-60cm of vertical erosion between April 2016 and July 2016, after a period of relatively little change (November 2015-April 2016). Examination of wave heights and periods at Jeffreys Ledge between April and July 2016 indicate that wave heights did not exceed 2.5m during this period (NDBC, 2016). Overall, these beaches generally did not fully rebuild their berms by the end of the study period (Figure 6-6).

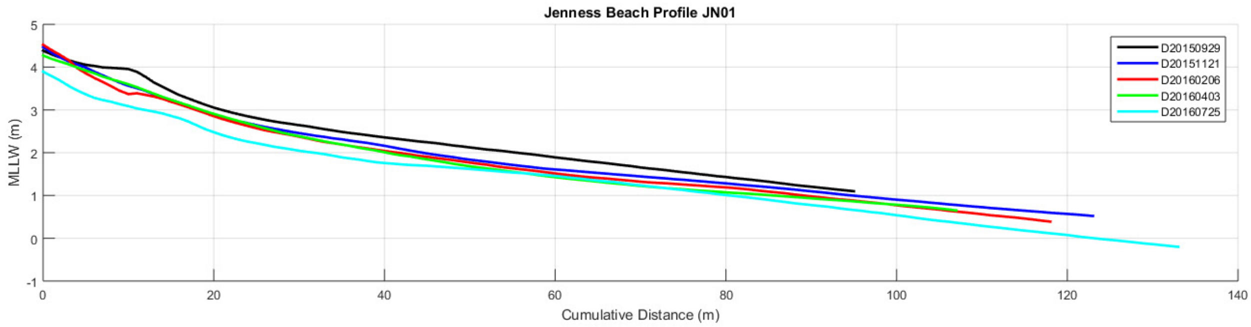

Figure 6-5: Beach profiles at Jenness Beach station JN01. Note that after an initial erosional episode between 09/29/15 and 11/21/15, there was very little erosion until after 04/03/16, despite the winter conditions.

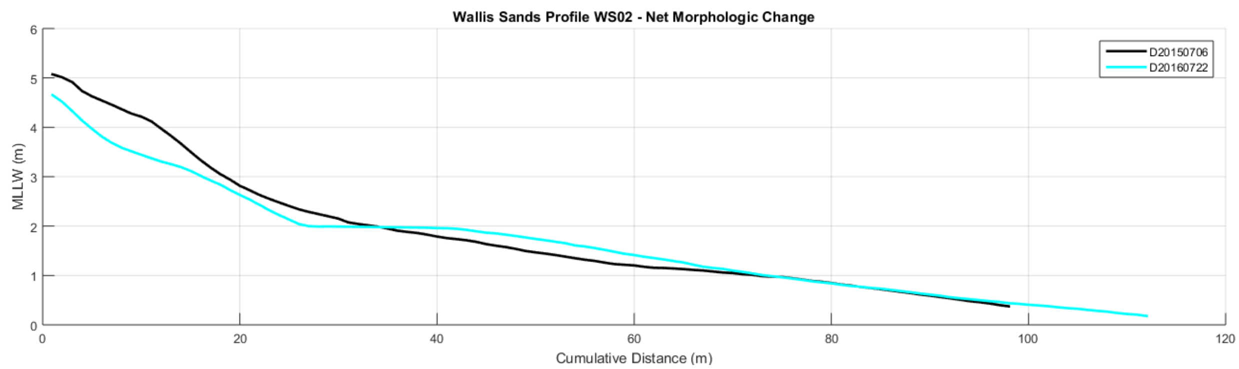

Figure 6-6: Net morphologic change at Wallis Sands station WS02 over the study period. Note the incomplete rebuilding of the small berm by the end of the study period.

Every station at North Hampton Beach, the northern three Hampton Beach stations, and Seabrook Beach began the study period with large, well developed berms. These berms were also significantly eroded during the fall and early winter (September to December, 2015) (Figure 6-7).

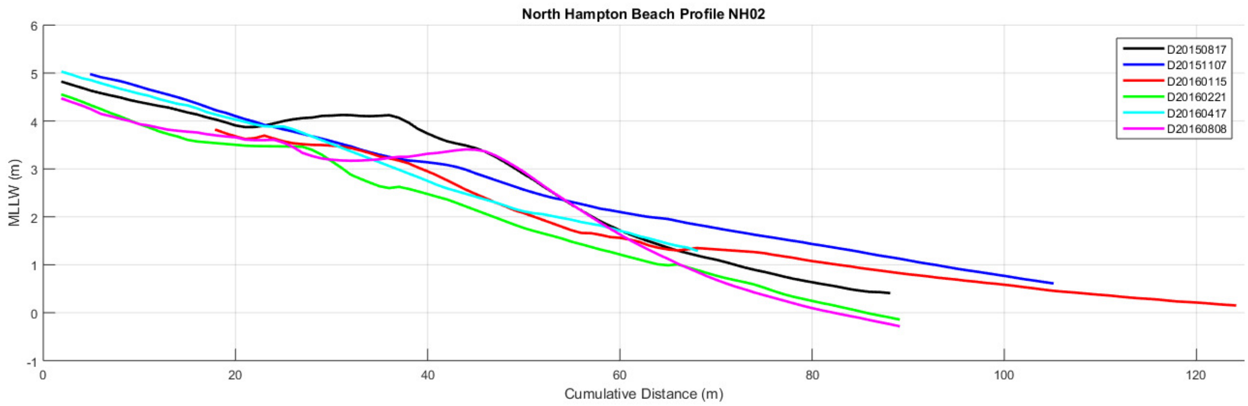

Figure 6-7: Beach profiles at North Hampton Beach station NH02. Note that after an initial major erosional episode between 08/17/15 and 01/15/16, there was very little erosion until after 04/17/16, when the beach began to rebuild to its 08/08/16 level.

The berms on these beaches also generally failed to rebuild to their starting elevation (summer 2015) or morphology by the end of the study period (summer 2016). For example, the berm at all three stations at North Hampton Beach approached, but did not rebuild to the original summer 2015 berm elevation, as the upper parts of the berm, including the berm crest, were 50-100cm lower in elevation in August 2016 than in August 2015 (Figure 6-8).

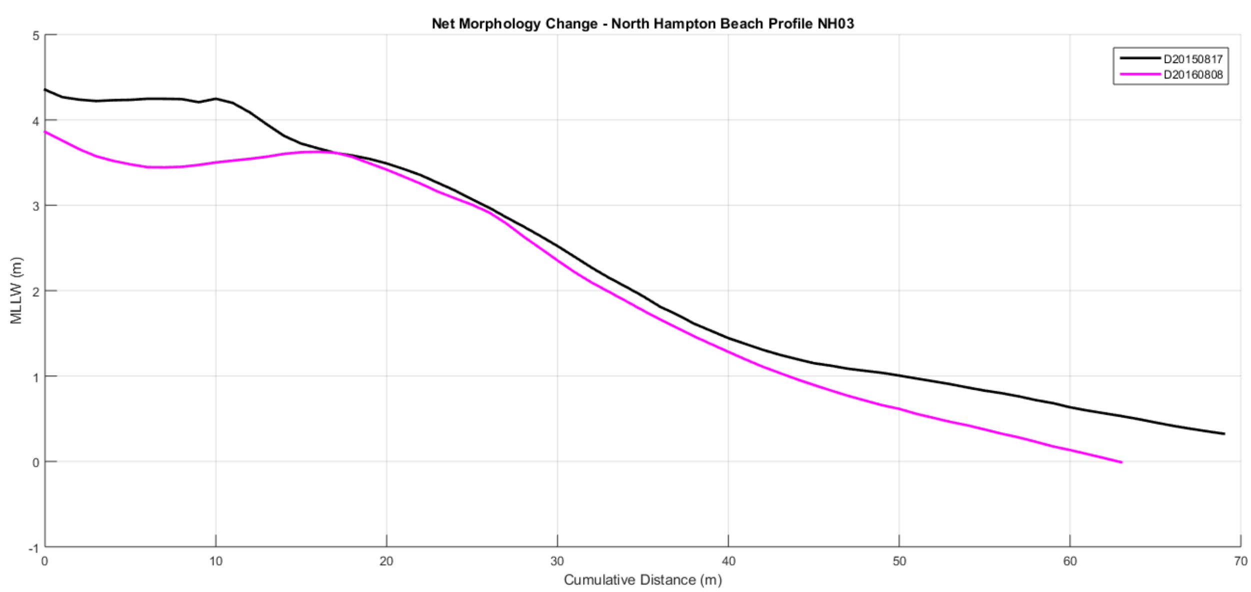

Figure 6-8: Net morphologic change at North Hampton station NH03 over the study period. Note the incomplete rebuilding of the large berm by the end of the study period.

At Hampton Beach, the berm at the northern station (HA01) accreted significantly, did not rebuild to its original morphology, while at station HA02, there was minor accretion over the study period (Figure 5-23). The berm on the southern half of Hampton Beach (HA03 and HA04) eroded early in the study and had rebuilt very little by the end of the study (Figure 5-24). On Seabrook Beach, the berm at the northern three stations (SE01-SE03) approached or rebuilt to the original summer 2015 berm size, but the berm at the southern station (SE04) was over 100cm lower in elevation in August 2016 in comparison to August 2015 (Figure 5-28 and Figure 5-29).

The incomplete rebuilding of the berms at most stations suggests that, despite the mildness of the 2015-2016 winter weather, the beaches generally failed to rebuild to their original summer 2015 elevation and morphology by summer 2016, even at those beaches which have significant sediment volume, as evidenced by their large berms. However, it is likely that the beaches would have continued accreting after August 2016, and that the berms would have rebuilt during the early fall of 2016.

VOLUMETRIC TRENDS

When normalized by beach width, average net sediment volume change per meter of beach width along the profile lines ranged from a maximum of +0.86m^3/m (Foss Beach) to a minimum of -0.67m^3/m (Seabrook Beach) (Figure 6-9). Nine of the 24 stations experienced only minor net erosion or accretion during the study period, often less than the normalized volume change uncertainty of ±0.15m^3/m. Fifteen stations did have normalized net volume changes that exceeded the uncertainty and represent measurable change.

Jenness Beach, North Hampton Beach, and Seabrook Beach experienced the most severe net erosion (-0.59m^3/m, -0.36m^3/m, and -0.67m^3/m, respectively) over the study period. The cause of the major erosion at Jenness Beach is unknown. The fact that Jenness Beach eroded considerably in volume and elevation during the study is partially consistent with the results found by Leo (2000), in which Jenness Beach appeared to reach an erosional downcut limit over the time period September 1997 to September 1998. However, during this study, after the initial episode of erosion of Jenness Beach during the fall of 2015, there was a second episode of erosion of unknown origin between April and August of 2016. The cause of the net erosion on Seabrook Beach, especially on the southern end, over the study period is also unknown, however, it may be related to the major erosional problems currently faced to the south at Salisbury Beach and Plum Island, Massachusetts (U.S. Army Corps of Engineers, 2009). There was significant erosion over the study period at all three stations on North Hampton Beach (-0.36m^3/m, -0.33m^3/m, and -0.29m^3/m, at NH01, NH02, and NH03, respectively). North Hampton Beach is rather narrow (~60-80m at low tide), therefore, it may be more susceptible to erosion and large volume changes.

Foss Beach experienced considerable net accretion over the study period (+0.86m^3/m, and 0.35 m^3/m, at FO01 and FO02, respectively), perhaps related to the bedrock outcrops present in the nearshore (Figure 5-6). However, long-term monitoring is needed to determine if this is a continued trend. The northern half of Hampton Beach also experienced net accretion (0.26 m^3/m at station HA02). The effect of the daily summer bulldozing on the northern three stations at Hampton Beach on the morphology and sediment volume is unknown, however, it appears that only the existing Hampton Beach sediment is graded, and no sand is added or removed from the beach.

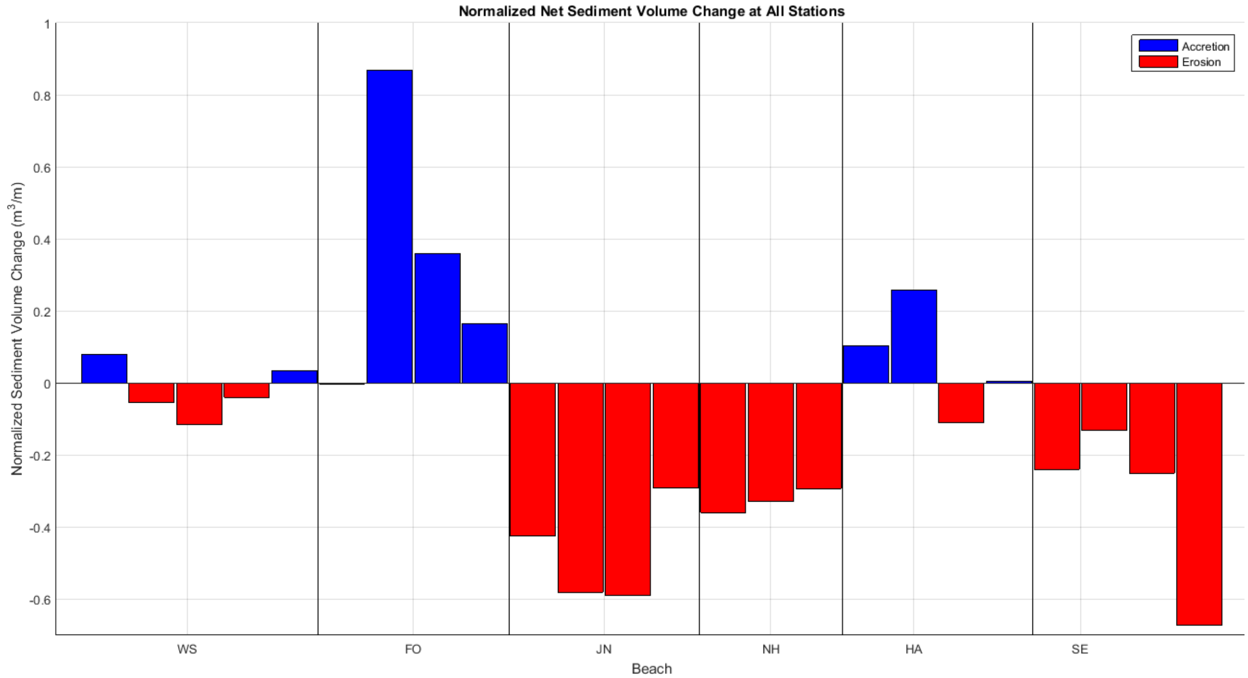

Figure 6-9: Net sediment volume change for all stations over the study period. Sediment volume change values normalized by the width of the beach at each station, resulting in average values of volume change per meter of beach width for each station. Stations are arranged in order, with north to the left and south to the right. Uncertainty is ±0.15m^3/m for normalized sediment volume changes.

These results of net sediment volume changes on NH beaches from this study stand in contrast to a long-term (decadal) LIDAR study of shoreline and volume change of the NH coast (Olson et al., 2016). That study determined that, based on LIDAR surveys, Hampton and Seabrook Beaches had positive net sediment volume changes (accretion) over the period 2000-2011, while all of the beaches north of Hampton Beach experienced negative net sediment volume changes (erosion) over the same period (Foss Beach experienced the most severe erosion) (Olson et al., 2016). However, this study found that Seabrook Beach suffered net erosion, as opposed to net accretion, while Foss Beach experienced major net accretion, as opposed to severe net erosion (Olson et al., 2016). In both this study and Olson et al. (2016), however, Jenness and North Hampton Beaches experienced net erosion. These differences in long-term (decadal) and short-term (annual) volume changes suggest that beach sediment volume change on NH beaches is highly variable on both annual and decadal time scales. However, this study only spanned fourteen months, and consequently cannot predict long-term trends in NH beach sediment volume change.

SEDIMENTOLOGICAL TRENDS

The beaches of NH show a general trend of transitioning from dissipative finer grained sand beaches with gravel in the northern parts of the coast to intermediate and reflective medium and coarse sand beaches in the southern parts of the coast (see CLASSIFICATION OF NEW HAMPSHIRE BEACHES, below). In nearshore bathymetric maps, bathymetric obstructions are visible as separating most of the northern beaches (Figure 1-2), suggesting that nearshore bathymetric highs may interrupt regional longshore sediment transport. Additionally, offshore surficial sediment mapping indicates that there are more gravel and gravel mixes present offshore of the northern NH beaches, while there is more slightly gravelly sand and sand bodies present offshore of the southern NH beaches (Ward et al., 2016b). Although there are several extensive sand bodies on the nearshore continental shelf of the Western Gulf of Maine (Ward et al., 2016b), whether or not that sand is naturally available to NH beaches is unknown.

Sediment samples collected summer 2015 were composed of a range of grain sizes, predominately pebbly sand or granular sand (Appendix 1). The strong presence of gravel at every beach (even during accretionary summer conditions) (Figure 5-2, Figure 5-7, Figure 5-12, and Figure 5-17) suggests glacial sources for beach sediments, possibly the headlands that bound most of the beaches or reworked glacial shelf deposits (Kelley and Belknap, 1991; Barnhardt et al., 1997; Belknap et al., 2002).

Gravel ramps of various sizes formed on the upper beach at several of the northern beaches, including Foss Beach, Jenness Beach, and the northern part of North Hampton Beach. The largest and steepest of these gravel ramps formed at Foss Beach, where the gravel (mostly pebbles and cobbles) built up far enough vertically on the riprap and upper beach to bury all the station markers for several months (Figure 5-7). At Foss Beach, the gravel ramp appears to build up during the winter as the finer sediments (sands) of the lower beach are eroded away. The formation of these gravel ramps on the upper beach suggests that the increased wave swash energy during fall and winter storms both erodes the finer sediments (sand) and pushes the larger sediments (gravel) up onto the upper beach.

CLASSIFICATION OF NEW HAMPSHIRE BEACHES

Beaches were classified using a combination of the Wright and Short (1984) method (based on profile morphology and seasonal change of the profile), and the sediment grain size (Table 6-1). See CHAPTER 5. RESULTS for description of classification categories.

The northernmost and southernmost Wallis Sands stations (WS01 and WS05), which are protected on one or both sides by bedrock and/or a groin (at WS01), were dissipative, granular fine and medium sand beaches with little seasonality (Figure 5-1). The central Wallis Sands stations (WS03, WS04, and WS05), which are more exposed, demonstrated much greater seasonal variability, ranging from intermediate to dissipative granular fine and medium sand beaches. Overall, Wallis Sands was classified as a dissipative granular fine and medium sand beach.

The sandy lower beach on Foss Beach was dissipative, and experienced vertical erosion and accretion, rather than feature formation and loss (e.g. berms). The lower beach of Foss Beach remained a dissipative, granular and pebbly fine sand beach throughout the study. A steep gravel ramp was developed or exposed during the winter and spring on the upper beach at all stations. Taking into consideration the dissipative lower beach and the steep gravel ramp, Foss Beach was classified as an intermediate granular and pebbly fine sand beach.

Jenness Beach was a dissipative, granular and pebbly fine sand beach. There were slightly more intense erosional and accretional periods at the northern stations compared to the southern stations, suggesting that the southern stations are protected by the bedrock outcrops that can be seen offshore in aerial photographs (Figure 5-11).

North Hampton Beach was classified as an intermediate, granular and pebbly medium sand beach with major seasonality in morphology. The norther station (NH01) is much less exposed than the southern two stations (NH02 and NH03) and tended to undergo much larger vertical erosional and accretional changes than NH02 and NH03.

Hampton Beach was morphologically very dynamic, with most changes occurring on the berm. At the northern three stations (HA01, HA02, and HA03), the beach was often reflective at high tide and dissipative at low tide. The southernmost station (HA04) behaves very unlike the northern three stations, and was a flat, dissipative beach for most of the study. Overall, Hampton Beach was classified as a reflective, granular medium and coarse sand beach that shows major seasonal dependence in its morphology.

Seabrook Beach was morphologically and sedimentologically dynamic, with great seasonality. Despite major accretion between January and April 2016, the entire beach suffered net erosion during the study period, most severely at the southern end. The beach ranged from reflective during the summer to intermediate during the winter. Overall, Seabrook Beach was classified as a reflective, granular medium and coarse sand beach.

Table 6-1: Summary of beach classification based on overall morphology and sediment grain size.

Beach Name	Beach Classification
Wallis Sands	Dissipative granular fine to medium sand
Foss Beach	Intermediate granular and pebbly fine sand
Jenness Beach	Dissipative granular and pebbly fine sand
North Hampton Beach	Intermediate granular and pebbly medium sand
Hampton Beach	Reflective granular medium to coarse sand
Seabrook Beach	Reflective granular medium to coarse sand

STORM RESPONSE

There were several key differences between the two storm events that occurred during the study period (Joaquin and Jonas). Most importantly, Joaquin was 900km offshore when it passed by the GOM, while Jonas impacted the east coast directly. Wave heights were consistently larger with longer wave periods during Jonas as compared to Joaquin (Figure 5-31 and Figure 5-38). The largest waves that occurred during Joaquin had shorter periods (Figure 5-31), suggesting that the waves were locally generated. Smaller, longer period waves likely generated by the storm directly arrived several days later. Waves came from an east-southeasterly direction during both storm events (Figure 5-32 and Figure 5-39). Both storms brought long period swell (7-10 seconds) to the coast (Figure 5-31 and Figure 5-38). Sustained wind speeds were higher for a longer period during Jonas than for Joaquin (Figure 5-33 and Figure 5-40). Winds had no preferential direction during either storm (Figure 5-34 and Figure 5-41).

Morphologic changes at Hampton Beach suggest that Joaquin had minimal impact, primarily due to its distance offshore. After the storm passed the Gulf of Maine and wave heights decreased the beach began to recover quickly (Figure 5-35 and Figure 5-36). This suggests that sediment eroded during the storm was available for recovery on Hampton Beach after the storm (Hayes, 1972). Surveys on Seabrook Beach during and after the passing of the storm demonstrate that there was major erosion of the berm at the southern end of the beach (station SE04) (Figure 5-37).

The response of Hampton Beach to Jonas was much more pronounced and severe than the response to Joaquin. Jonas caused major erosion at the northern three stations (HA01 - HA03) (60-70cm of vertical erosion and 6-8m of berm crest retreat), and very little change at the southern Hampton station (HA04) (Figure 5-42). HA04 had already eroded significantly from summer 2015 levels, and eroded little during the storm. The northern three stations were affected much more intensely, suffering considerable berm retreat and vertical erosion.

CHAPTER 7. CONCLUSIONS

Six New Hampshire beaches were studied over the period of July 2015 to August 2016 for geomorphologic, elevation, and sediment volume changes. In addition, sediment samples were collected during summer 2015 in order to characterize the beaches using sediment grain size. During the study, a novel method was developed for correcting irregularities in measured profiles and interpolating the data to straight, shore-perpendicular, overlying lines.

The seasonal behavior of each beach, in addition to sediment grain size, were used to classify the six beaches, which fell into two broad, regional categories of beach-types. The two dominant beach-types of New Hampshire are: the northern beaches, which include Wallis Sands, Foss Beach, and Jenness Beach, and the southern beaches, which include North Hampton Beach, Hampton Beach, and Seabrook Beach.

The NH beaches transition from northern to southern beaches between North Hampton and Hampton Beaches. The northern beaches tend to be dissipative, bimodal granular and pebbly fine and medium sand welded barrier beaches. These beaches tend to have little sediment volume overall, and tended to erode quickly in the fall and early winter, then erode very little until summer, when they began to rebuild. The gravel population on the northern beaches increases considerably during the fall and winter, and several of the beaches built up a gravel ramp on the upper beach (e.g. Foss Beach). The southern beaches are intermediate to reflective unimodal granular medium and coarse sand barrier beaches. These beaches are much larger and have much larger sediment volumes overall. They also had larger, well-defined berms in the summer, and most of the morphologic and erosional changes occurred to the berm, whether as vertical erosion/accretion or as berm retreat/advance.

Due to onshore and offshore topographic and bathymetric features, which likely interrupt longshore sediment transport, sediment movement is likely in an onshore/offshore direction for the northern beaches. This is evidenced by the presence of headlands and offshore bathymetric highs at the northern and southern end of every northern beach. The southern beaches likely transition to both onshore/offshore and alongshore transport. The northern beaches appeared to reach a critical erosional downcut limit, generally in October or November of 2015, after which there was little vertical erosion despite storms and winter wave conditions. The southern beaches did not appear to reach such a downcut limit, likely due to their larger overall sediment volumes. The strong presence of gravel at every beach, especially the northern beaches, suggests a nearby glacial sediment source, likely offshore glacial deposits and/or the beach headlands.

Nine of the 24 stations ended the study period with minor normalized net sediment volume changes (less than the uncertainty limit). Foss Beach and Hampton Beach had stations that experienced normalized net accretion over the study period, while Jenness Beach, North Hampton Beach, Hampton Beach, and Seabrook Beach had stations that experienced normalized net erosion. The fact that 38% of stations (9 of 24) experienced no measurable net sediment volume changes and 21% of stations (5 of 24) experienced measurable net accretion suggests that the beaches were relatively stable during this study period. One beach (Foss Beach) accreted significantly over the study period, on the order of $+0.87 m^3/m$, however, the cause of the major net accretion seen on this beach is unknown and long-term monitoring is need to determine if this accretion is a trend. However, Jenness Beach, North Hampton Beach, and southern Seabrook Beach experienced major normalized net erosion, on the order of $-0.59 m^3/m$, $-0.36 m^3/m$, and $-0.67 m^3/m$, respectively. Despite the mildness of the 2015/2016 winter, these beaches still eroded significantly.

Two southern NH beaches had varying responses to two storm events: a far-offshore tropical cyclone and the other a local extratropical cyclone. The effects of the far-offshore tropical cyclone were much less severe than that of the extratropical cyclone, due to its distance offshore. The extratropical cyclone, which impacted the coast directly, had much more pronounced erosional effects.

The results of this study suggest that New Hampshire beaches are vulnerable to current and future threats of sea-level rise and more intense storms related to climate change. Many of the beaches experienced significant vertical erosion and sediment volume loss during the study period, and most beaches did not recover to pre-study levels by the end of the study. This lack of recovery was not driven by an extremely stormy winter season, as only two storm events occurred during the study period. However, a fourteen-month study is not long enough to determine long-term coastal trends with certainty. Future works should address specific beach sediment sources and transport mechanisms and evaluate New Hampshire coastal resiliency in greater detail and over longer time scales.

REFERENCES

3.0: Gulf of Maine Resource Information (No. Offshore Wind Feasibility Study), 2009. University of Maine.

ArcGIS, 2014. ESRI.

Ashtech, 1998. Precise Differential Navigation and Surveying, PNAV. Magellan Corp.

Barnhardt, W.A., Belknap, D.F., Kelley, J.T., 1997. Stratigraphic evolution of the inner continental shelf in response to late Quaternary relative sea-level change, northwestern Gulf of Maine. Geological Society of America Bulletin 109, 612–630.

Barnhardt, W.A., Gehrels, W.R., Kelley, J.T., 1995. Late Quaternary relative sea-level change in the western Gulf of Maine: Evidence for a migrating glacial forebulge. Geology 23, 317–320.

Beardsley, R.C., Butman, B., 1974. Circulation on the New England Continental Shelf: Response to Strong Winter Storms.

Belknap, D.F., Anderson, B.G., Anderson, R.S., Anderson, W.A., Borns, H.W.J., Jacobson, G.L., Kelley, J.T., Shipp, R.C., Smith, D.C., Stuckenrath, R., Jr., Woodrow, B.T., Tyler, D.A., 1987. Late Quaternary sea-level changes in Maine. SEPM 41, 71–85.

Belknap, D.F., Kelley, J.T., Gontz, A.M., 2002. Evolution of the glaciated shelf and coastline of the northern Gulf of Maine, USA. JCR 37–55.

Belknap, D.F., Shipp, R.C., Kelley, J.T., Schnitker, D., 1989. Depositional sequence modeling of the late Quaternary geologic history, west-central Maine coast, in: Tucker, R.D., Marvinney, R.G. (Eds.), Studies in Maine Geology 5: Quaternary Geology. Department of Conservation, Maine Geological Survey, Augusta, Maine, pp. 29–46.

Bennett, D.S., Bothner, W.A., Moench, R.H., Thompson, J.B., 1997. Generalized Bedrock Geologic Map of New Hampshire.

Berg, R., 2016. Hurricane Joaquin (Tropical Cyclone Report No. AL 112015). National Hurricane Center.

Birch, F.S., 1990. Radiocarbon dates of Quaternary sedimentary deposits on the inner continental shelf of New Hampshire. Northeastern Geology 12, 218–230.

Blondin, H., 2016. New Hampshire Inventory of Tidal Shoreline Protection Structures (New Hampshire Coastal Program No. R-WD-16-09). New Hampshire Department of Environmental Services, Portsmouth, New Hampshire.

Bloom, A.L., 1959. Late Pleistocene changes of sea level in southwestern Maine (Ph.D. Thesis). Yale University.

Blott, S.J., Pye, K., 2001. GRADISTAT: a grain size distribution and statistics package for the analysis of unconsolidated sediments. Earth Surface Processes and Landforms 26, 1237–1248. doi:10.1002/esp.261

Bradley, E., 1964. Geology and ground-water resources of southeastern New Hampshire (U.S. Geological Survey Water Supply Paper No. 1695). United States Geological Survey.

Donnelly, J.P., Bryant, S.S., Butler, J., Dowling, J., Fan, L., Hausmann, N., Newby, P., Shuman, B., Stern, J., Westover, K., Webb III, T., 2001. 700 yr sedimentary record of intense hurricane landfalls in southern New England. GSA Bulletin 113, 714–727.

Duffy, W., Belknap, D.F., Kelley, J.T., 1989. Morphology and stratigraphy of small barrier-lagoon systems in Maine. Marine Geology 88, 243–262.

Dyke, A.S., Andrews, J.T., Clark, P.U., England, J.H., Miller, G.H., Shaw, J., Veillette, J.J., 2002a. The Laurentide and Innuitian ice sheets during the Last Glacial Maximum. Quaternary Science Reviews 21, 9–31.

Dyke, A.S., Andrews, J.T., Clark, P.U., England, J.H., Miller, G.H., Shaw, J., Veillette, J.J., 2002b. Ice sheets and sea level of the Last Glacial Maximum. Quaternary Science Reviews 21, 9–31.

Earth Systems Research Center, 2017. NH GRANIT: New Hampshire's Statewide GIS Clearinghouse [WWW Document]. NH GRANIT. URL http://www.granit.unh.edu/

Federal Agency for Cartography and Geodesy of Germany, 2005. NTRIP [WWW Document]. GNSS Data Center. URL https://igs.bkg.bund.de/ntrip/about (accessed 10.23.16).

Fitzgerald, D.M., Van Heteren, S., 1999. Classification of paraglacial barrier systems: coastal New England, USA. Sedimentology 46, 1083–1108. doi:10.1046/j.1365-3091.1999.00266.x

FitzGerald, D.M., Van Heteren, S., Rosen, P.S., 1993. Distribution, Morphology, Evolution, and Stratigraphy of Barriers along the New England Coast (No. 16), Boston University Technical Report.

Folk, R.L., 1980. Petrology of Sedimentary Rocks. Hemphill Publishing Company, Austin, Texas.

Fucella, J.E., Dolan, R., 1996. Magnitude of Subaerial Beach Disturbance during Northeast Storms. Journal of Coastal Research 12, 420–429.

Goldsmith, R., Ratcliffe, N.M., Robinson, P., Stanley, R.S., Hatch, Jr., N.L., Shride, A.F., Weed, E.G.A., Wones, D.R., 1983. Bedrock Geologic Map of Massachusetts.

Haddad, T.C., Pilkey, O.H., 1998. Summary of the New England Beach Nourishment Experience (1935-1996). Journal of Coastal Research 14, 1395–1404.

Hapke, C.J., Himmelstoss, E.A., Kratzmann, M.G., List, J.H., Thieler, E.R., 2010. National Assessment of Shoreline Change: Historical Shoreline Change along the New England and Mid-Atlantic Coasts (Open-File Report No. 2010–1118). USGS.

Harrison, W., Lyon, C.J., 1963. Sea-level and Crustal Movements along the New England-Acadian Shore. The Journal of Geology 71, 96–108.

Hayes, M.O., 1979. Barrier Island Morphology as a Function of Tidal and Wave Regime, in: Barrier Islands from the Gulf of St. Lawrence to the Gulf of Mexico. Academic Press, New York, USA, pp. 1–27.

Hayes, M.O., 1972. Forms of sediment accumulation in the beach zone, in: Waves on Beaches, and Resulting Sediment Transport. Academic Press, New York, USA, pp. 297–356.

Hein, C.J., FitzGerald, D.M., Barnhardt, W.A., 2007. Holocene evolution of the Merrimack Embayment, Northern Massachusetts, interpreted from shallow seismic stratigraphy, in: Coastal Sediments' 07, Proceedings of the 6th International Symposium on Coastal Engineering and Science of Coastal Sediment Processes: New Orleans, LA. pp. 856–866.

Hill, H.H., Kelley, J.T., Belknap, D.F., Dickson, S.M., 2004. The Effects Of Storms And Storm-Generated Currents On Sand Beaches In Southern Maine, USA. Marine Geology 210, 149–168.

Hill, H.H., Kelley, J.T., Belknap, D.F., Dickson, S.M., 2002. Co-measurement of beaches in Maine, USA: volunteer profiling of beaches and annual meetings. Journal of Coastal Research SI 36, 374–380.

IPCC, 2014. IPCC, 2014: Climate Change 2014: Synthesis Report. Contribution of Working Groups I, II, and III to the Fifth Assessment Report of the Intergovernmental Panel on Climate Change (Fifth Assessment Report of the Intergovernmental Panel on Climate Change). Intergovernmental Panel on Climate Change, Geneva, Switzerland.

Kelley, J.T., 2004. Coastal bluffs of New England (U.S. Geological Survey Professional Paper No. 1693).

Kelley, J.T., Barber, D.C., Belknap, D.F., FitzGerald, D.M., van Heteren, S., Dickson, S.M., 2005. Sand budgets at geological, historical and contemporary time scales for a developed beach system, Saco Bay, Maine, USA. Marine Geology 214, 117–142. doi:10.1016/j.margeo.2004.10.027

Kelley, J.T., Belknap, D.F., 1991. Physiography, surficial sediments, and Quaternary stratigraphy of the inner continental shelf and nearshore region of the Gulf of Maine. Continental Shelf Research 11, 1265–1283.

Kelley, J.T., Belknap, D.F., Claesson, S., 2010. Drowned coastal deposits with associated archaeological remains from a sea-level "slowstand": Northwestern Gulf of Maine, USA. Geology 38, 695–698. doi:10.1130/G31002.1

Kelley, J.T., Dickson, S.M., Belknap, D.F., Stuckenrath, R., Jr., 1992. Sea-level change and late Quaternary sediment accumulation on the southern Maine continental shelf, in: Fletcher, C.H., Wehmiller, J.F. (Eds.), Quaternary Coasts of the United States: Marine and Lacustrine Systems, Special Publication of the Society of Economic Paleontologists and Mineralogists. pp. 23–34.

Kocin, P.J., Uccellini, L.W., 2004. A Snowfall Impact Scale Derived from Northeast Storm Snowfall Distributions. Bulletin of the American Meteorological Society 85, 177–194. doi:10.1175/BAMS-85-2-177

Koteff, C., Moore, R.B., 1994. Surficial geologic map of the Kingston quadrangle, Rockingham County, New Hampshire. Geologic Quadrangle Map GQ-1740.

Krishen, P., Wake, C., Huber, M., Knuuti, K., Stampone, M., 2014. Sea-level Rise, Storm Surges, and Extreme Precipitation in Coastal New Hampshire: Analysis of Past and Projected Future Trends (No. RSA 483-E). Science and Technical Advisory Panel, New Hampshire Coastal Risks and Hazards Committee.

Leo, M.E., 2000. The Geomorphology, Sedimentology, and Storm Response of Beaches Along the Glaciated Coast of the Western Gulf of Maine (New Hampshire and Southwestern Maine). University of New Hampshire.

Lyon, C.J., Harrison, W., 1960. Rates of Sumbergence of Coastal New England and Acadia. Science 132, 295–296.

Lyons, J.B., Bothner, W.A., Moench, R.H., Thompson, J.B., 2006. Bedrock Geologic Map of New Hampshire - A Digital Representation of the Lyons and others 1997 map and ancillary files.

Masselink, G., Hughes, M., Knight, J., 2011. Introduction to Coastal Processes and Geomorphology, Second. ed. Hodder Education, New York, USA.

MathWorks, Inc., 2014. MATLAB R2014a. The MathWorks, Inc., Natick, Massachusetts.

Mayfield, M., 1992. Preliminary Report Hurricane Bob. National Hurricane Center.

Moore, R.B., 1987. Evidence indicative of former grounding-lines in the Great Bay Region of New Hampshire (Unpublished MS Thesis). University of New Hampshire, Durham, NH.

National Geodetic Survey, 2016a. User Friendly CORS (UFCORS) v4.0 [WWW Document]. National Geodetic Survey: Positioning America for the Future. URL http://www.ngs.noaa.gov/UFCORS/ (accessed 4.30.16).

National Geodetic Survey, 2016b. OPUS: Online User Positioning Service [WWW Document]. National Geodetic Survey. URL https://www.ngs.noaa.gov/OPUS/

National Geodetic Survey, 2014. The NGS Data Sheet (Survey Marks Datasheets). National Oceanic and Atmospheric Administration.

National Ocean Service, 2016. Estimation of Vertical Uncertainties in VDatum [WWW Document]. NOAA: Vertical Datum Transformation. URL http://vdatum.noaa.gov/docs/est_uncertainties.html

NDBC, 2016. Station 44098 - Jeffrey's Ledge, NH (160) [WWW Document]. National Data Buoy Center. URL www.ndbc.noaa.gov/station_history.php?station=44098

NDBC, 2009a. Climatic Summary Table - Station: IOSN3 [WWW Document]. National Data Buoy Center. URL www.ndbc.noaa.gov/data/climatic/IOSN3.txt

NDBC, 2009b. Climatic Summary Table - Station: 44007 [WWW Document]. National Data Buoy Center. URL http://www.ndbc.noaa.gov/data/climatic/44007.txt

NERACOOS, 2016. NERACOOS (Northeastern Regional Association of Coastal Ocean Observing Systems): Ocean and Climate Display [WWW Document]. The Gulf of Maine Research Institute's Ocean Data Products. URL neracoos.org/datatools

Nicholls, R.J., Orlando, S.P., 1993. A new dataset on the depth of disturbance and vertical erosion on beaches during storms.

Niederoda, A.W., Swift, D.J.P., Figgueiredo, A.G., Freeland, G.L., 1985. Barrier island evolution, middle Atlantic shelf, USA, Part II. Marine Geology 63, 363–396.

Nielson, J.W., 1989. The Formation of New England Coastal Fronts. AMS, Monthly Weather Review 117, 1380–1401.

NOAA, 2016. Sea Level Trends - 8419870 Seavey Island, Maine [WWW Document]. NOAA Tides & Currents. URL https://tidesandcurrents.noaa.gov/sltrends/sltrends_station.shtml?stnid=8419870 (accessed 10.18.16).

NOAA, 2015. VDatum, Vertical Datums Transformation. NOAA/NOS.

NOAA, 2013a. Portland, ME - Station ID: 8418150 [WWW Document]. NOAA Tides & Currents. URL https://tidesandcurrents.noaa.gov/waterlevels.html?id=8418150

NOAA, 2013b. Mean Sea Level Trend 8418150 Portland, Maine [WWW Document]. NOAA Tides & Currents. URL tidesandcurrents.noaa.gov/sltrends/sltrends_station.shtml?stnid=8418150

NOAA, 2013c. Fort Point, NH - Station ID: 8423898 [WWW Document]. NOAA Tides & Currents. URL https://tidesandcurrents.noaa.gov/stationhome.html?id=8423898

NOAA NCEI, 2016. Climate at a Glance: U.S. Time Series [WWW Document]. NOAA National Centers for Environmental Information. URL www.ncdc.noaa.gov/cag/time-series/us/27/0/tavg/ytd/12/1895-2016?base_prd=true%firstbaseyear=1901%lastbaseyear=2000

Novotny, R.F., 1969. The geology of the seacoast region, New Hampshire. New Hampshire Department of Resources and Economic Development, Concord, N.H.

Oldale, R.N., 1989. Timing and mechanisms for the deposition of the glaciomarine mud in and around the Gulf of Maine; a discussion of alternative models, in: Studies in Maine Geology, Quaternary Geology. pp. 1–10.

Oldale, R.N., Colman, S.M., Jones, G.A., 1993. Radiocarbon Ages from two submerged strandline features in the Western Gulf of Maine and a sea-level curve for the Northeastern Massachusetts coastal region. Journal of Quaternary Research 40, 38–45.

O'Leary, M., 2016. January 2016 blizzard ranked Category 4 on Northeast snowfall scale [WWW Document]. National Oceanic and Atmospheric Administration. URL http://www.noaa.gov/january-2016-blizzard-ranked-category-4-northeast-snowfall-scale (accessed 7.5.16).

Olson, N.F., Chormann, R., 2016. New Hampshire beaches: Shoreline Movement and Volumetric Change: BOEM/New Hampshire Cooperative Agreement (Contract M14ACOOO10) Technical Report (in review). BOEM Marine Minerals Branch.

Olson, N.F., Chormann, R., Ward, L.G., 2016. Change analysis of New Hampshire's beaches from multiple airborne LIDAR collections, historical charts, and orthophotography. Geological Society of America Abstracts with Programs 48.

Pilkey, O.H., Cooper, J.A.G. (Eds.), 2012. "Alternative" Shoreline Erosion Control Devices: A Review, in: Pitfalls of Shoreline Stabilization: Selected Case Studies. Springer Science+Business Media Dordrecht.

Pilkey, O.H., Wright, H.L., 1988. Seawalls Versus Beaches. Journal of Coastal Research SI 41–64.

Rockingham Planning Commission, 2015. From Tides to Storms: Preparing for New Hampshire's Future Coast: Assessing Risk and Vulnerability of Coastal Communities to Sea Level Rise and Storm Surge. Rockingham Planning Commission, Exeter, New Hampshire.

Sallenger, A.H., Doran, K.S., Howd, P.A., 2012. Hotspot of accelerated sea-level rise on the Atlantic coast of North America. Nature Climate Change Letters 5. doi:10.1038/NCClimate1597

Schimel, A., 2011. wgs2utm.m. MetOcean Solutions, Ltd., New Plymouth, New Zealand.

Shaw, J., Piper, D.J.., Fader, G.B.J., King, E.L., Todd, B.J., Bell, T., Batterson, M.J., Liverman, D.G.E., 2006. A conceptual model of the glaciation of Atlantic Canada. Quaternary Science Reviews 25, 2059–2081.

Thieler, E.R., Hammar-Klose, E.S., 1999. National Assessment of Coastal Vulnerability to Sea-Level Rise: Preliminary Results for the U.S. Atlantic Coast (U.S. Geological Survey Open-File Report No. 99–593). United States Geological Survey, Woods Hole, Massachusetts.

Tuttle, S.D., 1960. Evolution of the New Hampshire Shore Line. Bulletin of the Geological Society of America 71, 1211–1222.

Uchupi, E., Bolmer, S.T., 2008. Geologic evolution of the Gulf of Maine region. Earth-Science Reviews 91, 27–76. doi:10.1016/j.earscirev.2008.09.002

U.S. Army Corps of Engineers, 2016a. Hampton Beach Shore and Bank Protection Project [WWW Document]. U.S. Army Corps of Engineers. URL www.nae.usace.army.mil/Missions/Civil-Works/Shore-Bank-Protection/New-Hampshire/Hampton/

U.S. Army Corps of Engineers, 2016b. Wallis Sands State Beach Shore and Bank Protection Project [WWW Document]. U.S. Army Corps of Engineers. URL www.nae.usace.army.mil/Missions/Civil-Works/Shore-Bank-Protection/New-Hampshire/Wallis-Sands/

U.S. Army Corps of Engineers, 2009. Newburyport Harbor and Plum Island and Salisbury Beaches, Newbury, Newburyport and Salisbury, Massachusetts: 204 Beneficial Use of Dredged Material Detailed Project Report (Detailed Project Report and Environmental Assessment for Beneficial

Use of Dredged Materials from Maintenance Dredging No. 204). U.S. Army Corps of Engineers, New England District.

Wake, C., Burakowski, E., Kelsey, E., Hayhoe, K., Stoner, A., Watson, C., Douglas, E., 2011. Climate Change in the Piscataqua/Great Bay Region: Past, Present, and Future, in: Carbon Solutions New England. University of New Hampshire, Durham, NH, p. 54.

Ward, L.G., Adams, J.R., 2001. A Preliminary Assessment of Tidal Flooding along the New Hampshire Coast: Past, Present, and Future. New Hampshire Office of Emergency Management and the Office of State Planning Coastal Program.

Ward, L.G., McPherran, K.A., McAvoy, Z.S., Vallee-Anziani, M., 2016a. New Hampshire beaches: Sediment characterization: BOEM/New Hampshire Cooperative Agreement (Contract M14ACOOO10) Technical Report (in review). BOEM Marine Minerals Branch.

Ward, L.G., Vallee-Anziani, M., McAvoy, Z.S., 2016b. New Hampshire and vicinity continental shelf: Morphologic features and surficial sediments; BOEM/New Hampshire Cooperative Agreement (Contract M14ACOOO10) Technical Report (in review). BOEM Marine Minerals Branch.

Ward, L.G., Zaprowski, B.J., Trainer, K.D., Davis, P.T., 2008. Stratigraphy, pollen history and geochronology of tidal marshes in a Gulf of Maine estuarine system: Climatic and relative sea level impacts. Marine Geology 256, 1–17. doi:10.1016/j.margeo.2008.08.004

Wentworth, C.K., 1922. A scale of grade and class terms for clastic sediments. Journal of Geology 30, 377–392.

Wones, D.R., Goldsmith, R., 1991. Intrusive rocks of eastern Massachusetts, Chapter I (U.S. Geological Survey Professional Paper No. 1366–E–J).

Wright, L.D., Short, A.D., 1984. Morphodynamic variability of surf zones and beaches: a synthesis. Marine geology 56, 93–118.

APPENDIX 1. GRAIN SIZE ANALYSIS RESULT TABLES

The following six tables include detailed information about the grain size analysis of every sample taken during the summer 2015 sampling campaign (Ward et al., 2016a). Information includes date taken, sample location, textural group, sediment name, grain size mode, percentages of gravel, sand, and mud, mean grain size, sorting, and weight of each phi fraction. Abbreviations include "g" (gravel/gravelly), "s" (sand/sandy), "m" (mud/muddy), "v" (very), "f" (fine), "md" (medium), "c" (coarse), "PS" (poorly sorted), "MS" (moderately sorted), "MWS" (moderately well sorted), "VWS" (very well sorted), "Uni" (unimodal), "Bi" (bimodal). Parentheses represent "slightly", as in "(g)S" means "slightly gravelly sand". Tables are arranged in order by beach. The final set of tables are the results of the loss on ignition (LOI).

Wallis Sands		D20150610 WS01			D20150610 WS02			D20150706 WS03			D20150803 WS04				D20150610 WS05		
		A	B	C	A	B	C	A	B	C	A	B	C	D	A	B	C
	Textural Group	(g)S	(g)S	(g)S	(g)S	(g)S	(g)S	(g)S	(g)S	(g)S	(g)S	(g)S	(g)S	(g)S	S	(g)S	(g)S
	Sediment Name	(vfg)fS	(vfg)mdS	(vfg)fS	(vfg)mdS	(vfg)cS	(vfg)mds	(vfg)fS	(vfg)mdS	(vfg)fS	(vfg)mdS	(vfg)fS	(vfg)mdS	(fg)mdS	mdS	(vfg)mdS	(vfg)mdS
	Sed. Name (Wentworth)	(gr)fS	(gr)mdS	(gr)fS	(gr)mdS	slgmS	(gr)mdS	(gr)fS	(gr)mdS	(gr)fS	mdS	fS	mdS	mdS	mdS	(gr)mdS	(gr)mdS
	Sorting	PS	MS	MS	MWS	MWS	MS	MWS	MS	MWS	MWS	MWS	MWS	MWS	MWS	MWS	MWS
	Modes	Uni	Uni	Uni	Uni	Uni	Uni	Uni	Uni	Uni	Uni	Uni	Uni	Uni	Uni	Uni	Uni
	%G	3.5	1.0	1.0	0.0	0.1	1.5	0.1	1.2	0.6	0.0	0.2	0.4	0.4	0.0	0.0	O.2
	%S	96.0	98.6	98.8	99.7	99.5	98.2	99.8	98.7	99.3	100.0	99.8	99.5	99.6	100.0	100.0	99.5
	%M	0.5	0.4	0.2	0.2	0.4	0.3	0.1	0.1	0.1	0.0	0.0	0.1	0.0	0.0	0.0	0.3
	Mean - phi	1.5	1.6	1.6	1.1	1.1	1.4	2.0	1.7	1.9	1.8	2.0	1.7	1.7	1.6	1.8	1.3
	Mean mm	0.363	0.340	0.319	0.475	0.472	0.379	0.245	0.315	0.270	0.293	0.246	0.311	0.299	0.337	0.291	0.397
	Sorting - phi	1.149	0.872	0.869	0.560	0.688	0.840	0.56	0.75	0.61	0.63	0.52	0.66	0.53	0.50	0.56	0.63
	Skewness	-0.234	-0.171	-0.255	0.018	0.156	-0.120	-0.316	-0.281	-0.252	-0.267	-0.177	-0.101	-0.142	-0.110	-0.148	-0.075
	Kurtosis	0.909	0.893	0.929	0.98	0.91	0.897	1.373	1.165	1.241	1.027	1.147	1.024	1.192	1.033	0.969	1.009
	D10 - phi	-0.2	0.3	0.4	0.3	0.2	0.2	1.1	0.6	1.0	0.8	1.3	0.7	1.0	0.9	1.0	0.5
	D50 - phi	1.6	1.7	1.8	1.1	1.0	1.4	2.1	1.8	2.0	1.9	2.1	1.7	1.8	1.6	1.8	1.4
	D90 - phi	2.8	2.6	2.7	1.8	2.0	2.4	2.6	2.4	2.5	2.4	2.7	2.4	2.4	2.2	2.4	2.1
	D10 - microns	0.872	1.265	1.349	1.252	1.167	1.133	2.188	1.472	2.018	1.766	2.397	1.670	2.040	1.865	2.049	1.456
	D50 - microns	3.054	3.150	3.475	2.076	2.005	2.632	4.357	3.430	3.923	3.670	4.225	3.314	3.402	3.042	3.547	2.570
	D90 - microns	6.842	5.916	6.303	3.525	3.984	5.112	6.216	5.363	5.599	5.384	6.345	5.411	5.151	4.654	5.345	4.298
	Sample Wt. (g)	61.3	84.8	98.5	55.4	49.3	57.2	61.8	90.4	73.4	59.1	66.3	97.9	53.3	46.1	97.8	108.8
Class (ϕ)	-3.0																
	-2.5																
Gravel	-2.0	0.2		0.2					0.1	0.2			0.1	0.2			
	-1.5	1.3	0.4	0.1		0.2	0.8	0.1	0.5	0.2		0.1	0.1	0.1			
	-1.0	2.0	0.5	0.7	0.0	0.0	0.6	0.1	0.6	0.2	0.0	0.1	0.2	0.0		0.0	0.2
	-0.5	3.3	1.2	1.2	0.2	0.3	1.6	0.2	1.2	0.4	0.1	0.1	0.2	0.1	0.0	0.1	0.5
	0.0	5.4	2.9	2.7	2.1	2.5	3.7	0.6	2.0	0.8	0.6	0.2	0.8	0.2	0.1	0.2	1.6
	0.5	8.8	7.3	5.9	11.7	15.7	9.0	2.2	4.5	2.3	3.2	0.9	3.3	1.5	1.5	1.1	5.9
	1.0	13.5	14.9	13.1	32.4	31.2	18.7	5.1	8.8	5.6	9.4	3.7	10.8	6.8	10.5	7.2	19.5
	1.5	12.4	16.6	14.4	32.3	21.8	19.5	6.7	13.6	10.8	14.0	9.1	18.8	16.6	28.6	19.2	30.5
Sand	2.0	13.9	19.4	19.5	17.6	18.6	21.7	22.4	33.3	31.2	30.0	28.7	33.9	45.2	42.3	33.7	29.5
	2.5	20.9	25.0	27.8	3.0	8.6	19.3	48.7	28.5	38.1	36.1	42.3	23.8	24.8	15.1	32.2	10.6
	3.0	14.6	10.2	12.8	0.3	0.7	4.3	13.0	6.0	9.3	6.1	13.2	6.5	3.7	1.7	5.9	1.4
	3.5	2.2	1.1	1.4	0.1	0.1	0.5	0.9	0.8	0.7	0.4	1.6	1.4	0.5	0.2	0.3	0.1
	4.0	1.0	0.0	0.0	0.0	0.0	0.0	0.1	0.0	0.0	0.0	0.0	0.0	0.1	0.0	0.0	0.0
Mud	<4.0	0.5	0.4	0.2	0.2	0.4	0.3	0.1	0.1	0.1	0.0	0.0	0.1	0.0	0.0	0.0	0.3

Foss Beach		D20150718 FO02			D20150718 FO03			D20150718 FO04		
		A	B	C	A	B	C	A	B	C
Textural Group		(g)S	S	(g)S	gS	gS	gS	gS	S	S
Sediment Name		(vfg)fS	fS	(vfg)fS	fgfS	fgfS	fgfS	fgfS	fS	fS
Sed. Name (Wentworth)		(gr)fS	fS	(gr)fS	pfS	pfS	pfS	pfS	fS	fS
Sorting		WS	WS	WS	MS	PS	PS	PS	VWS	VWS
Modes		Uni	Uni	Uni	Uni	Bi	Bi	Bi	Uni	Uni
%G		0.1	0.0	0.3	6.1	27.2	20.0	14.6	0.0	0.0
%S		99.9	99.9	99.5	93.7	72.7	79.9	85.3	99.8	99.8
%M		0.0	0.1	0.2	0.2	0.1	0.1	0.1	0.2	0.2
Mean - phi		2.5	2.3	2.5	2.2	0.8	1.1	1.5	2.3	2.3
Mean mm		0.174	0.197	0.181	0.218	0.564	0.452	0.346	0.197	0.199
Sorting - phi		0.49	0.388	0.44	0.84	1.97	1.84	1.54	0.33	0.33
Skewness		0.274	0.143	0.114	-0.425	-0.780	-0.732	-0.722	0.220	0.178
Kurtosis		0.928	1.486	1.05	4.78	0.53	0.816	4.722	1.385	1.43
D10 - phi		2.0	1.8	2.0	0.9	-2.3	-2.1	-1.8	2.0	2.0
D50 - phi		2.4	2.3	2.4	2.2	2.2	2.2	2.2	2.3	2.3
D90 - phi		3.2	2.9	3.0	2.7	2.7	2.9	2.8	2.8	2.8
D10 - microns		0.247	0.278	0.247	0.527	4.872	4.205	3.598	0.247	0.248
D50 - microns		0.189	0.205	0.187	0.213	0.225	0.218	0.211	0.204	0.206
D90 - microns		0.107	0.136	0.126	0.151	0.151	0.139	0.141	0.139	0.142
Sample Wt. (g)		68.7	84.6	70.7	66.9	144.3	89.5	63.8	85.0	95.0
Class (ϕ)	-3.0									
	-2.5									
Gravel	-2.0				3.3	24.2	11.7	9.3		
	-1.5	0.1		0.3	1.6	1.5	4.1	2.5		
	-1.0	0.0		0.0	1.2	1.6	4.2	2.9		
Sand	-0.5	0.1	0.2	0.1	1.7	1.4	3.8	1.2	0.0	
	0.0	0.2	0.3	0.2	1.2	1.0	1.9	0.5	0.0	0.0
	0.5	0.3	0.4	0.4	0.6	0.4	0.6	0.2	0.0	0.0
	1.0	0.4	0.6	0.5	0.5	0.2	0.3	0.2	0.2	0.2
	1.5	0.9	1.2	1.0	0.7	0.3	0.5	0.6	0.6	0.5
	2.0	6.2	10.4	5.9	8.1	3.8	4.5	5.0	6.2	7.9
	2.5	49.7	61.6	47.2	63.5	49.2	43.5	52.9	69.3	69.4
	3.0	23.0	20.1	35.1	15.6	13.4	20.8	22.2	19.2	18.4
	3.5	19.1	5.0	8.8	1.7	3.0	3.9	2.4	3.8	3.3
	4.0	0.1	0.1	0.2	0.1	0.1	0.1	0.1	0.3	0.1
Mud	<4.0	0.1	0.1	0.2	0.2	0.1	0.1	0.1	0.2	0.2

Jenness Beach		D20150611 JN01			D20150611 JN02			D20150611 JN03			D20150803 JN04			
		A	B	C	A	B	C	A	B	C	A	B	C	D
Textural Group		(g)S	sG	(g)S	(g)S	sG	(g)S	sG	(g)S	(g)S	(g)S	(g)S	(g)S	gS
Sediment Name		(vfg)mdS	svfgfS	(fg)fS	(vfg)fS	sfG	(vfg)fS	smdG	(vfg)fS	(fg)fS	(vfg)fS	(fg)fS	(fg)fS	vfgS
Sed. Name (Wentworth)		(gr)mS	sgrG	(p)fS	(gr)fS	spG	(gr)fS	spG	(gr)fS	(p)fS	(g)fS	(p)fS	(p)fS	pfS
Sorting		MWS	PS	PS	WS	PS	MS	VPS	WS	PS	MWS	MWS	WS	PS
Modes		Uni	Bi	Uni	Uni	Bi	Uni	Bi	Uni	Bi	Uni	Uni	Uni	Uni
%G		0.1	52.8	5.0	0.0	37.4	1.8	60.7	0.0	1.7	0.2	1.5	1.3	14.3
%S		99.7	47.1	95.0	99.8	62.4	98.0	39.3	99.5	98.1	99.7	98.5	98.6	85.7
%M		0.2	0.1	0.0	0.2	0.1	0.2	0.0	0.5	0.2	0.1	0.0	0.1	0.0
Mean - phi		1.3	-0.9	2.1	2.0	0.0	2.1	-1.6	2.3	1.9	2.4	2.4	2.5	1.9
Mean mm		0.395	1.839	0.228	0.244	0.994	0.240	3.076	0.200	0.272	0.195	0.186	0.180	0.265
Sorting - phi		0.690	1.141	1.071	0.435	1.674	0.816	2.606	0.433	1.046	0.504	0.520	0.047	1.056
Skewness		0.023	0.346	-0.572	0.031	-0.384	-0.340	0.672	-0.057	-0.503	-0.028	-0.084	0.017	-0.555
Kurtosis		0.948	1.280	1.901	1.008	0.531	1.089	0.498	1.029	1.449	1.137	1.206	1.112	2.971
D10 - phi		0.5	-2.0	0.2	1.5	-2.3	0.8	-4.2	1.7	0.3	1.7	1.7	1.9	-1.5
D50 - phi		1.3	-1.1	2.4	2.0	0.6	2.2	-3.1	2.3	2.3	2.3	2.4	2.4	2.1
D90 - phi		2.3	0.8	3.0	2.6	1.9	2.9	2.4	2.9	2.9	2.9	3.0	3.0	2.6
D10 - microns		0.701	3.954	0.896	0.344	5.060	0.557	18.095	0.311	0.829	0.318	0.308	0.260	2.819
D50 - microns		0.400	2.077	0.186	0.243	0.661	0.219	8.441	0.201	0.203	0.197	0.184	0.184	0.235
D90 - microns		0.207	0.568	0.128	0.161	0.271	0.134	0.192	0.138	0.130	0.130	0.126	0.126	0.162
Sample Wt. (g)		60.0	62.4	100.1	106.2	152.3	91.0	135.4	90.8	127.9	84.8	82.6	87.4	87.6
Class (ϕ)	-4.0							15.8						
	-3.5							25.2						
	-3.0							10.7						
	-2.5							5.8						
Gravel	-2.0		9.4	2.6		33.2	0.8	1.2		0.9		1.2	0.7	5.9
	-1.5		18.5	0.8		2.6	0.4	1.4		0.4		0.1	0.4	4.2
	-1.0	0.1	24.9	1.6	0.0	1.7	0.6	0.6	0.0	0.4	0.2	0.2	0.2	4.2
	-0.5	0.4	16.2	2.2	0.0	2.0	0.9	0.8	0.1	0.4	0.3	0.1	0.2	1.1
	0.0	1.6	11.8	2.1	0.0	2.7	1.3	0.7	0.2	0.4	0.3	0.2	0.2	0.0
	0.5	7.2	6.9	2.3	0.1	5.5	2.2	0.8	0.3	13.7	0.4	0.4	0.3	0.0
	1.0	22.1	3.7	3.5	0.5	11.8	5.5	1.1	0.9	1.2	1.1	1.1	0.7	0.1
Sand	1.5	28.7	2.1	4.7	5.8	19.3	10.7	2.5	3.0	2.5	3.5	2.8	1.6	1.0
	2.0	22.7	1.8	7.0	39.8	14.6	15.9	10.0	14.8	7.6	13.3	9.2	6.4	24.5
	2.5	12.9	2.3	25.9	40.1	5.4	28.8	16.7	46.0	35.1	43.0	36.9	42.0	45.8
	3.0	3.4	1.8	40.4	11.5	0.8	28.6	5.9	34.2	30.8	31.3	38.4	37.8	10.5
	3.5	0.8	0.4	6.9	1.8	0.3	4.1	0.8	0.0	6.2	6.5	8.9	9.1	2.4
	4.0	0.0	0.0	0.1	0.1	0.0	0.1	0.0	0.0	0.1	0.1	0.3	0.4	0.1
Mud	<4.0	0.2	0.1	0.0	0.2	0.2	0.2	0.0	0.5	0.2	0.1	0.0	0.1	0.0

North Hampton		D20150817 NH01			D20150817 NH02				D20150817 NH03			
		A	B	C	A	B	C	D	A	B	C	D
Textural Group		S	S	gS	(g)S	(g)S	(g)S	S	S	gS	gS	(g)S
Sediment Name		mdS	mdS	fgmdS	(fg)mdS	(vfg)mdS	(vfg)mdS	mdS	mdS	vfgmdS	vfgmdS	(vfg)mdS
Sed. Name (Wentworth)		mdS	mdS	pmdS	(p)mdS	(gr)mdS	(gr)mdS	mdS	mdS	grmdS	grmdS	(p)mdS
Sorting		WS	MS	PS	WS	MS	MS	MWS	WS	PS	PS	MWS
Modes		Uni	Uni	Bi	Uni	Uni	Uni	Uni	Uni	Bi	Uni	Uni
%G		0.0	0.0	25.7	0.8	4.3	4.3	0.0	0.0	14.2	12.9	2.1
%S		100.0	100.0	74.3	99.2	95.7	95.7	100.0	100.0	85.8	87.1	97.9
%M		0.0	0.0	0.0	0.0	0.0	0.0	0.0	0.0	0.0	0.0	0.0
Mean - phi		1.7	1.6	0.6	1.5	1.4	1.5	1.2	1.7	0.8	0.8	1.3
Mean mm		0.302	0.328	0.674	0.346	0.377	0.343	0.425	0.301	0.593	0.578	0.394
Sorting - phi		0.455	0.796	1.821	0.495	0.790	0.737	0.627	0.387	1.346	1.309	0.597
Skewness		-0.072	-0.260	-0.620	-0.190	-0.048	-0.436	-0.005	-0.054	-0.479	-0.512	-0.185
Kurtosis		1.376	1.348	0.668	1.108	1.660	1.942	0.992	1.361	0.944	0.996	1.181
D10 - phi		1.1	0.4	-2.2	0.8	0.1	0.5	0.5	1.2	-1.4	-1.4	0.6
D50 - phi		1.7	1.7	1.5	1.6	1.6	1.7	1.2	1.7	1.2	1.2	1.4
D90 - phi		2.3	2.4	2.4	2.1	2.1	2.2	2.0	2.3	2.1	2.0	2.0
D10 - microns		0.463	0.733	4.625	0.568	0.904	0.709	0.717	0.443	2.690	2.557	0.682
D50 - microns		0.299	0.306	0.344	0.332	0.332	0.317	0.425	0.299	0.439	0.429	0.380
D90 - microns		0.201	0.186	0.192	0.236	0.236	0.215	0.253	0.210	0.240	0.254	0.256
Sample Wt. (g)		82.3	80.1	117.5	66.1	84.0	101.6	62.8	87.2	106.5	129.7	81.3
Class (ϕ)	-3.0											
	-2.5											
Gravel	-2.0			17.6	0.5	1.6	2.0			5.4	5.9	1.5
	-1.5			4.1	0.2	1.3	1.1			4.0	3.0	0.3
	-1.0			4.0	0.1	1.4	1.2			4.8	4.0	0.3
Sand	-0.5	0.0	2.8	4.1	0.4	1.9	1.4	0.2	0.0	5.8	6.1	0.7
	0.0	0.2	3.5	3.0	0.6	2.6	1.7	1.8	0.2	6.6	6.3	1.3
	0.5	0.9	4.2	2.9	2.2	4.0	2.6	8.3	0.6	7.3	7.3	4.2
	1.0	5.0	8.3	4.2	9.3	8.6	6.5	24.5	3.8	10.6	10.6	14.7
	1.5	17.4	15.2	7.5	27.7	19.9	17.0	32.1	15.4	14.7	15.0	33.9
	2.0	54.5	37.9	29.1	47.0	46.8	50.4	24.1	61.1	29.6	33.1	35.4
	2.5	18.1	20.5	16.7	10.7	10.5	13.3	7.1	17.0	10.1	7.3	7.0
	3.0	3.4	6.7	5.6	1.0	1.1	2.5	1.7	1.8	1.1	1.1	0.7
	3.5	0.5	1.0	1.1	0.2	0.2	0.3	0.3	0.1	0.1	0.1	0.1
	4.0	0.0	0.1	0.1	0.0	0.0	0.0	0.0	0.0	0.0	0.0	0.0
Mud	<4.0	0.0	0.0	0.0	0.0	0.0	0.0	0.0	0.0	0.0	0.0	0.0

Hampton Beach		D20150618 HA01			D20150617 HA03				D20150707 HA04			
		A	B	C	A	B	C	D	A	B	C	D
Textural Group		(g)S	(g)S	(g)S	(g)S	(g)S	(g)S	S	(g)S	(g)S	(g)S	S
Sediment Name		(vfg)cS	(vfg)mdS	(vfg)fS	(vfg)cS	(vfg)cS	(vfg)mdS	mdS	(vfg)fS	(vfg)mdS	(vfg)mdS	fS
Sed. Name (Wentworth)		(gr)cS	(gr)mdS	(gr)fS	(gr)cS	(gr)cS	(gr)mdS	mdS	(gr)fS	(gr)mdS	(gr)mdS	fS
Sorting		MS	MWS	MS	PS	MS	MS	MWS	PS	MS	MS	WS
Modes		Uni	Uni	Uni	Bi	Uni	Bi	Uni	Uni	Uni	Uni	Uni
%G		1.1	0.3	0.2	0.6	4.7	0.1	0.0	1.1	0.5	2.0	0.0
%S		98.3	99.7	99.6	99.1	95.3	90.1	99.8	98.9	99.4	97.9	99.9
%M		0.6	0.0	0.2	0.3	0.0	9.8	0.2	0.0	0.1	0.1	0.1
Mean - phi		0.7	1.0	1.8	1.2	0.5	1.6	1.6	1.6	1.4	1.3	2.1
Mean mm		1.576	2.024	3.375	2.342	1.376	2.992	2.965	2.973	2.715	2.454	4.196
Sorting - phi		0.797	0.671	0.806	1.028	0.910	0.925	0.647	1.068	0.773	0.960	0.482
Skewness		0.080	-0.082	-0.281	-0.007	0.062	0.306	0.012	-0.244	0.027	-0.072	-0.091
Kurtosis												
D10 - phi		-0.3	0.1	0.6	-0.1	-0.7	0.7	0.7	0.0	0.5	0.0	1.5
D50 - phi		0.6	1.0	1.9	1.2	0.4	1.5	1.6	1.7	1.4	1.3	2.1
D90 - phi		1.8	1.9	2.7	2.5	1.7	3.3	2.4	2.8	2.4	2.4	2.7
D10 - microns		1.267	0.919	0.675	1.072	1.624	0.599	0.612	0.971	0.701	0.976	0.350
D50 - microns		0.652	0.485	0.267	0.426	0.744	0.345	0.336	0.299	0.373	0.399	0.232
D90 - microns		0.293	0.276	0.155	0.178	0.309	0.104	0.191	0.144	0.188	0.185	0.150
Sample Wt. (g)		71.1	71.6	117.0	113.1	72.2	77.8	69.3	73.6	69.3	86.0	73.5
Class (ϕ)	-3.0											
	-2.5											
	-2.0								0.3		0.8	
Gravel	-1.5	0.4		0.0	0.1	0.9	0.1		0.2	0.2	0.5	
	-1.0	0.8	0.3	0.2	0.5	3.9	0.0		0.6	0.3	0.7	
	-0.5	4.3	1.9	0.6	3.1	9.0	0.0	0.1	2.2	0.6	2.0	0.0
	0.0	15.5	3.8	2.3	8.0	17.1	0.2	0.5	5.9	1.8	5.2	0.2
	0.5	23.9	16.0	5.5	14.4	22.0	2.6	3.7	9.7	6.5	10.7	0.4
	1.0	21.5	25.4	9.3	17.7	22.0	14.7	13.6	13.7	18.1	17.5	1.9
	1.5	17.5	28.7	13.9	13.5	12.0	29.9	27.1	11.7	26.4	18.9	6.2
Sand	2.0	11.5	19.1	22.3	16.4	7.6	31.1	32.4	11.8	23.1	19.6	31.3
	2.5	3.1	4.0	30.3	16.1	4.1	9.7	15.5	22.6	15.1	15.3	43.7
	3.0	0.7	0.5	13.2	8.0	1.1	1.6	4.9	18.3	6.3	6.9	12.8
	3.5	0.3	0.2	2.0	1.9	0.3	0.3	1.8	2.9	1.5	1.6	3.2
	4.0	0.1	0.0	0.1	0.1	0.0	0.0	0.2	0.1	0.1	0.1	0.2
Mud	<4.0	0.5	0.0	0.2	0.3	0.0	9.8	0.2	0.0	0.1	0.0	0.1

Seabrook Beach		D20150719 SE01				D20150719 SE02				D20150719 SE03			
		A	B	C	D	A	B	C	D	A	B	C	D
Textural Group		S	(g)S	(g)S	(g)S	(g)S	(g)S	(g)S	(g)S	(g)S	(g)S	(g)S	(g)S
Sediment Name		mdS	(vfg)mdS	(vfg)mdS	(vfg)mdS	(vfg)cS	(vfg)fS	(vfg)mdS	(vfg)cS	(vfg)cS	(vfg)fS	(vfg)mdS	(vfg)cS
Sed. Name (Wentworth)		mdS	mdS	mdS	mdS	cS	mdS	mdS	cS	cS	mdS	mdS	cS
Sorting		MWS	MWS	MS	MS	MS	MS	MWS	MWS	MS	PS	MWS	MWS
Modes		Uni	Uni	Uni	Uni	Uni	Uni	Uni	Uni	Uni	Uni	Uni	Uni
%G		0.0	0.1	0.3	0.2	1.4	0.9	0.0	0.1	1.0	0.8	0.2	0.0
%S		100.0	99.9	99.6	99.8	98.6	99.1	100.0	99.9	99.0	99.2	99.8	100.0
%M		0.0	0.0	0.1	0.0	0.0	0.0	0.0	0.0	0.0	0.0	0.1	0.0
Mean - phi		1.3	1.0	1.5	1.7	0.8	1.8	1.8	0.8	0.7	1.3	1.8	0.7
Mean mm		2.544	2.014	2.912	3.322	1.689	3.470	3.494	1.765	1.647	2.505	3.413	1.579
Sorting - phi		0.563	0.654	0.743	0.756	0.913	0.844	0.602	0.631	0.907	1.092	0.621	0.601
Skewness		0.052	0.007	-0.339	-0.163	-0.033	-0.476	-0.106	0.068	0.076	-0.296	-0.114	0.076
Kurtosis		0.888	0.977	1.220	1.035	0.842	1.570	1.135	0.981	0.863	0.752	1.131	1.070
D10 - phi		0.6	0.1	0.4	0.7	-0.4	0.2	1.0	0.1	-0.4	-0.3	1.0	0.0
D50 - phi		1.3	1.0	1.7	1.8	0.8	2.0	1.8	0.8	0.7	1.6	1.8	0.6
D90 - phi		2.1	1.9	2.3	2.6	1.9	2.6	2.5	1.7	1.9	2.5	2.5	1.4
D10 - microns		0.640	0.904	0.782	0.635	1.328	0.845	0.487	0.955	1.308	1.200	0.515	1.035
D50 - microns		0.393	0.501	0.313	0.288	0.585	0.246	0.280	0.575	0.628	0.334	0.286	0.646
D90 - microns		0.233	0.275	0.199	0.162	0.269	0.168	0.181	0.307	0.265	0.173	0.183	0.370
Sample Wt. (g)		52.0	52.9	65.6	96.6	83.3	89.0	68.0	61.4	65.3	45.6	75.1	57.1
Class (ϕ)	-3.0												
	-2.5												
Gravel	-2.0						0.2						
	-1.5				0.1	0.2	0.2			0.1	0.2		
	-1.0		0.1	0.3	0.0	1.2	0.5	0.0	0.1	1.0	0.6	0.2	0.0
	-0.5	0.1	0.8	1.2	0.7	6.2	2.4	0.3	0.5	5.6	4.4	0.2	1.2
	0.0	0.6	4.7	4.3	2.2	15.2	4.5	0.8	6.4	16.5	10.6	0.9	9.8
	0.5	1.9	14.9	5.9	4.0	17.1	4.4	1.8	22.6	20.1	11.0	2.3	29.8
	1.0	25.1	29.6	8.5	9.5	18.3	4.3	5.7	34.0	19.2	10.4	6.9	33.9
	1.5	31.7	27.3	15.8	18.1	18.7	7.8	17.0	21.7	15.8	10.0	17.0	17.4
Sand	2.0	28.3	17.3	39.1	25.9	16.5	23.7	35.7	11.5	13.9	16.3	36.4	6.3
	2.5	10.3	4.5	21.8	26.2	5.5	39.9	29.2	2.5	6.6	25.6	27.2	1.1
	3.0	1.5	0.6	2.8	11.8	0.8	11.0	8.5	0.5	1.0	9.9	8.1	0.3
	3.5	0.3	0.2	0.3	1.5	0.3	1.0	0.8	0.2	0.1	1.0	0.7	0.1
	4.0	0.1	0.0	0.0	0.0	0.0	0.0	0.0	0.0	0.0	0.1	0.0	0.0
Mud	<4.0	0.0	0.0	0.1	0.0	0.0	0.0	0.0	0.0	0.0	0.0	0.0	0.0

Wallis Sands		
Sample	Date Collected (YYYYMMDD)	% LOI
WS01A	20150610	0.21
WS01B	20150610	0.34
WS01C	20150610	0.34
WS02A	20150610	0.16
WS02B	20150610	0.22
WS02C	20150610	0.34
WS03A	20150706	0.40
WS03B	20150706	0.40
WS03C	20150706	0.37
WS04A	20150803	0.32
WS04B	20150803	0.38
WS04C	20150803	-----
WS04D	20150803	-----
WS05A	20150610	0.17
WS05B	20150610	0.26
WS05C	20150610	-----

Jenness Beach		
Sample	Date Collected (YYYYMMDD)	% LOI
JN01A	20150611	-----
JN01B	20150611	-----
JN01C	20150611	-----
JN02A	20150611	0.49
JN02B	20150611	0.38
JN02C	20150611	0.38
JN03A	20150611	0.22
JN03B	20150611	0.36
JN03C	20150611	0.32

Foss Beach		
Sample	Date Collected (YYYYMMDD)	% LOI
FO02A	20150718	0.23
FO02B	20150718	0.35
FO02C	20150718	0.34
FO03A	20150718	0.31
FO03B	20150718	0.25
FO03C	20150718	0.36
FO04A	20150718	0.35
FO04B	20150718	0.24
FO04C	20150718	0.26

North Hampton Beach		
Sample	Date Collected (YYYYMMDD)	% LOI
NH01A	20150817	0.18
NH01B	20150817	0.31
NH01C	20150817	0.30
NH02A	20150817	0.15
NH02B	20150817	0.19
NH02C	20150817	0.31
NH02D	20150817	0.15
NH03A	20150817	0.13
NH03B	20150817	0.57
NH03C	20150817	-----
NH03D	20150817	-----

Hampton Beach		
Sample	Date Collected (YYYYMMDD)	% LOI
HA01A	20150618	0.16
HA01B	20150618	0.17
HA01C	20150618	0.25
HA03A	20150618	0.26
HA03B	20150618	0.20
HA03C	20150618	0.13
HA03D	20150618	0.14
HA04A	20150618	0.19
HA04B	20150618	0.17
HA04C	20150618	0.18
HA04D	20150618	-----

Seabrook Beach		
Sample	Date Collected (YYYYMMDD)	% LOI
SE01A	20150719	0.13
SE01B	20150719	0.14
SE01C	20150719	0.20
SE01D	20150719	0.28
SE02A	20150719	0.19
SE02B	20150719	0.25
SE02C	20150719	0.29
SE02D	20150719	0.18
SE03A	20150719	0.23
SE03B	20150719	0.23
SE03C	20150719	0.26
SE03D	20150719	0.17

APPENDIX 2. GNSS ROVER DATA PROCESSING STEPS

The following are the detailed steps taken to process the GNSS Rover data from the raw files collected in the field to the final interpolated profiles.

1. Atmospheric corrections were applied to the raw GNSS data. Differential correction data were downloaded from the Salisbury, Massachusetts (MASA) Continuously Operating Reference Station (CORS) National Geodetic Service (NGS) website for the time period of the survey (National Geodetic Survey, 2016a).
2. The raw GNSS data file from the survey were integrated with the differential corrections from the CORS station using Ashtech's Precise Differential Surveying and Navigation (PNAV) software (Ashtech, 1998). The file produced by PNAV for the survey contained the following information: date, time, latitude and longitude (relative to the WGS84 ellipsoid), antenna elevation (relative to the WGS84 ellipsoid), root mean square error (RMS) of the errors in the east, north, and up position data, the position dilution of precision (PDOP), relating to the geometry of the satellite coverage, the number of satellites used to determine position (SVs), and the velocity of the rover in the east, north, and up directions.
3. The corrected data from the survey was loaded into MATLAB using code (readpp.m) written by Dr. Thomas Lippmann at the University of New Hampshire Center for Coastal and Ocean Mapping. The survey data was edited in MATLAB to remove data of poor quality by setting threshold criteria of: RMS (root mean square) errors ≤ 0.1, PDOP (position dilution of precision) ≤ 0.1, and SVs (number of satellites) ≥ 5. These thresholds were recommended for this study by Dr. Lippmann.

4. The latitude and longitude data (referenced to the WGS84 ellipsoid) were converted into Universal Transverse Mercator (UTM) Easting and Northing coordinates using wgs2utm.m in MATLAB (Schimel, 2011). The elevation data were adjusted to take into account the height of the antenna pole and the height from the pole to the antenna reference point (1.84m and 6.7cm, respectively).
5. Using the start and end times of each profile recorded in the field, the data for each individual profile were separated out from the rest of the survey data.
6. Following profile data extraction, the profile line was straightened, the position data set to evenly-spaced distances (1m apart), and elevations at the new positions were interpolated in MATLAB. In order to calculate cumulative distances to the plot beach profiles, it was essential that every profile be perfectly straight. If profiles were not perfectly straight (due to slight variations in the walking path of each survey and the uncertainties in the GNSS positions data), the cumulative distance calculated for a profile would be too long, and the profile shape would appear distorted. This would cause the geomorphologic features to appear in incorrect locations on the profile, especially on the steeper parts of the profile (Figure 4-6 and Figure 4-7). This would also be problematic for calculating sediment volume changes.
7. Therefore, an idealized, straight profile line was created using the same starting and ending points at each station, chosen so that the straightened profiles would overlie each other and be perpendicular to the beach. A vector of linear, evenly spaced points (1m apart) was generated, beginning at the chosen starting point of that station and ending at the chosen end point of that station. Then, the angle (theta) between the actual survey line and the idealized profile line was calculated in MATLAB using the four-quadrant inverse tangent (atan2.m). New Easting coordinates were generated for the idealized profile line by starting with the Easting coordinate of the profile starting point and adding the value of each vector value multiplied by the cosine of

the angle theta: $Enew = E(1) + (Dist .* \cos(\theta))$, where Dist is the vector of evenly spaced points, and ".*" multiplies every value of the vector Dist by cos(Θ). New Northing coordinates were generated in the same manner, except that the vector was multiplied by the sine of theta: $Nnew = N(1) + (Dist .* \sin(\theta))$.

8. In order to interpolate the elevation values at each of the new position values of the idealized profile, a surface was created in MATLAB using the profile data. The surface was necessary because griddata.m cannot confidently interpolate points along a single profile line because there are so few neighbors (bilinear interpolation [linear interpolation in two dimensions] requires at least four adjacent values). The surface was generated by creating two identical copies of the original profile line, 5m perpendicular distance to each side of the original profile line. From this surface, the new elevation values were bilinearly interpolated. On Seabrook Beach, where a lack of station markers made returning to the same starting point in the field difficult, this surface was extended to 10m to each side of the original profile line.
9. The copies of the profile line were created in the following way. A rotation matrix was used to rotate the original profile line in Euclidean space to an orthonormal coordinate system. Two copies of the original profile line were created in MATLAB, one 5m to each side (±5m perpendicular to the profile) of the measured profile line. The three profile lines acted as a surface, from which the elevations at the idealized profile points could be interpolated linearly (griddata.m).
10. The interpolated elevation data were transformed from the WGS84 reference ellipsoid to Mean Lower Low Water (MLLW) using VDatum (NOAA, 2015) for visualization purposes.
11. The cumulative sum of the idealized distance data for the profile was calculated and plotted against the interpolated MLLW elevation data for each profile line in the survey to create beach profiles.

APPENDIX 3. COMPARISONS OF CORRECTED AND UNCORRECTED PROFILES

To determine the accuracy and acceptability of the profile interpolation methodology, uncorrected and corrected (interpolated) profile data were compared at ten stations. The following figures are comparisons of uncorrected and corrected profile at stations from each beach. The position figures show corrected and uncorrected profile positions and are plotted as UTM Easting vs. Northing coordinates (m). The profile elevation figures show corrected and uncorrected elevations for the same station, and are plotted as UTM Easting coordinates (m) vs. WGS84 Ellipsoidal Elevation (m). Due to the fact that profiles generally do not trend directly East, the values on the Easting scales of the position figures appear shorter than the Easting scales on the distance vs. elevation figures; however, for the purpose of comparison, examining the profiles as elevation vs Easting is sufficient for elevation differences between corrected and uncorrected profiles to be seen.

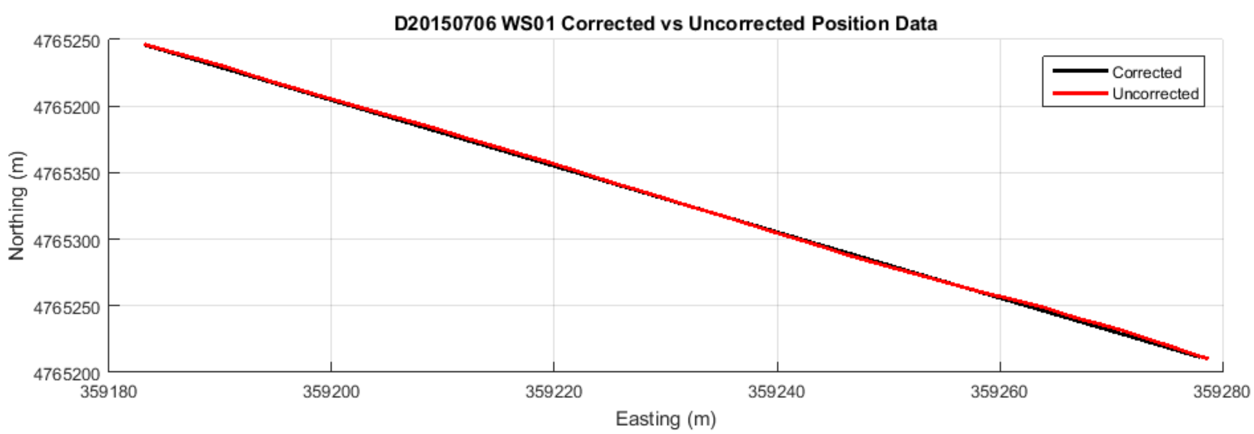

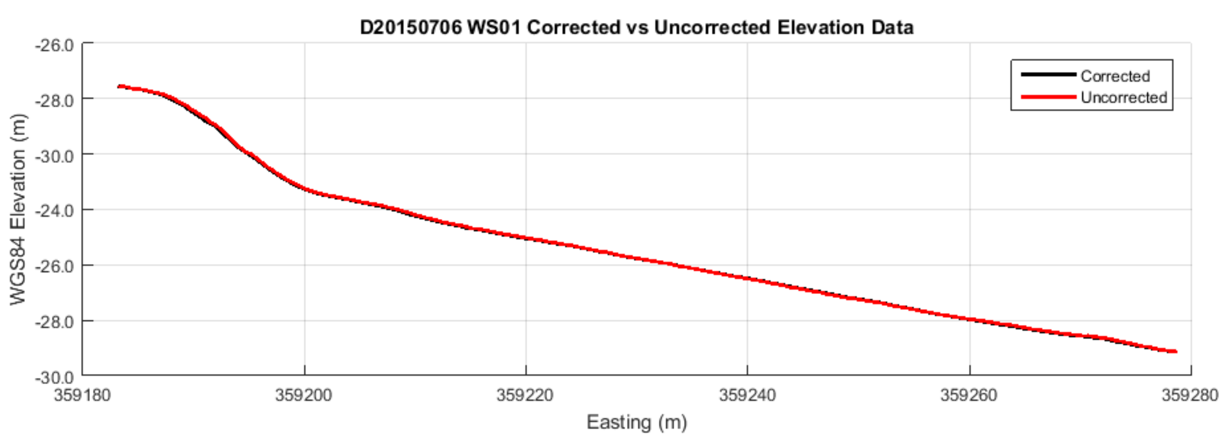

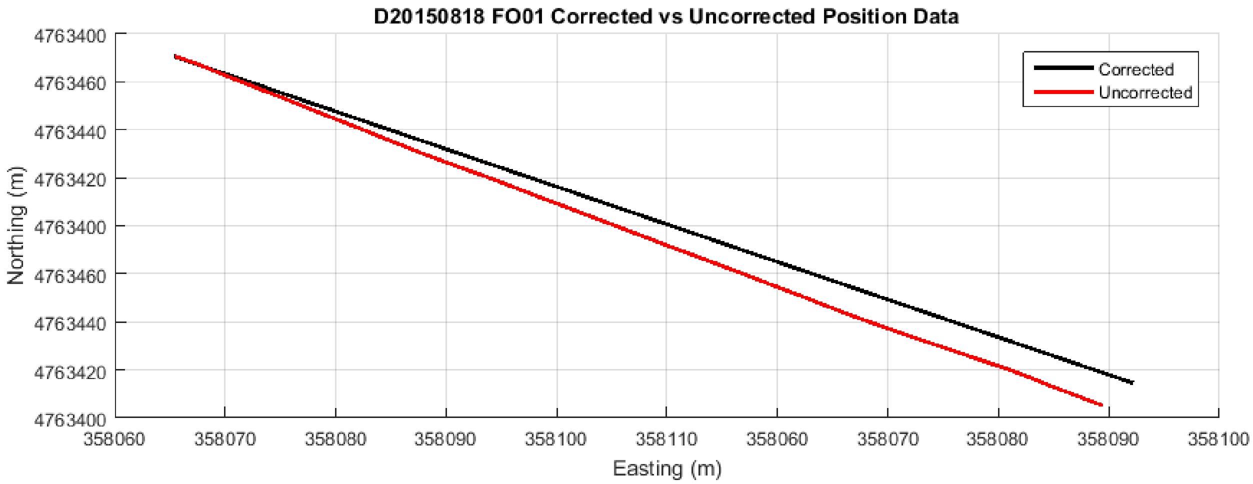
D20150818 FO01 Corrected vs Uncorrected Position Data
Corrected
Uncorrected
Northing (m)
Easting (m)

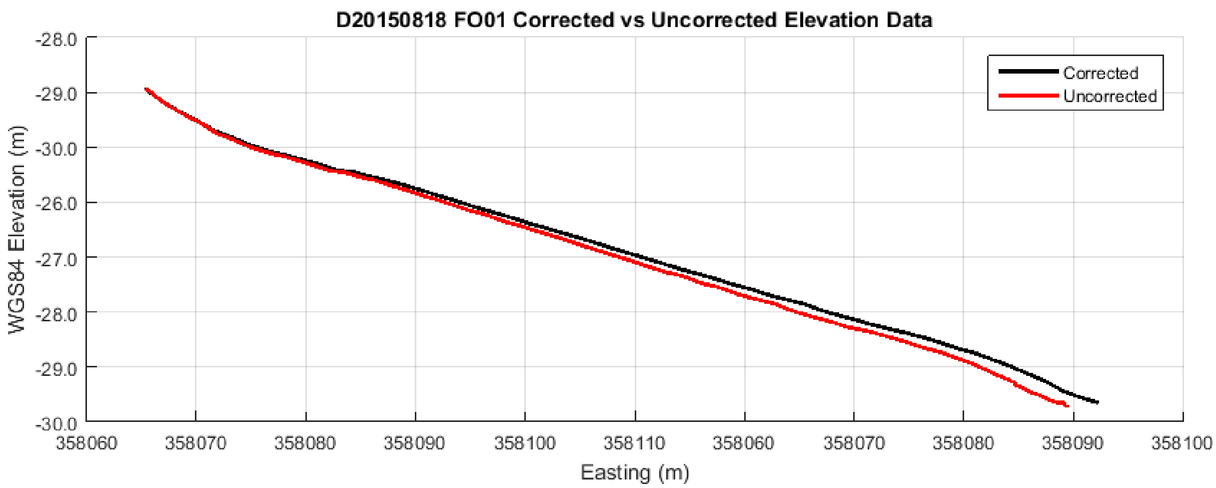
D20150818 FO01 Corrected vs Uncorrected Elevation Data
Corrected
Uncorrected
WGS84 Elevation (m)
Easting (m)

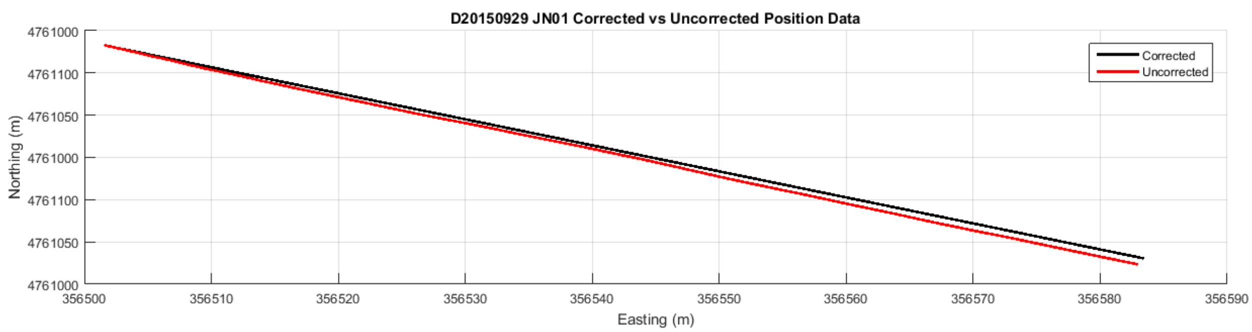
D20150929 JN01 Corrected vs Uncorrected Position Data
Corrected
Uncorrected
Northing (m)
Easting (m)

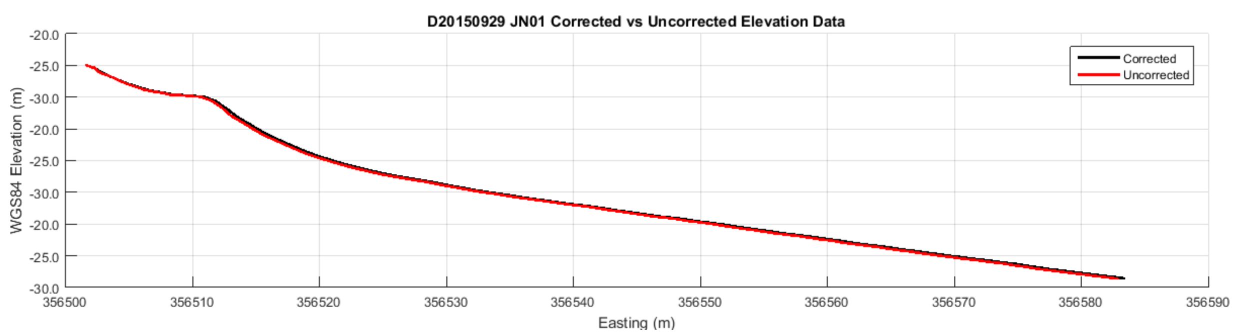
D20150929 JN01 Corrected vs Uncorrected Elevation Data
Corrected
Uncorrected
WGS84 Elevation (m)
Easting (m)

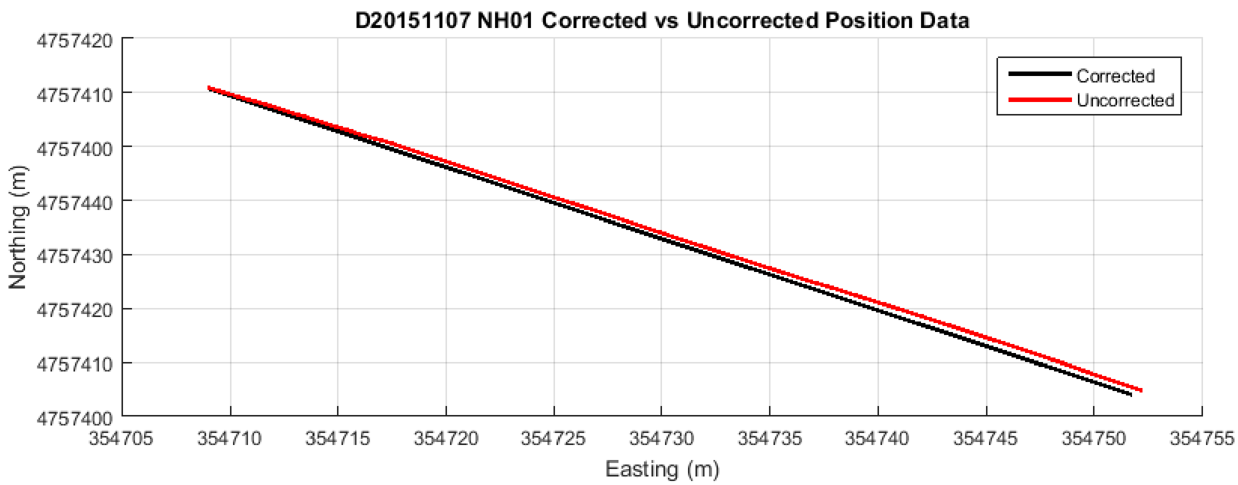
D20151107 NH01 Corrected vs Uncorrected Position Data
Northing (m)
Easting (m)
Corrected
Uncorrected

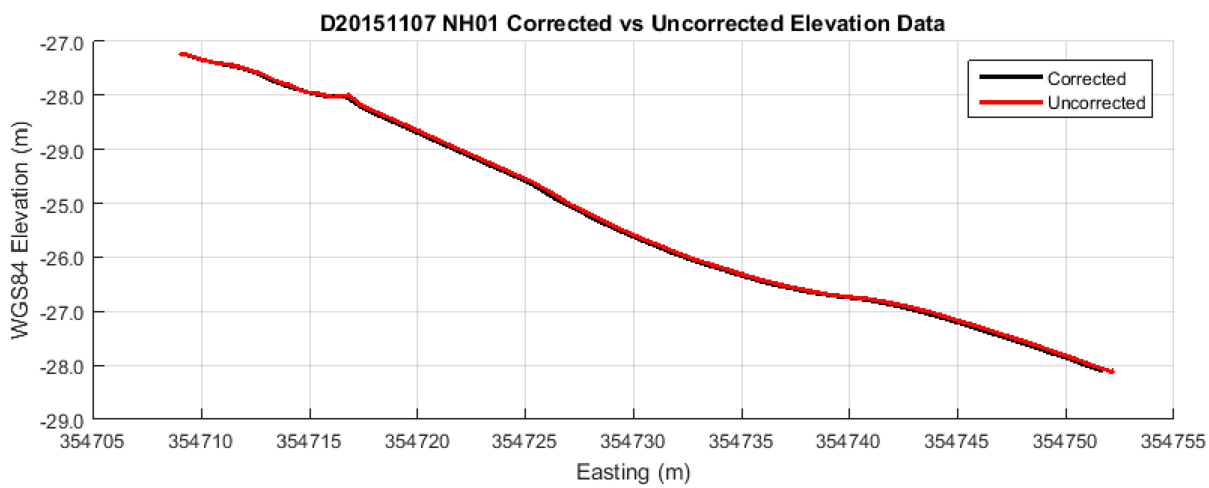
D20151107 NH01 Corrected vs Uncorrected Elevation Data
WGS84 Elevation (m)
Easting (m)
Corrected
Uncorrected

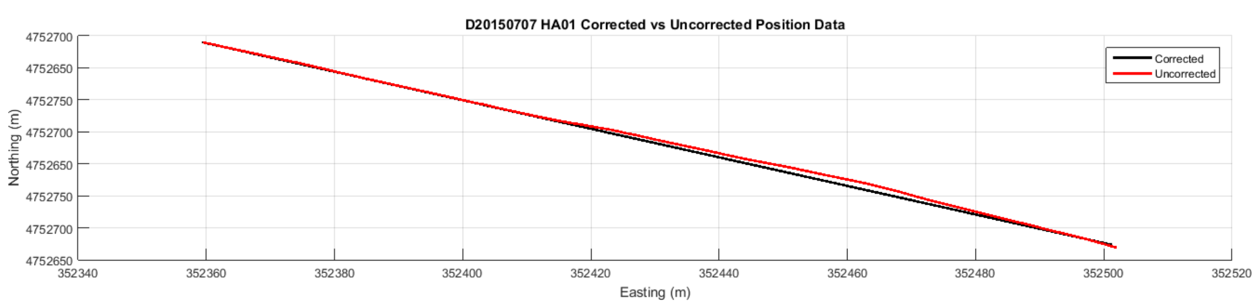
D20150707 HA01 Corrected vs Uncorrected Position Data
Northing (m)
Easting (m)
Corrected
Uncorrected

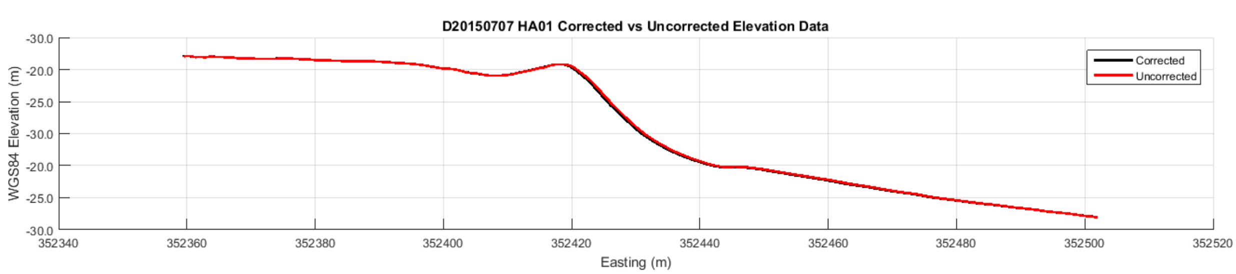
D20150707 HA01 Corrected vs Uncorrected Elevation Data
WGS84 Elevation (m)
Easting (m)
Corrected
Uncorrected

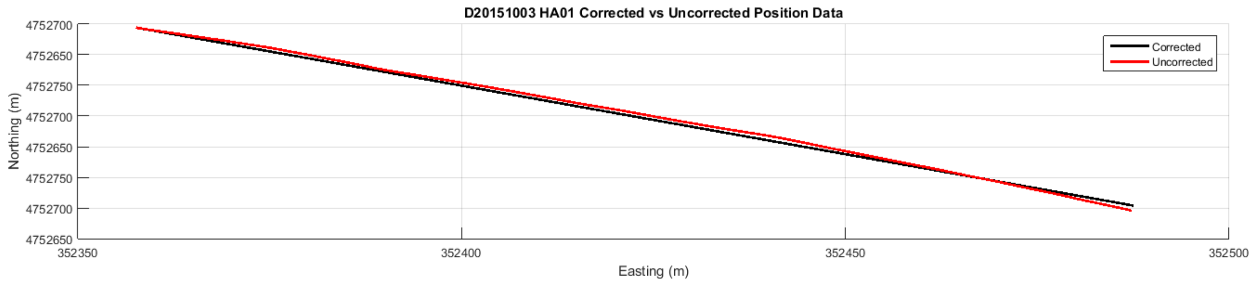
D20151003 HA01 Corrected vs Uncorrected Position Data
Northing (m)
Easting (m)
Corrected
Uncorrected

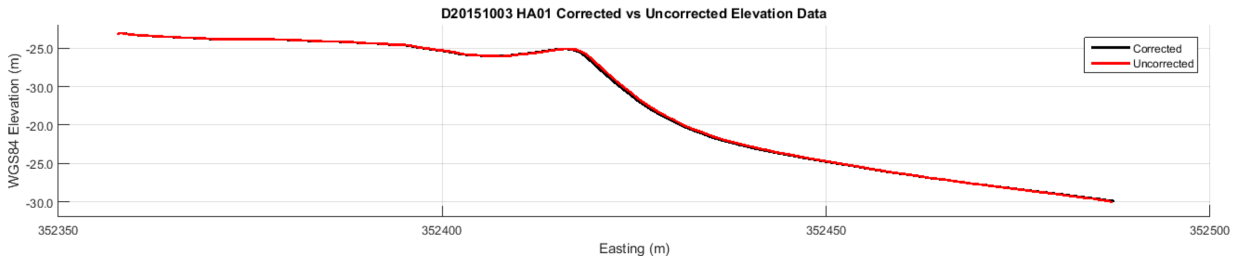
D20151003 HA01 Corrected vs Uncorrected Elevation Data
WGS84 Elevation (m)
Easting (m)
Corrected
Uncorrected

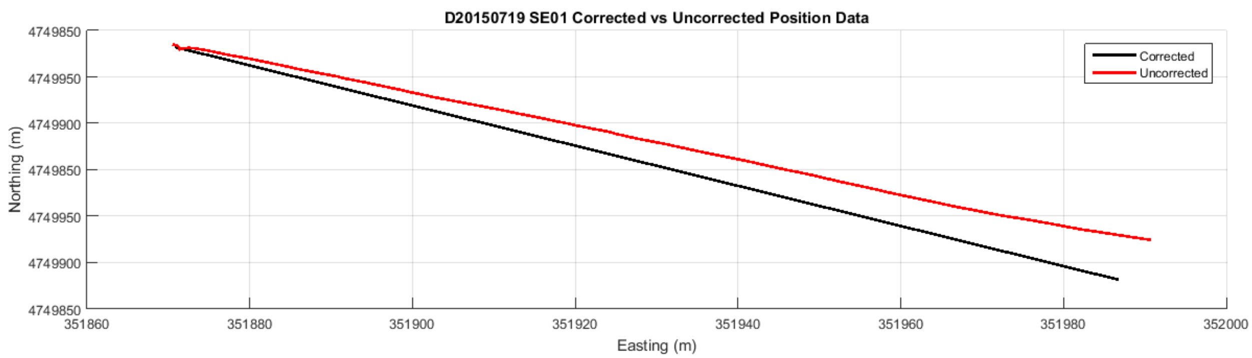
D20150719 SE01 Corrected vs Uncorrected Position Data
Northing (m)
Easting (m)
Corrected
Uncorrected

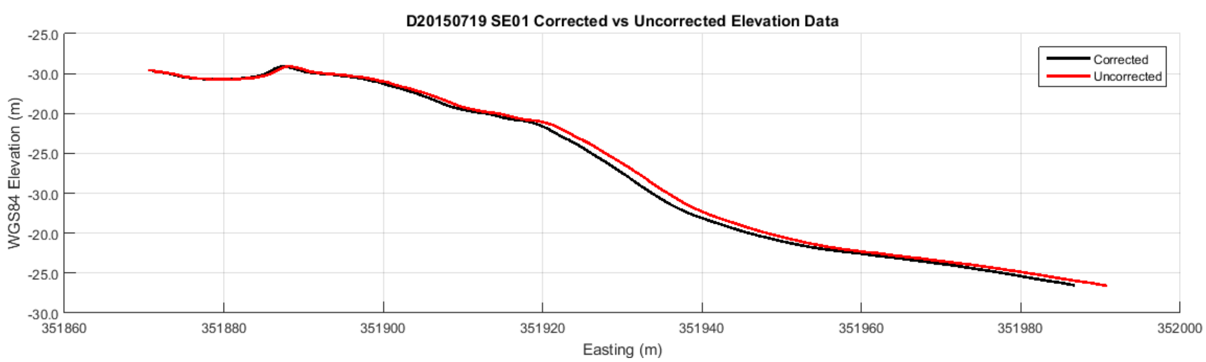
D20150719 SE01 Corrected vs Uncorrected Elevation Data
WGS84 Elevation (m)
Easting (m)
Corrected
Uncorrected

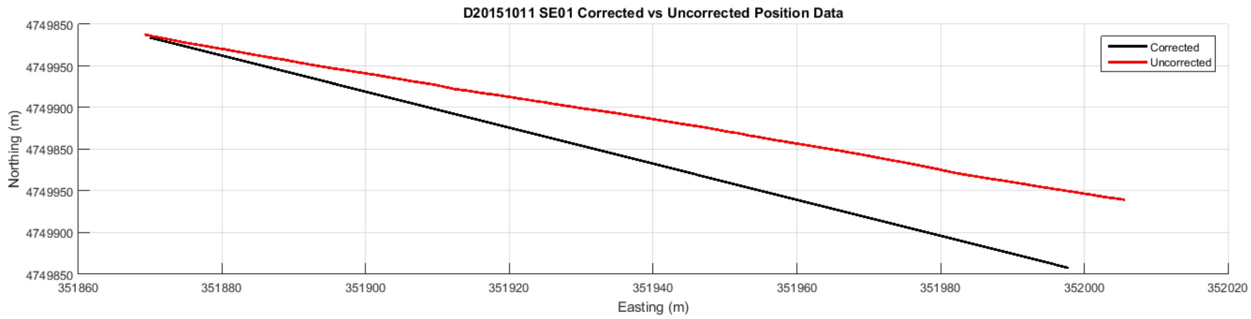
D20151011 SE01 Corrected vs Uncorrected Position Data
Corrected
Uncorrected
Northing (m)
Easting (m)

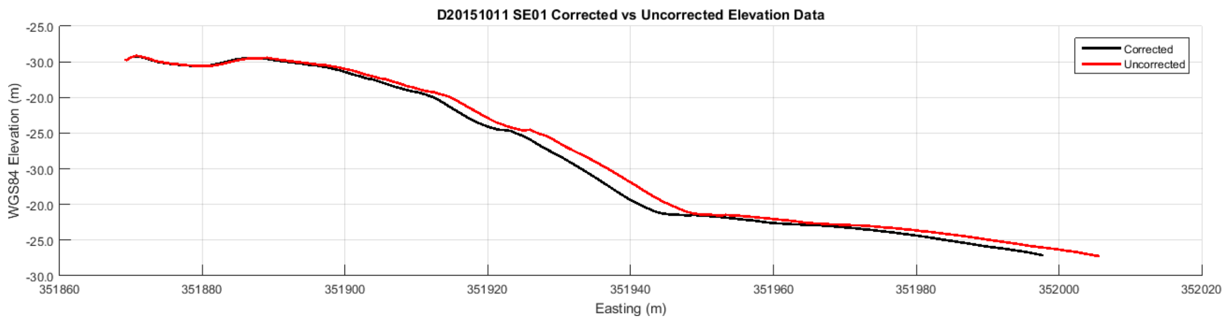
D20151011 SE01 Corrected vs Uncorrected Elevation Data
Corrected
Uncorrected
WGS84 Elevation (m)
Easting (m)

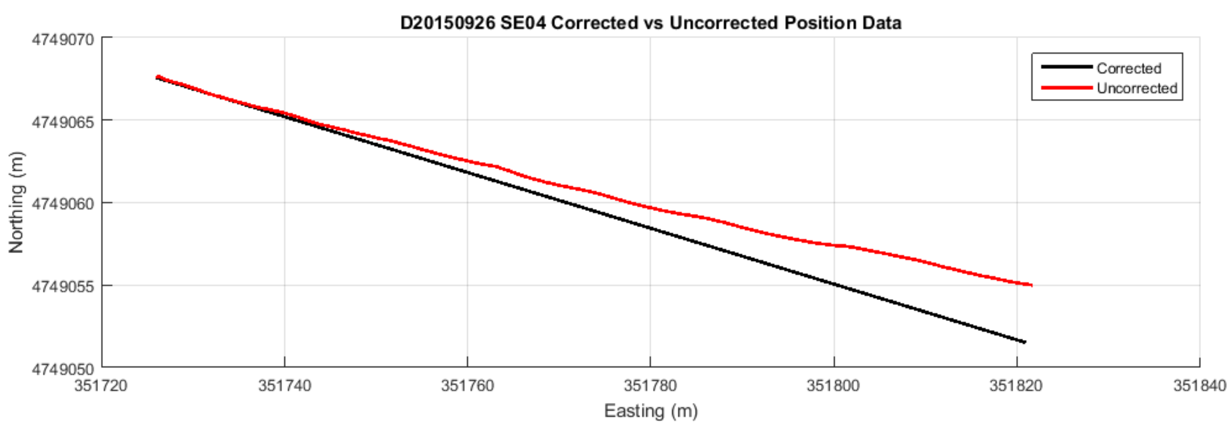
D20150926 SE04 Corrected vs Uncorrected Position Data
Corrected
Uncorrected
Northing (m)
Easting (m)

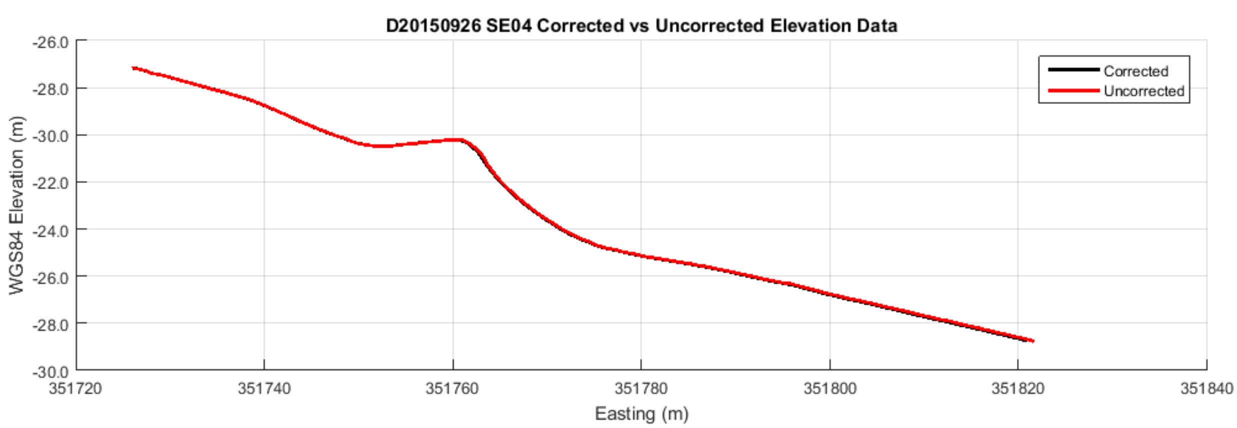
D20150926 SE04 Corrected vs Uncorrected Elevation Data
Corrected
Uncorrected
WGS84 Elevation (m)
Easting (m)

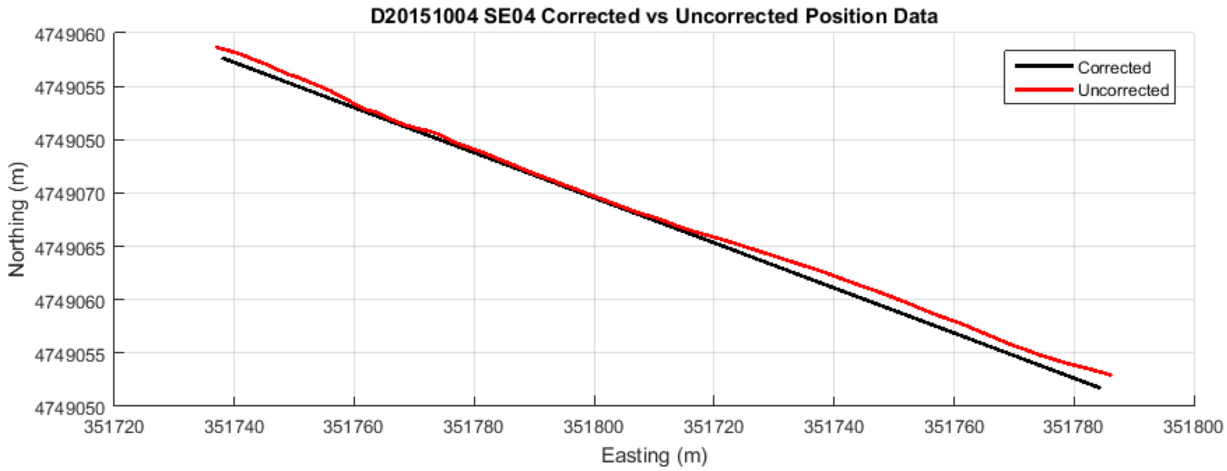
D20151004 SE04 Corrected vs Uncorrected Position Data
Northing (m)
Easting (m)
Corrected
Uncorrected
4749060
4749055
4749050
4749070
4749065
4749060
4749055
4749050
351720
351740
351760
351780
351800
351720
351740
351760
351780
351800

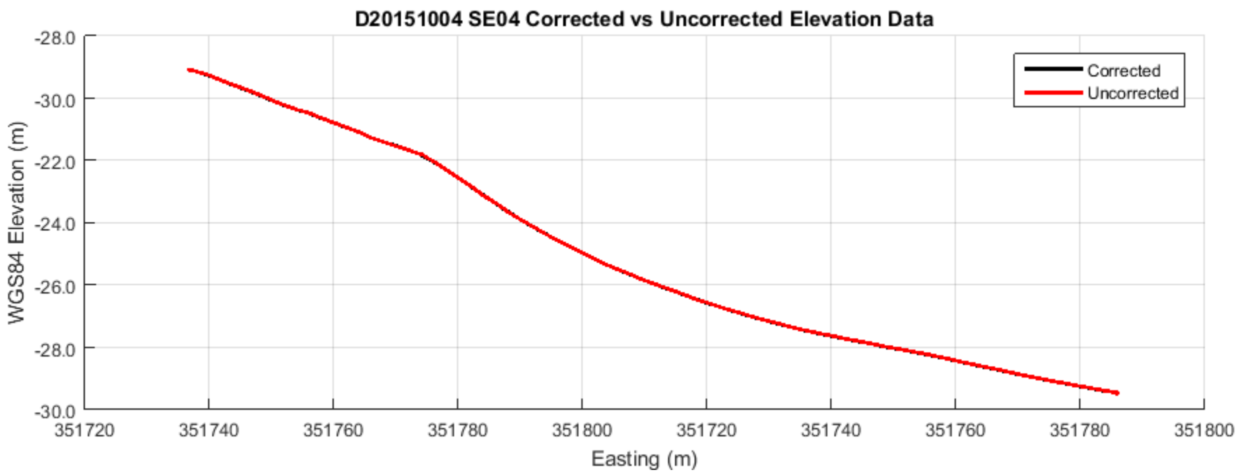
D20151004 SE04 Corrected vs Uncorrected Elevation Data
WGS84 Elevation (m)
Easting (m)
Corrected
Uncorrected
-28.0
-30.0
-22.0
-24.0
-26.0
-28.0
-30.0
351720
351740
351760
351780
351800
351720
351740
351760
351780
351800

APPENDIX 4. DETAILED PROFILE BEHAVIOR

The following tables include detailed changes in profiles at each station between every survey, including vertical erosion/accretion, change in berm slope, horizontal change in berm crest position, sediment volume change, and various comments. Tables are arranged in order by beach, station, then date.

Station	Dates	Vert. Change (cm)	Accretion/Erosion Location	Berm Slope Change	Berm Crest Position Change (m)	Sed. Vol. Change (m^3)	Comments
WS01	07/06/15 to 10/25/15	+20	Beach face, LTT			+18.3	
WS01	10/25/15 to 01/14/16	-40	Beach face		-5	-15.3	
WS01	01/14/16 to 04/02/16	-80	Seawall, LTT	Decreased		-50.5	
WS01	04/02/16 to 07/22/16	+60	Berm face, LTT	Increased	+15	+55.9	Berm formed
WS02	07/06/15 to 10/25/15	+40	LTT			+23.5	
WS02	10/25/15 to 01/14/16	-30	Berm face	Increased		-14.3	
WS02	01/14/16 to 04/02/16	-30	Upper LTT			-8.6	
WS02	04/02/16 to 07/22/16	-50 +30	Upper beach Berm toe			-6.1	Ridge formed
WS03	07/06/15 to 10/25/15	-30 +20	Berm face LTT		+4	+3.3	
WS03	10/25/15 to 01/14/16	-40	Upper beach, berm			-12.6	Lost berm
WS03	01/14/16 to 04/02/16	-30	Upper LTT			-16.8	Ridge formed
WS03	04/02/16 to 07/22/16	-50 +40	Upper Beach LTT			+13.9	Ridge formed
WS04	08/03/15 to 10/25/15	-30	Berm		-8	-0.2	Ridge formed
WS04	10/25/15 to 01/14/16	-40	Berm			-2.0	Lost berm
WS04	01/14/16 to 04/02/16	-40	Upper LTT			-13.2	
WS04	04/02/16 to 07/22/16	+50	Upper LTT	Increased		+11.3	Berm formed
WS05	10/25/15 to 04/02/16	-30	Upper beach			-8.9	Ridge formed
WS05	04/02/16 to 07/22/16	+30 +60	Berm Upper LTT			+12.4	Berm formed, ridge formed

Table 7-1: Analysis of profile measurements for Wallis Sands monitoring stations, including station number, dates of the surveys of the two profiles examined, the vertical erosion/accretion magnitude, the location(s) of the vertical erosion/accretion, the visually qualitative change in berm face slope, the magnitude of progradation/retrogradation of the berm crest, the change in sediment volume for a 1m wide section of beach along the profile, and any other morphologic features gained/lost between surveys.

Station	Dates	Vert. Change (cm)	Accretion/Erosion Location	Berm Slope Change	Berm Crest Position Change (m)	Sed. Vol. Change (m^3)	Comments
FO01	08/18/15 to 11/08/15	-90	Upper beach	Decreased		-26.8	
FO01	11/08/15 to 02/07/16	+40 +60	Upper beach Lower beach			+15.1	
FO01	02/07/16 to 04/09/16	+10 -10	Upper beach Lower beach			-2.3	
FO01	04/09/16 to 08/09/16	+70	Upper beach	Decreased		+13.8	
FO02	08/18/15 to 11/08/15	-90	Upper beach			-29.4	
FO02	11/08/15 to 02/07/16	+30	Entire profile			+13.8	
FO02	02/07/16 to 04/09/16	-20	Upper beach			-2.2	Runnel formed
FO02	04/09/16 to 08/09/16	+90 +40	Mid-beach Upper and lower	Decreased		+61.2	
FO03	11/08/15 to 04/09/16	+50 +30	Upper beach Lower beach			+12.1	Runnel formed
FO03	04/09/16 to 08/09/16	+40	Upper beach	Decreased		+5.8	
FO04	11/08/15 to 04/09/16	+90	Lower beach	Increased		+10.5	Berm formed
FO04	04/09/16 to 08/09/16	-40	Mid-beach			-2.2	Lost berm

Table 7-2: Analysis of profile measurements for Foss Beach monitoring stations, including station number, dates of the surveys of the two profiles examined, the vertical erosion/accretion magnitude, the location(s) of the vertical erosion/accretion, the visually qualitative change in berm face slope, the magnitude of progradation/retrogradation of the berm crest, the change in sediment volume for a 1m wide section of beach along the profile, and any other morphologic features gained/lost between surveys.

Station	Dates	Vert. Change (cm)	Accretion/Erosion Location	Berm Slope Change	Berm Crest Position Change (m)	Sed. Vol. Change (m^3)	Comments
JN01	09/29/15 to 11/21/15	-40 -30	Upper beach Lower beach			-18.5	Lost berm
JN01	11/21/15 to 02/06/16	-20	Upper beach			-8.7	
JN01	02/06/16 to 04/03/16	+20	Upper beach			-3.1	
JN01	04/03/16 to 07/25/16	-50	Upper beach	Decreased		-19.8	
JN02	09/29/15 to 11/21/15	-60	Berm			-12.7	Lost berm
JN02	11/21/15 to 02/06/16	-10	Entire profile			-9.0	
JN02	02/06/16 to 04/03/16	-20	Lower beach			-7.7	
JN02	04/03/16 to 07/25/16	-60 -40	Upper beach Lower beach			-39.0	
JN03	09/29/15 to 11/21/15	-20	Upper beach			-10.1	
JN03	11/21/15 to 02/06/16	-30	Upper beach			-22.8	
JN03	02/06/16 to 04/03/16	+10	Lower beach			+2.1	
JN03	04/03/16 to 07/25/16	-40 -50	Upper beach LTT			-38.8	Ridge formed
JN04	09/29/15 to 11/21/15	-30	Upper beach			-16.7	
JN04	11/21/15 to 02/06/16	-20	Upper beach			-10.6	Ridge formed
JN04	02/06/16 to 04/03/16	-20	Lower beach			-7.1	

Table 7-3: Analysis of profile measurements for Jenness Beach monitoring stations, including station number, dates of the surveys of the two profiles examined, the vertical erosion/accretion magnitude, the location(s) of the vertical erosion/accretion, the visually qualitative change in berm face slope, the magnitude of progradation/retrogradation of the berm crest, the change in sediment volume for a 1m wide section of beach along the profile, and any other morphologic features gained/lost between surveys.

Station	Dates	Vert. Change (cm)	Accretion/Erosion Location	Berm Slope Change	Berm Crest Position Change (m)	Sed. Vol. Change (m^3)	Comments
NH01	08/17/15 to 11/07/15	-50 +60	Upper beach Lower beach	Decreased		-32.9	Lost berm
NH01	11/07/15 to 01/15/16	-40	Entire profile			-12.3	
NH01	01/15/16 to 02/21/16	-30	Lower beach			-5.6	
NH01	02/21/16 to 04/17/16	+60	Upper beach	Increased		+19.3	
NH01	04/17/16 to 08/08/16	+110 -40	Berm Back-berm, LTT	Increased		+13.4	Berm formed
NH02	08/17/15 to 11/07/15	-80 +90	Upper beach Lower beach	Decreased		-15.6	Lost berm
NH02	11/07/15 to 01/15/16	-40	Lower beach			-48.2	Berm formed
NH02	01/15/16 to 02/21/16	+90	Lower beach		-6	+21.2	
NH02	02/21/16 to 04/17/16	+60 +50	Upper beach Lower beach			+19.5	
NH02	04/17/16 to 08/08/16	-60 +100	Upper beach, LTT Berm	Increased	+21	+6.8	Berm formed
NH03	08/17/15 to 11/07/15	-80 +50	Upper beach Lower beach	Decreased		-13.9	Lost berm
NH03	11/07/15 to 01/15/16	-50	Entire profile			-23.8	
NH03	01/15/16 to 02/21/16	-80	Lower beach			-19.5	
NH03	02/21/16 to 04/17/16	+70	Lower beach	Increased		+28.1	
NH03	04/17/16 to 08/08/16	+110 -40	Berm Back-berm, LTT	Increased		+14.6	Berm formed

Table 7-4: Analysis of profile measurements for North Hampton Beach monitoring stations, including station number, dates of the surveys of the two profiles examined, the vertical erosion/accretion magnitude, the location(s) of the vertical erosion/accretion, the visually qualitative change in berm face slope, the magnitude of progradation/retrogradation of the berm crest, the change in sediment volume for a 1m wide section of beach along the profile, and any other morphologic features gained/lost between surveys.

Station	Dates	Vert. Change (cm)	Accretion/Erosion Location	Berm Slope Change	Berm Crest Position Change (m)	Sed. Vol. Change (m^3)	Comments
HA01	07/07/15 to 10/03/15	-50 +40	Upper beach Lower beach	Decreased	-2	+1.5	
HA01	10/03/15 to 10/10/15	-30	Berm face	Increased		-2.1	
HA01	10/10/15 to 12/05/15	+50	Berm face	Increased		+10.2	
HA01	12/05/15 to 01/17/16	-60 +40	Upper berm Lower berm	Decreased	-8	-5.4	
HA01	01/17/16 to 01/30/16	-60	Berm face	Decreased	-8	-4.6	
HA01	01/30/16 to 02/20/16	-60	Berm face	Decreased	-6	-3.7	
HA01	02/20/16 to 04/16/16	+110	Berm face	Increased	+9	+33.3	
HA02	10/03/15 to 10/10/15	+80	Berm face	Increased		+53.2	
HA02	10/10/15 to 12/05/15	-50	Berm face	Increased		-26.5	Ridge formed
HA02	12/05/15 to 01/17/16	-50	Berm face	Increased		-0.9	Ridge formed
HA02	01/17/16 to 01/30/16	-60 +50	Berm face Berm crest	Decreased	-9	-0.8	
HA02	01/30/16 to 02/20/16	-50	Berm face	Decreased	-5	+1.2	
HA02	02/20/16 to 04/16/16	+30	LTT			+2.8	
HA02	04/16/16 to 08/22/16	-50 +40	Back berm Lower beach	Increased	+16	+4.0	
HA03	07/07/15 to 10/03/15	+50	Berm crest	Increased		+36.3	
HA03	10/03/15 to 10/10/15	-50	Berm	Increased	-2	-31.8	Ridge formed
HA03	10/10/15 to 12/05/15	-30	Berm face	Decreased	-4	-9.1	
HA03	12/05/15 to 01/17/16	-40	Berm face	Decreased	-6	-5.7	
HA03	01/17/16 to 01/30/16	-60	Berm face	Decreased	-7	-20.31	Ridge formed
HA03	01/30/16 to 02/20/16	+40	Back berm	Decreased	-13	+13.9	
HA03	02/20/16 to 04/16/16	+40	Berm face	Increased	+11	+2.4	
HA04	10/03/15 to 10/10/15	-20	Lower beach	Increased	-8	+2.5	Ridge formed
HA04	10/10/15 to 12/05/15	-40	Berm face	Decreased		-13.5	
HA04	12/05/15 to 01/17/16	-30	Mid-beach	Decreased		-12.7	Lost berm
HA04	01/17/16 to 01/30/16	-20	Mid-beach	Decreased		-8.1	
HA04	01/30/16 to 02/20/16	-20	Mid-beach	Decreased		-5.3	
HA04	02/20/16 to 04/16/16	+20	Mid-beach	Increased		+23.4	
HA04	08/04/16 to 08/22/16	+40	Berm	Increased		+14.4	Berm formed

Table 7-5: Analysis of profile measurements for Hampton Beach monitoring stations, including station number, dates of the surveys of the two profiles examined, the vertical erosion/accretion magnitude, the location(s) of the vertical erosion/accretion, the visually qualitative change in berm face slope, the magnitude of progradation/retrogradation of the berm crest, the change in sediment volume for a 1m wide section of beach along the profile, and any other morphologic features gained/lost between surveys.

Station	Dates	Vert. Change (cm)	Accretion/Erosion Location	Berm Slope Change	Berm Crest Position Change (m)	Sed. Vol. Change (m³)	Comments
SE01	07/19/15 to 10/11/15	-50	Berm face	Decreased	-6	-9.8	
SE01	10/11/15 to 12/06/15	+40	Berm face	Increased		+10.2	
SE01	12/06/15 to 01/31/16	-90	Upper berm, LTT	Decreased		-56.4	
SE01	01/31/16 to 04/10/16	+170 +100	Berm crest LTT	Increased		+71.2	Huge berm formed
SE01	04/10/16 to 08/05/16	-50	Back berm	Decreased	-6	-31.4	
SE02	07/19/15 to 12/06/15	-40	Berm toe	Increased		+16.9	
SE02	12/06/15 to 01/31/16	-100	Berm crest, berm base	Increased		-45.0	
SE02	01/31/16 to 04/10/16	+130 +120	Berm crest Berm base	Increased		+40.5	Major berm build up
SE02	04/10/16 to 08/05/16	-50	Berm			-21.3	
SE03	07/19/15 to 10/03/15	-70	Berm crest	Decreased	-6	-5.1	
SE03	10/03/15 to 01/31/16	-80 -100	Berm crest Berm base	Decreased	+9	-16.7	
SE03	01/31/16 to 04/10/16	+60	Berm face			+23.7	
SE03	04/10/16 to 08/05/16	-50 -30	Back berm LTT			-18.8	
SE04	09/26/15 to 10/04/15	-150	Berm	Decreased	-13.5	-39.5	Lost berm
SE04	10/04/15 to 10/11/15	+60 -50	Upper berm Lower berm	Increased		+15.7	Berm formed
SE04	10/11/15 to 12/06/15	+30	Berm			-9.8	
SE04	12/06/15 to 01/31/16	-80	Upper berm	Increased		-41.6	
SE04	01/31/16 to 04/10/16	+120	Upper berm	Increased		+40.6	Major berm build up
SE04	04/10/16 to 08/05/16	-30 +50	Back berm Berm base			-11.2	Ridge formed

Table 7-6: Analysis of profile measurements for Seabrook Beach monitoring stations, including station number, dates of the surveys of the two profiles examined, the vertical erosion/accretion magnitude, the location(s) of the vertical erosion/accretion, the visually qualitative change in berm face slope, the magnitude of progradation/retrogradation of the berm crest, the change in sediment volume for a 1m wide section of beach along the profile, and any other morphologic features gained/lost between surveys.